Electricity-based Mobility

Analysis of greenhouse gas emissions in the context of an evolving energy system

Authors

Martin Rüdisüli[a], Christian Bach[c], Christian Bauer[e], Didier Beloin-Saint-Pierre[b], Urs Elber[a], Sherif Fahmy[f], Gil Georges[d], Robert Limpach[a], Giacomo Pareschi[d], Ramachandran Kannan[e], Sinan Teske[a]

[a] Urban Energy Systems Laboratory, Swiss Federal Laboratories for Materials Science and Technology, Empa, Dübendorf, Switzerland

[b] Technology and Society Laboratory, Swiss Federal Laboratories for Materials Science and Technology, Empa, St. Gallen, Switzerland

[c] Automotive Powertrain Technologies Laboratory, Swiss Federal Laboratories for Materials Science and Technology, Empa, Dübendorf, Switzerland

[d] Aerothermochemistry and Combustion Systems Laboratory, Institute of Energy and Process Engineering, ETH Zürich, Zürich, Switzerland

[e] Laboratory for Energy Systems Analysis, Paul Scherrer Institut (PSI), Forschungsstrasse 111, 5232 Villigen, Switzerland

[f] Distributed Electrical Systems Laboratory – Power Systems group, EPFL STI IEL DESL ELL 037, Station 11, 1015 Lausanne

July 2021

Acknowledgement

The study was mandated and financed by the Competence Center for Energy and Mobility (CCEM) of the ETH Domain. The authors express their gratitude to CCEM as well as to Urs Elber (Empa, PSI) and Jürg Christener (FHNW) for their project support.

Contents

Nomenclature

GHG = Greenhouse gas (CO_2-eq)
CO_2-eq = CO_2 equivalent
NG = natural gas (from the grid)
SNG = Synthetic natural gas
CCS = Carbon Capture and Storage
EBM = Electricity based-mobility
BEV = Battery Electric Vehicle
H_2-FCEV = Hydrogen-based Fuel Cell Electric Vehicle
SNG-V = SNG vehicle
ICEV = Internal Combustion Engine Vehicle
HEV-p = Hybrid Electric Vehicle (petrol)
CH = Switzerland
EU = EU-28 (not including Estonia, Latvia, Lithuania)
LC = Low carbon
LCA = Life Cycle Assessment
LCIA = Life Cycle Impact Assessment
LCI = Life Cycle Inventory
CCGT = Combined Cycle Gas Turbine
SFOE = Swiss Federal Office of Energy (Bundesamt für Energie BFE)
PHS = Pumped-hydro Storage
PV = Photovoltaics
ELYSE = Electrolysis
METH = Methanation
SMR = Steam Methane Reforming

EUSTEM = European Swiss TIMES Electricity Model
RNW_SOL = Renewable Solar PV electricity generation
RNW_WIND = Renewable Wind electricity generation
RNW_OTHERS = Other renewable electricity generation
RNW_GEO = Renewable geothermal electricity generation
RNW_CSP = Renewable Concentrated Solar Power electricity generation
RNW_TIDE = Renewable wave and tidal power electricity generation
STG_BAT = Stationary Battery
HYD_PUMP = Pumped-hydro storage (PHS)
HYD_DAM = Hydro storage electricity generation
HYD_RUN = Run-of-the-River electricity generation
NUC = Nuclear electricity generation
GAS_CCS = Gas-fired electricity generation (with CCS)
GAS_B = Gas-fired electricity generation (baseload)
OIL = Oil-fired electricity generation
COAL_CCS = Coal-fired electricity generation (with CCS)
COAL_B = Coal-fired electricity generation (baseload)

Executive summary

Electricity-Based Mobility (EBM) refers to vehicles that use electricity as their primary source of energy, either directly as Battery Electric Vehicles (BEV) or indirectly as Fuel Cell Electric Vehicles (H2-FCEV) or Synthetic Natural Gas Vehicles (SNG-V). Within this project, the Greenhouse Gas (GHG) emissions reduction potential of EBM vehicles is investigated considering both evolving vehicle fleets and Swiss and European electricity systems.

For all three EBM scenarios (BEV, H_2-FCEV and SNG-V) the same vehicle market development in Switzerland is derived from the current and foreseeable legislative CO_2 reduction targets on newly registered passenger cars. These EBM scenarios are compared with a reference scenario ("non-EBM") relying on conventional and hybridized Internal Combustion Engine Vehicles (ICEV/HEV) fueled by fossil gasoline (60%) and diesel (40%). While a strong growth of EBM in newly registered vehicles is expected with no more new fossil fueled ICEV after 2040, the resulting share of EBM in the entire vehicle stock linearly grows up to 55% by 2050, while the rest of vehicles is expected to decrease to 40% Hybrid Electric Vehicles (HEV) and 5% ICEV. In this regard, it is expected that the entire passenger car fleet will grow from 4.5 million vehicles in 2020 driving 50 billion vehicle-km (vkm) to 6 million vehicles in 2050 with a total mileage of 62 billion vkm. Aspects such as vehicle sharing or autonomous driving are not considered in this study.

The average real-world end energy demand, defined as Tank/Battery-to-Wheel consumption for BEV is assumed to be, on average, 20 kWh/100km today, decreasing to 17 kWh/100km by 2050; for H_2-FCEV it is 35 kWh_{LHV}/100km (1.05 kgH_2/100km) today and decreases to 28 kWh_{LHV}/100km by 2050 (0.85 kgH_2/100km); and for SNG-V it is 750 kWh_{LHV}/100km (5.5 kg/100km) today with a decrease to 490 kWh_{LHV}/100km (3.6 kg/100km) until 2050. For all scenarios, Life Cycle Assessment (LCA) data are used to quantify GHG emissions, including the whole vehicle manufacturing and disposal cycle as well as the end-energy production, distribution and supply.

The supply chain of EBM end-energy is modeled at an hourly resolution, starting from today's Swiss energy supply and demand including imports of electricity and fossil natural gas. The electricity demand from consumers other than passenger cars is fixed and electricity supply from nuclear power is assumed to be phased out by 2034. For domestic electricity supply from PV, three expansion scenarios are considered: a least-cost expansion to an annual production of 13 TWh as well as two exogenously defined larger expansions to 32 and 52 TWh by 2050. For imported electricity, two GHG intensity scenarios are used: a Low Carbon (LC) import scenario and a scenario based on import electricity from natural gas operated Combined Cycle Gas Turbine (CCGT) power plants. The LC scenario is linked to an annual average GHG intensity of 330 g CO2/kWh in 2020, which is gradually reduced to 80 g CO2/kWh until 2050 by using less conventional-thermal energy, more renewable energy as well as Carbon Capture and Storage (CCS) technologies. In turn, the CCGT scenario features a GHG intensity of 440 g CO2/kWh in 2020 and a reduction to 360 g CO2/kWh until 2050 by efficiency measures.

Figure 1 summarizes the key findings of this study with respect to systemic GHG emissions (including all life-cycle GHG emissions) associated with the three EBM (BEV, H2-FCEV, SNG-V) and “non-EBM” powertrains for the three PV expansion (13, 32 and 52 TWh PV) and two import GHG scenarios ("LC" and "CCGT") for all years 2015 to 2050. A distinction between "additional SNG production" and "curtailment" of excess electricity is made. Arrows indicate the additional GHG emissions of the EBM fleet added on top of GHG emissions tied to the base electricity demand (dark grey area). GHG savings of EBM against the reference “non-EBM” fleet are displayed as a light grey area along with their absolute numbers in 2050. GHG savings due to sector coupling (“add. SNG prod.”) are displayed as in the light blue area with negative values.

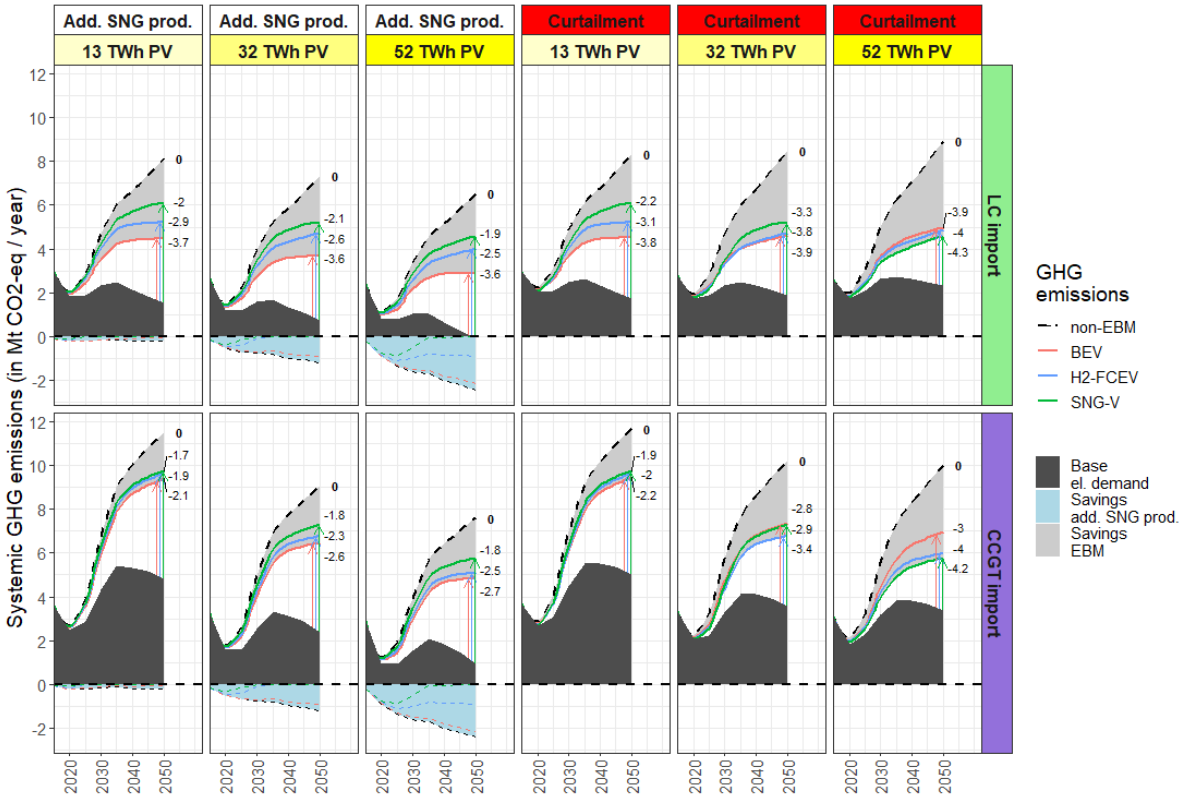

Figure 1 Overall (systemic) GHG emissions for all EBM (BEV, H2-FCEV, SNG-V) and "non-EBM" powertrain scenarios in all PV expansion (13, 32, 52 TWh PV) and import GHG content (LC, CCGT) scenarios. A distinction between "additional SNG production" and "curtailment" of excess electricity is made. The dark grey area shows the GHG emissions of the base electricity demand in the electricity sector (without mobility). The light grey area shows GHG savings of EBM powertrains against the "non-EBM" fleet.

Due to the increased electricity demand of EBM, GHG emissions in the electricity sector increase (shown by the arrows in Figure 1). At the same time, GHG emissions from non-EBM vehicles, operated with fossil fuels decrease, resulting in an overall GHG emission reduction by all three EBM powertrains in all investigated scenarios. This overall GHG mitigation is on the one hand limited by the amount of installed PV and on the other hand by the GHG intensity of imported electricity.

If low carbon (LC) electricity is imported when the domestic electricity production cannot meet the demand (which is mainly the case in winter) and if there is no excess electricity that must be curtailed (three top left diagrams in Figure 1), that is, if all electricity is either used directly or can be converted to additional SNG for use in other energy sectors (e.g. heavy-duty transportation, industry, etc.), then BEV always show the lowest systemic GHG emissions among all EBM powertrains due to their highest Tank-to-Wheel (TTW) efficiency and no additional conversion steps. By 2050, depending on the assumed PV expansion, between -3.7 and -3.6 Mt CO_2-eq can be saved by a corresponding BEV fleet compared to a "non-EBM" fleet. In turn, if electricity must be curtailed (three top right diagrams in Figure 1), by 2050 an overall GHG reduction between -2.2 (SNG) and -3.8 (BEV) Mt CO_2-eq per year occurs in the 13 TWh PV scenario, between -3.3 (SNG) and -3.9 (BEV) Mt in the 32 TWh PV as well as between -3.9 (BEV) and -4.3 (SNG) Mt in the 52 TWh PV scenario. If carbon-intensity CCGT electricity must be imported, an overall GHG reduction between -1.9 (SNG) and -2.2 (BEV) Mt per year results in the 13 TWh PV scenario, between -2.9 (SNG, BEV) and -3.5 (H2-FCEV) Mt in the 32 TWh PV as well as between -3.0 (BEV) and -4.3 (SNG) Mt for the 52 TWh PV scenario (three bottom right diagrams in Figure 1).

To identify potential problems that BEV might have on low-voltage distribution grid's static security (i.e. nodal voltage, branch current and slack node apparent power magnitudes within safety bounds), this study employs a stochastic Monte-Carlo based load-flow method. This method yields the probabilities of violating different grid static constraints depending on the percentage of BEV penetration in the local grid as well as the season, day-type (weekday vs. weekend) and hour of the day. The method was applied to two real-world low-voltage grids in Switzerland and revealed that, depending on the characteristics of the grid, beyond a certain percentage of BEV penetration, their additional load becomes harmful to the grid's static security and actions such as grid reinforcement, smart charging or grid-aware placement of charging stations are needed to fully deploy BEV mobility in such local grids.

1. Introduction

In many countries - such as in Switzerland - the mobility sector still emits one of the largest shares of greenhouse gas (GHG) emissions in the entire energy system (BAFU, 2019; Solaymani, 2019). An electricity-based mobility (EBM) with low life-cycle GHG emissions - along with other low environmental impacts - is one option to reduce GHG emissions by gradually substituting fossil fuels operated internal combustion engine vehicles (ICEV) (Hirschberg et al., 2016; Schlögl, 2017). Three promising EBM technologies are Battery Electric Vehicles (BEV), Fuel Cell Electric Vehicles (H_2-FCEV) and Synthetic Natural Gas Vehicles (SNG-V). All of these technologies use electricity directly or indirectly as their fuel: while BEV directly operate on electricity from the grid, H_2-FCEV and SNG-V indirectly use electricity as stored H_2 and SNG previously produced by electrolysis (ELYSE) and - in case of SNG - by an additional methanation (METH). Both BEV and H_2-FCEV feature an electric motor, which is fed with electricity from an on-board battery or a fuel cell system, respectively, while SNG-V operate as conventional ICEV or HEV.

Each EBM technology features a different well-to-wheel efficiency (well-to-tank plus tank-to-wheel) as well as storability of their fuels (Hänggi et al., 2019). While BEV feature a high tank-to-wheel efficiency (Bauer et al., 2015; Cox et al., 2020; Hirschberg et al., 2016), their energy demand can economically only be stored for short terms (hours to days). In turn, SNG-V have a rather low well-to-wheel efficiency due to losses in the electricity conversion to SNG (well-to-tank) and the internal combustion engine based powertrain (tank-to-wheel). However, SNG can be stored for longer durations (seasons) in the existing natural gas (NG) grid and thus SNG-V feature a large flexibility with regard to the electricity used to produce SNG. Moreover, due to impending improvements (incl. hybridization) of ICEV, their tank-to-wheel efficiency may also become more efficient (Cox et al., 2020; Nordelöf et al., 2014; Taylor, 2008). H_2-FCEV are between BEV and SNG-V both in terms of their well-to-wheel efficiency as well as in their storage flexibility (days to weeks). And, H_2-FCEV are still in their infancy, therefore, substantial technological improvements can be expected (Hawkins et al., 2012; Züttel et al., 2010).

For all EBM technologies, to feature overall (systemic) low GHG emissions, renewable electricity with a low carbon footprint must be used (Ajanovic and Haas, 2019; Bauer et al., 2015; Berrill et al., 2016; Hertwich et al., 2015; Sacchi et al., 2020). Conversely, if conventional thermal power plants (e.g. gas or coal) are used to meet the additional electricity demand of EBM, no effective GHG mitigation will occur[1] (Cox et al., 2020). From a GHG mitigation point of view, the decisive factor is the GHG emissions per km traveled including all direct and indirect ("grey") GHG emissions from operation, fuel supply as well as manufacturing of the vehicles and other infrastructure. Thus, the introduction of EBM must occur in parallel to an expansion of renewable electricity generation. However, in the near to mid-term future, it is unlikely that all electricity in Switzerland (and the EU) will stem from renewable sources. Moreover, as many European countries phase out nuclear power, a gap of low carbon base-load electricity must be filled (Díaz Redondo and van Vliet, 2015; Rüdisüli et al., 2019). Renewable electricity from hydropower is already well exploited (in Switzerland), and hence difficult to increase, while the potential and exploitability of other intermittent and stochastic renewable energy technologies such as photovoltaics (PV) and wind are still vague (Suisse Eole, 2020; Walch et al., 2020)]. As an alternative to increasing domestic renewable electricity production, also importing more electricity from abroad is an option to fill this gap, however, then this imported electricity must also feature a low GHG content (Romano et al., 2018).

In particular, renewable electricity from PV has a clear diurnal and seasonal pattern with peaks at noon and in summer, which generally do not match electricity demand peaks in the evening/morning and in winter, respectively. While diurnal discrepancies between demand and supply may be offset by local

[1] Converting biomass or natural gas to hydrogen via reforming and/or gasification processes with CCS represents an alternative to electrolysis, which would not induce additional electricity demand and still exhibits comparatively low or even negative GHG emissions (Antonini et al., 2020). However, such hydrogen production pathways have not been considered within this study.

smart grids (e.g. demand side management) and well-connected grids with short-term electricity storage such as batteries and pumped hydro storage (PHS), a sustainable energy system with high PV shares must in particular be able to cope with seasonal demand and supply discrepancies by adequate long-term (seasonal) storage. As seasonal storage of electricity (e.g. in PHS and batteries) is economically not sensible, it is still viable to store electricity seasonally by converting it to chemical energy carriers such as H_2 and SNG via power-to-gas (PtG) (Kober et al., 2019; Reiter and Lindorfer, 2015; Van Der Giesen et al., 2014; Zhang et al., 2017). Despite its relatively high costs and conversion losses, PtG is a promising option to promote and exploit the full potentials of PV, in particular with respect to mobility (Teske et al., 2019).

Several studies have been conducted with regard to the environmental (e.g. GHG) life-cycle assessment (LCA) of EBM technologies, in particular with regard to BEV (Hawkins et al., 2012; Nordelöf et al., 2014). Other EBM technologies have also been investigated by Bauer et al. (2015) in a novel LCA scenario analysis framework with conventional and hybrid ICEV as well as BEV and FCEV taking into account electricity and H_2 supply chains from fossil, nuclear and renewable energy resources. The H_2 supply chain for H_2-FCEV was further investigated by Wulf and Kaltschmid (2018) for a broad variety of renewable and fossil H_2 production pathways. Building on the work of the THELMA project (Hirschberg et al., 2016) and the SCCER project “Mobility, Supply of Electricity, and Heat and Electricity Storage” (Cox et al., 2020) conducted an attributional LCA study (with global sensitivity and uncertainty analysis) on the environmental impacts of current and future passenger cars in Switzerland including BEV, H_2-FCEV and SNG-V.

To properly evaluate and compare the GHG mitigation potential of EBM in a systemic way, their different fuel supply pathways have to be analyzed in a dynamic and evolving energy system. There are several studies with emphasis on such a systemic integration of EBM into the energy (electricity) system, however, they either do not have adequate temporal resolution to capture short-term dynamics (e.g. momentary demand and supply peaks) (Gül, 2008; Seixas et al., 2015) or they are specific to one country (Arnhold et al., 2017) or they investigate only BEV (Klettke et al., 2018; Longo et al., 2019). A Switzerland-specific study with an intra-annual hourly time resolution has been conducted by Kannan and Hirschberg (2016). They used the Swiss TIMES energy system model (STEM) (Kannan and Turton, 2014) to investigate the interactions between the Swiss mobility (including BEV, FCEV, yet no SNG-V) and the electricity system in a technology-rich, cost-optimal modelling framework with a time horizon 2010 till 2100 for a conservative (business-as-usual BAU) and low-carbon scenario (new energy policy NEP) (Prognos, 2012). They also accounted for cross border electricity trading and associated GHG contents of import electricity by employing the CROSSTEM model (Pattupara and Kannan, 2016). They found that e-mobility (BEV) supports decarbonization of the car fleet even if electricity is supplied from large domestic gas power plants or relatively low cost sources of imported electricity. They based their analysis on averaged hourly profiles for typical weekdays and weekends in three seasons (summer, winter, and intermediate season).

This study grounds on methods of these above-mentioned studies and extends them to study the life-cycle GHG mitigation potential of all three EBM powertrains in an evolving Swiss and European energy system in an as dynamic and as comprehensive way as necessary. In this respect, in particular the impact of curtailment of renewable electricity due to a diurnal and seasonal mismatch of demand and supply is addressed. Therefore, the primary research question is how and under what circumstances the selective use of low carbon electricity and subsequent enhanced storability (flexibility) of H_2 and SNG can be used to offset this seasons mismatch despite the additional energy losses associated with H_2-FCEV and SNG-V compared to overall more efficient but less flexible BEV or fossil fuels based ICEV powertrains.

To this end, 1) the evolution of EBM powertrains and their hourly end-energy demand in the Swiss passenger cars fleet is modeled such that legislative GHG emission targets are fulfilled, 2) the evolution of the Swiss and European electricity generation mix and their associated GHG emissions are modelled based on national and European energy strategies as well as 3) life-cycle GHG emissions of individual generation technologies such that 4) EBM powertrains and their supply chain can be modelled dynamically and comprehensively with respect to energy demand, supply and storage at an hourly time resolution to 5) effectively reduce GHG emissions in the energy system.

This study primarily investigates technological and physical aspects of EBM in the Swiss energy system. Socio-economic aspects, although also of high relevance to the topic, are out of the scope of this study.

This report is structured as follows: In Chapter 2, the evolution of a GHG emissions compliant Swiss passenger cars fleet and their annual and hourly energy demand are modelled. In Chapter 3, the evolution of the Swiss and European electricity system is shown. Chapter 4 provides the life-cycle GHG emissions of power supply technologies as well as conventional and EBM vehicle technologies. In Chapter 5, a dynamic analysis of systemic GHG emissions in the fuel supply chain of EBM fuels is conducted. Chapter 6 shows the impact of additional BEV mobility in two case study low-voltage electricity grids. In Chapter 7, the main findings of this report are summarized as recommendations for policy makers, Chapter 8, shows the limitations of this study and, based on these, provides an outlook for further study.

2. Mobility evolution and demand

2.1. Introduction

The rising urgency to address climate change is pushing regulators to tighten the GHG emissions requirements from all sectors of the economy. The European Union and Switzerland have set new ambitious targets for the average CO_2 emissions of newly registered cars for the upcoming decade based on a tank-to-wheel approach. These goals can only be met by extensively introducing plugin vehicles However, to consider not only tank-to-wheel but also all emissions, the greenhouse gas emissions were investigated based on an LCA approach for the following vehicle concepts:

- Battery electric vehicles (BEV)
- Fuel-cell electric vehicles (H_2-FCEV)
- Synthetic natural gas vehicles (SNG-V)

These three powertrains are collectively labelled as electricity-based mobility (EBM). The end-energy- and corresponding electricity- demand of each powertrain is estimated based on their assumed penetration in the future Swiss passenger car fleet. To this end, a fleet evolution scenario is established, in which EBM powertrains are introduced such that Switzerland's targets for average CO_2 emissions of newly registered passenger cars can be fulfilled. It must be noted that this fleet scenario just provides an adequate comparison with reasonable technological diffusion rates, but does not claim any predictive accuracy.

2.2. Design of a CO_2 legislation-compliant fleet

In this section, we introduce the mobility framework that serves as the basis for assessing the penetration of powertrain.

Each powertrain is analyzed independently during its hypothetical diffusion in the stock of Swiss passenger cars. We thus design three fleet evolution scenarios, where in each case a single powertrain is introduced in the fleet and the other two are excluded. These fleet scenarios are designed in order to guarantee a fair and unbiased comparison between the different powertrain technologies.

The stock of passenger cars is split into three technological segments:

- Internal combustion engine vehicles (ICEV), which include mild 48 V hybrid cars
- Full hybrid electric vehicles (HEV)
- Electricity-based mobility, which in each scenario will consist respectively of BEV, H2-FCEVs or SNG-V

For sake of simplicity, no plug-in version of HEV, H2-FCEV and SNG powertrains is included in the analysis. Similarly, we make no distinction in terms of car market segments, since the added complexity would not contribute towards the goal of the project and the assignment of powertrains to the different market segments would be strongly arbitrary.

2.2.1. Modelling the stock of newly registered vehicles

The BEV and H_2-FCEV fleet scenarios are designed so that the stock of new passenger cars fully complies with the legislation in terms of normative CO_2 emission targets. For an easier comparison, the same market penetration was also used for the SNG-V scenario. All legal limits used for the scenarios are presented in Table 1.

Table 1 Legal emission limits used to model the Swiss fleet of new passenger cars.

Year	Target (NEDC) g CO2 / km	Phase-in	Super credits
2020	95	85%	2.00
2021	95	90%	1.67
2022	95	95%	1.33
2023	95	100%	1.00
2025	95 - 15% = 80.75	100%	1.00
2030	95 - 37.5% = 59.38	100%	1.00
2050	0	70%	1.00

The phase-in indicates the share of the fleet of new cars that must meet the legal requirements, while the super-credits specify the weighting of low-emitting vehicles (here, EBM) towards the calculation of the average emissions. Until 2023 we make use of the already approved Swiss norms (Bundesrat, 2020), while for 2025 and 2030 we assume that Switzerland will, as often done, take over the European legislation (EU, 2019). However, while the time horizon addressed in the project spans until 2050, there is no official limit set after 2030. We thus add a hypothetical restriction for 2050, namely that 70% of new cars should be EBM. This estimate comes from the 2050 goal of the European roadmap to decrease transport-related CO_2 emissions by 70% compared to 2008 (EU, 2011). We also observe that total emissions from passenger cars have been relatively constant in Switzerland between 2008 and 2016 (BAFU, 2019).

For sake of simplicity, we base the emission targets on the New European Driving Cycle (NEDC), although from 2020 new models are certified according to the World harmonized Light-duty vehicles Test Procedure (WLTP). This decision is acceptable as long as the emissions of new cars entering the fleet are also given according to the NEDC. The current and future NEDC emissions assumed for the three technological segments introduced above are provided in Figure 2, together with fleet target values presented in Table 1.

The emissions values for cars registered in 2015 and 2016 are extracted from "MOFIS" (ASTRA, 2020). For future emission values we employ the study of Cox and Bauer (2018), which provides approximate energy consumption figures for a future average car, specifically designed for 2040. We thus use the estimated relative improvements in energy consumption between future and current vehicles (-33% for ICEVs, -17% for HEVs) to set the emission levels in 2040. Between 2016 and 2040, we assign a constant linear decrease in CO_2 emissions, while after 2040 we assume no further technological improvement for ICEVs and HEVs. The same study (Cox and Bauer, 2018) includes 48V hybrids in the ICEV segment, hence employing the same convention here adopted.

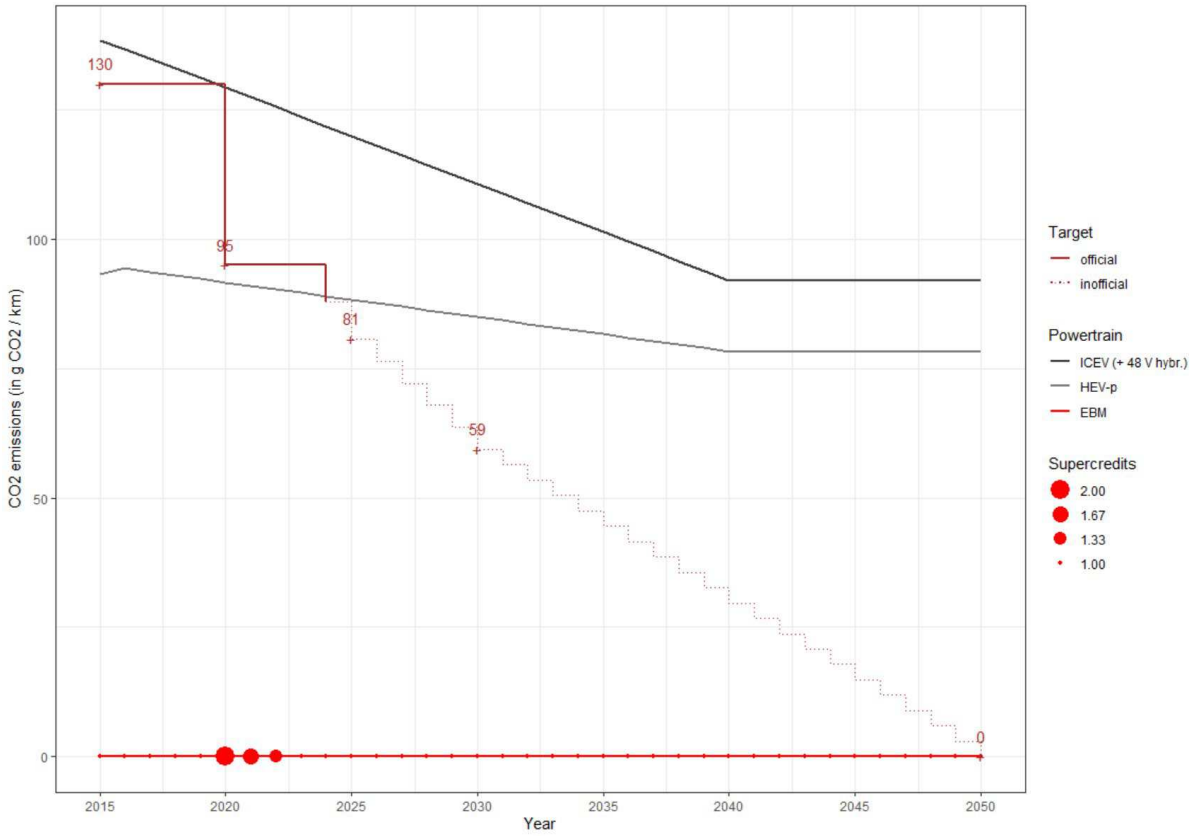

Figure 2 Evolution of the normative GHG emissions (in g CO2-eq/km) of different powertrain technologies and of the legislative targets according to NEDC.

To determine the market shares of a 3-segment fleet there is a need for 3 constraints; the first two have already been introduced, namely setting the sum of the market shares to 100% and imposing the compliance with the emission targets. As a third constraint, we specify the share of HEVs among non-EBM, i.e. the ratio between HEVs and the sum of ICEVs and HEVs. We set the ratio to linearly increase from 2.7% in 2017 (BFE, 2020) to 100% in 2040, year by which various countries and cities pledged to ban ICEVs (Wikipedia contributors, 2020).

The fleet market shares that result from complying with all three constraints are displayed in Figure 3. As expected, all ICEVs exit the market by 2040, while EBM occupy 70% of the market in 2050.

2.2.2. Modelling the stock of vehicles in the fleet

In order to translate the evolution of fleet market shares in a transition of the stock of moving vehicles we employ a simplified stock-flow cohort model. The model starts from the existing fleet in 2017 and then assumes the introduction of new cars every year with the composition given in Figure 3. The inflow of newly registered vehicles is assumed to steadily expand from 300'887 per year in 2018 (BFS, 2020a) (BFS, 2020a) to 427'000 per year in 2050. The growth rate of about 4'000 sales per year fits the observed trend in the last decade (BFS, 2020a) and allows it to hit 5'544'000 cars on the road in 2040, which is the central estimate of the Swiss transport outlook (ARE, 2016).

Regarding the cars' dismissal, we assume that all vehicles retire at the same age, regardless of their technology, as lifetime data of novel powertrains are still scarce. The cars' lifetime is calibrated to ensure a constant renovation of the fleet. Given the average sales in recent years (BFS, 2020a) and the current stock of passenger cars in Switzerland (BFS, 2020a), the lifetime ensuring regular fleet renewal rates amounts to 15 years. This value closely approaches the observed average lifetime of Swiss vehicles of 14.1 years (Oguchi and Fuse, 2015) . The resulting evolution of the stock of moving fleet is provided in Figure 4.

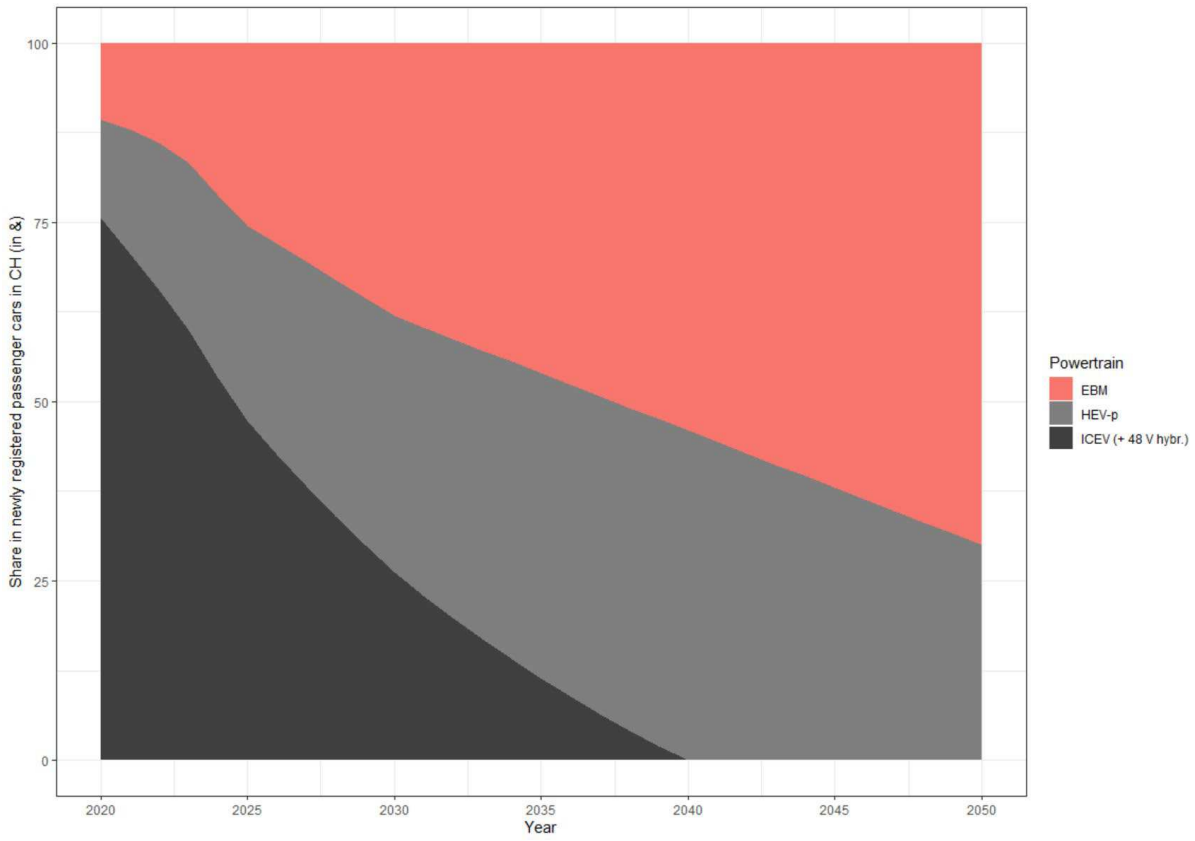

Figure 3 Evolution of the market shares of the three powertrains ICEV, HEV-p and EBM such that the average GHG emissions of the fleet of new vehicles always complies with the legislative targets in Figure 2.

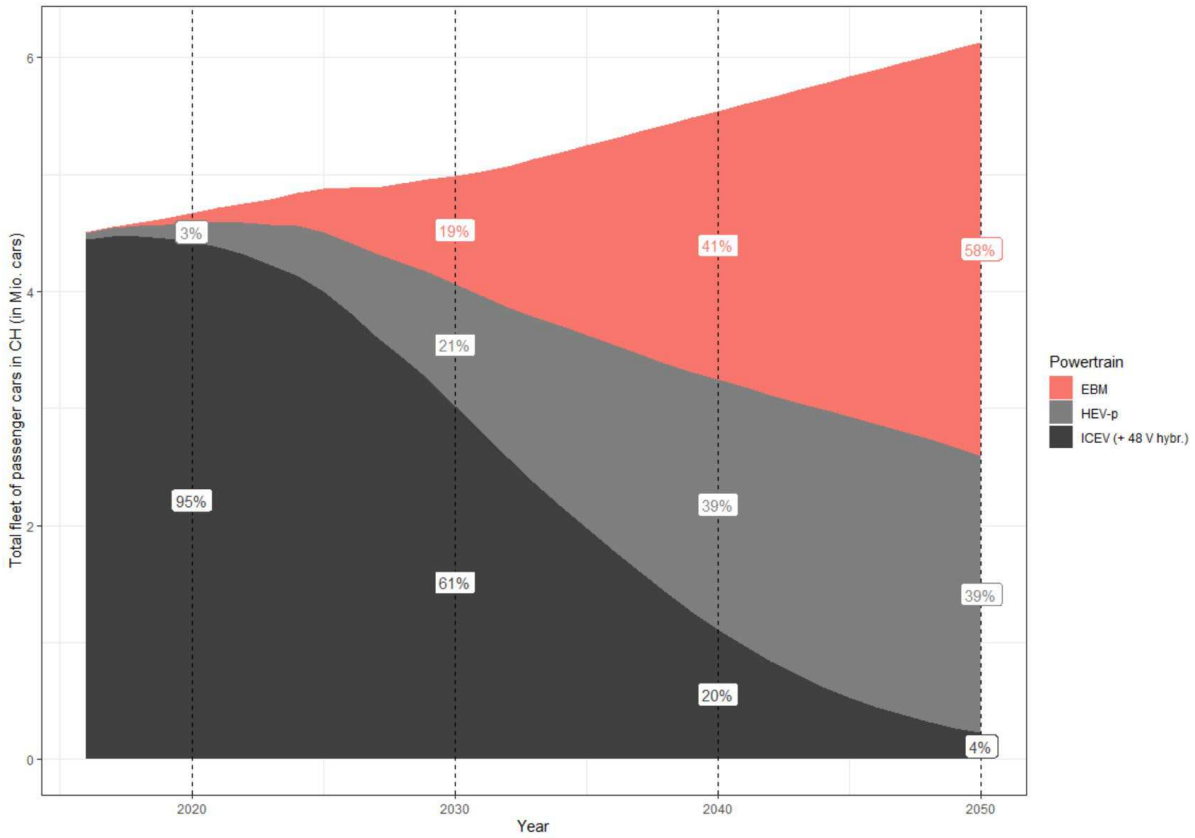

Figure 4 Evolution of the total Swiss passenger car fleet (areas) to comply with normative GHG emission targets of newly registered passenger vehicles. The penetration of powertrains (BEV, H_2-FCEV and SNG-V) is the red

area. In a benchmark scenario (non-), this red area will remain fossil fuels-based with 60% gasoline and 40% diesel ICEV for all years until 2050.

Figure 4 shows that EBM and HEVs slowly take over the entire fleet, with only a few ICEVs (all converted to 48V hybrids) still left in circulation in 2050. The overall fleet size grows to reflect the prognosis of the Swiss transportation outlook (ARE, 2016). The obtained fleet is used in all scenarios as a calculation basis for the derivation of the end-energy demand from each powertrain segment. Depending on the scenario, the EBM segment embodies BEVs, FCEVs or SNGVs.

2.3. End-energy demand of the future Swiss fleet

2.3.1. Yearly end-energy demand of the Swiss fleet

To model the future energy demand of the Swiss fleet we require two inputs:

- the specific energy consumption [kWh/vkm] at the refueling/charging stations
- the total yearly performance of the Swiss fleet (or of specific segments) [vkm]

For the former, we employ again the study of Cox and Bauer (2018), which provides tank-to-wheel (TTW) energy consumption data for all powertrains with current (2017) and future (2040) designs. For the years in between we linearly interpolate the energy consumption, while after 2040 we maintain the same values as in 2040, hence assuming that no further technological improvement occurs.

This approach is consistent with the extrapolation of future GHG emission values performed in the previous chapters. We must note that TTW energy consumption approximately represents the net energy demand at refueling stations for all powertrains but BEVs, which suffer from non-negligible charging losses. These losses are estimated to be around 15% (Cox and Bauer, 2018) and are added to the final specific energy demand of BEVs. The evolution of the specific energy demands for all EBM, each in terms of its own fuel, is provided in Figure 5.

Although these consumption values refer to new vehicles registered in a given year, we use them to compute the total energy consumption of all moving cars belonging to the same segment in that year. This choice is made because newly registered cars cover the lion's share of a fleet segment that is very quickly ramping up, which is the case of the EBM segment. Moreover, younger vehicles have larger annual mileage than older ones (Bolla et al., 2018) and this further increases the weight of newer cars in the fleet. Both factors contribute to shifting the fleet average consumption very close to the specific consumption of newly registered cars, hence endorsing the assumption here made. The resulting yearly energy demand may still be slightly underestimated, but the bias extent would be the same for all three types of EBM. Therefore, all observations and results from comparative analyses between various EBM would still hold true.

Figure 5 Present and future specific tank-to-wheel end-energy demand (TTW) of (BEV, H_2-FCEV, SNG-V) and "non-EBM" (60% gasoline and 40% diesel) at the charging / refueling station (BEV including 15% charging losses).

As for the total Swiss performance of passenger cars, we rely again on the Swiss transport outlook (ARE, 2016). We specifically start from the 2040 estimate of vkm for *Motorisierter Individualverkehr* (MIV) according to the Sprawl scenario. This worst-case scenario has been chosen since it most closely approximates the vkm performance observed in last years (the Sprawl forecast for 2020 is 58'225 Mvkm, while the performance in 2017 was already 60'743 Mvkm (BFS, 2019), hence overshooting even the worst-case scenario).

Since we are only interested in the vkm performance of Swiss cars, we subtract from the outlook the performance shares of motorbikes and foreign cars (BFS, 2019). The resulting vkm performance for Swiss passenger cars in 2040 is 57'231 Mvkm, a growth of 14% compared to 2017. As usual, between 2017 and 2040 the total annual performance is linearly interpolated, while after 2040 we apply a constant growth of 0.8% per year as observed in the last modelled decade of the Sprawl scenario (ARE, 2016). With the introduced inputs, we can derive the annual energy demand from each car segment in the fleet for every year until 2050. Among the different segments, we are particularly interested in the yearly energy demand of EBM, i.e. of BEVs, FCEVs or SNGV depending on the scenario. The evolution of energy demand from these powertrain segments is presented in Figure 6.

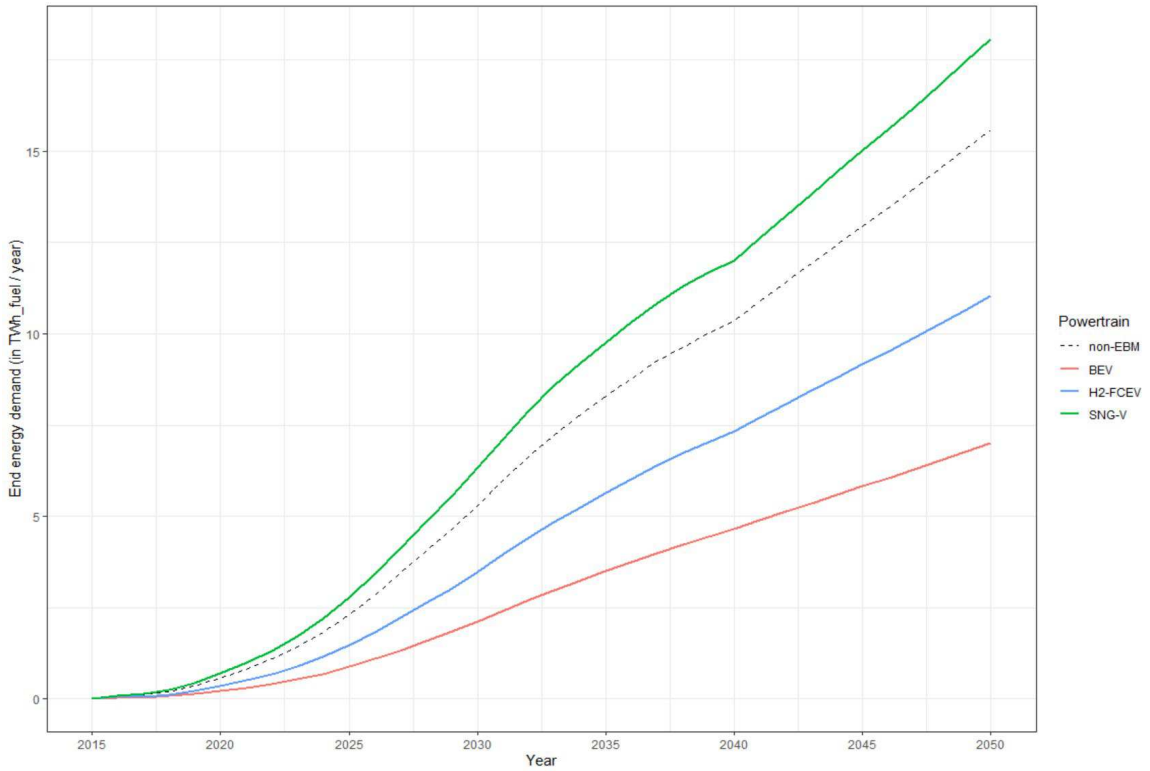

Figure 6 Evolution of the annual tank-to-wheel (TTW) end-energy demand of EBM (BEV, H_2-FCEV, SNG-V) and non-EBM (60% gasoline and 40% diesel).

The annual end-energy demand of the EBM segments grows in parallel to their diffusion in the stock of moving vehicles. The difference in magnitude between the three technologies stems from the specific powertrain efficiencies. As reference, the total final consumptions of electricity and gas in Switzerland in 2017 were 58 TWh and 33 TWh, respectively (BFE, 2017). It is also important to note that in 2050 the EBM segment covers about 58% of the stock of passenger cars.

2.3.2. Hourly end-energy demand of the Swiss fleet

In order to assess the dynamic response of the energy system to the additional energy demand triggered by passenger cars, it is valuable to disaggregate this demand to an hourly level. Specifically, we set out to build hourly-resolved yearly charging/refueling profiles for every EBM segment. In order to model daily mobility we make use of the "Mikrozensus Mobilität und Verkehr" (MZMV) (BFS, 2020b), which is a household travel survey that contains information on 1-day movements of around 60'000 sampled Swiss residents. A detailed analysis of MZMV reveals that, while weekly patterns are notably pronounced, there is no significant seasonal variation in people's mobility. We thus exclude any monthly variability in our construction and the yearly profiles are assembled by concatenating 52 identical weekly curves.

To build these weekly profiles, we firstly derive the shape of the hourly refueling/recharging patterns regardless of the absolute magnitude. Then, for every year, the scenarios we scale up the profiles so that the resulting annual energy supplied matches the yearly aggregates computed in the previous section.

However, MZMV does not provide explicit refueling patterns of the tracked vehicles and we resort to employing additional sources. Regarding FCEVs and SNGVs, we assume that their refueling patterns would approximately resemble the trends of today's ICEVs, as all these powertrains are characterized by similar ranges and comparable refueling rates. From personal communication with Migrol's representatives, we obtained data on hourly and daily frequencies of customer visits at Migrol petrol

stations. This information allows the construction of weekly and, in turn, yearly refueling profiles for both FCEVs and SNGVs.

On the other hand, the range and charging limitations of BEV do not allow for the same approach. To derive the charging profiles of BEVs we adopt the methodology described in Pareschi et al. (2020). The authors assume that the cars tracked in a household travel survey such as MZMV are BEVs and create customizable charging opportunities at the locations where the original car was stopping. The authors then check how many BEV would successfully complete multiple consecutive days of movements without running out of charge. All the charging events of the BEVs that withstand the assessment are then recorded and aggregated to form charging profiles of a generic BEV fleet. The authors validate their approach by comparing the simulated charging profiles against empirical measurements extracted from multiple EV field tests.

For the purposes of this project, we assumed that all BEVs are equipped with a 40 kWh battery (most common battery size sold in Europe in 2017 (EAFO, 2020) and that all drivers can charge their BEVs at home through the standard 230 V socket at 2.3 kW. The latter value allows the vast majority of the simulated BEVs to fully recharge the batteries during the long night stop at home. The resulting charging profiles are then aggregated by day of the week and concatenated in order to build the weekly mould used as basis for the yearly electricity demand. Figure 7 shows a week sample of the hourly-resolved end-energy demand for all EBM in 2030.

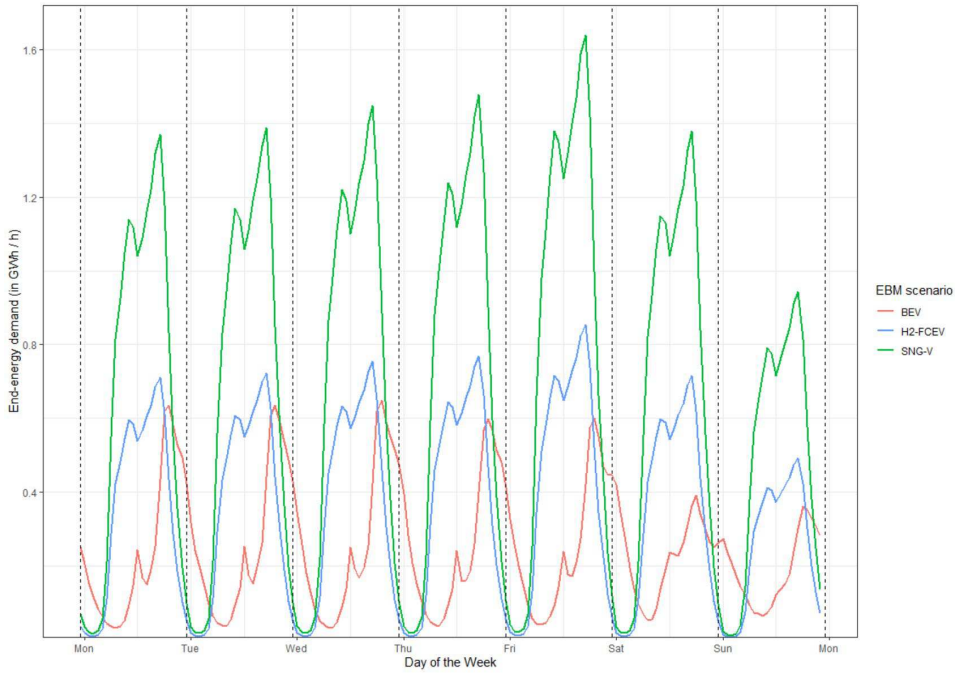

Figure 7 Hourly recharging/refueling profiles of EBM powertrains (BEV, H_2-FCEV and SNG-V) for one representative week in 2030. These weekly profiles are repeated throughout the year.

The hourly profiles of gas and hydrogen demands from SNG-Vs and H_2-FCEVs have similar shape since they derive from the same weekly mould obtained from Migrol's insights. The difference in magnitude comes from the higher powertrain efficiency of FCEVs compared to SNGVs. The demand for electricity is, however, the lowest thanks to the high efficiency of BEVs. Their charging profile shows a peak in the evenings, when BEVs come back home, followed by a slowly decreasing night demand, due to the low charging rate. The weekly trends of the three technologies are similar, with the weekend demand slightly lower than in the weekdays. As a reference, in 2017 the average electricity and gas demands in Switzerland were about 6700 MW and 3800 MW respectively.

3. Evolution of Swiss and European electricity generation mix

3.1. Introduction

In order to obtain the long-term evolution of electricity generation technologies towards a low carbon electricity system both in Switzerland and the EU, the technology-rich, bottom-up, least-cost optimization model EUSTEM (European Swiss TIMES electricity model) is used. To this end, we identify national portfolios consisting of existing and future power generation technologies, and assess the impacts of policies aimed to achieve a low-carbon electricity system. Potential pathways for decarbonization of the electricity sector are assessed in accordance with national energy policies (e.g. phase-out of nuclear and coal power plants), renewable energy targets, and trends of development of future power generation and transmission systems.

3.2. EUSTEM

EUSTEM is a multi-regional electricity model of Europe. The model is developed using the TIMES modelling framework – a least-cost optimization framework, i.e. EUSTEM identifies the least-cost combination of power plants and electricity generation mixes to satisfy exogenously given electricity demands within a policy setting. The policy settings are exogenous scenarios describing constraints on regional electricity systems such as renewable energy targets, restrictions on mining, GHG emissions, international electricity trade limits, taxes, etc. The model has a long model horizon with high intra-annual details at daily, seasonal, and weekly levels to account for variations in electricity supply and demand at an hourly time resolution. This high temporal resolution combines capacity expansion and ad-hoc dispatch in a single framework. For reliable projection of operation and investments, the electricity system (that includes electricity generation technologies, and power transmission and distribution grids) within a country is described with high technical details, including characteristics such as investment costs, operational and maintenance costs, fuel resource costs and availability, energy conversion efficiencies, technology availabilities, etc. For more details, refer to Pattupara (2016).

EUSTEM has 11 regions encompassing 20 of the 28 EU member states (plus Switzerland and Norway) as shown in Figure 8. It covers more than 95% of the total installed capacity and 94% of the total electricity generation of EU-28. Each of the regions are connected through aggregated interconnectors, which enable electricity trade between regions based on long run marginal cost of electricity supply. The model is calibrated by using the 2015 electricity statistics from ENTSO-E, Eurostat, and other national archives and includes detailed technical and operational description of existing power plants aggregated by plant type and fuel mix; and a wide range of new and emerging electricity generation technologies. For each of the regions, renewable energy resource potentials, CCS potentials, and region specific generation technologies are implemented.

Figure 8 Geographical coverage and regional aggregation in EUSTEM

The model has a time horizon until 2050 with 8 unequal intermediate time steps at 2015, 2020, 2025, 2030, 2035, 2040 and 2050. The time steps in near future are shorter in order to describe the impacts of policy and technology development on the transition in higher details. Each year in the model is divided into 288 chronological time slices, three representative days in four seasons. This facilitates description of intra-annual variability and processes within a year in each region.

3.2.1. Electricity demand

For the hourly and annual electricity demand profile, the 2015 electricity demand (BFE, 2015) is adopted for all years in EUSTEM until 2050 in CH and other EU regions. Electricity demand projections for Switzerland (CH) are based on the "Business-As-Usual" (BAU) scenario of the Swiss Energy Strategy 2050 (SES2050) (Prognos, 2012) and adjusted to reflect recent trends in the electricity demand. For example, actual demand in 2015 and 2017 were 58.3 TWh and 58.6 TWh, respectively, whereas projections in the SES2050 were 60.6 TWh and 61.4 TWh in 2015 and 2020. Thus, the future projection of SES2050 must be linearly adjusted to reflect the near-term trend. Demand projections for other regions in EUSTEM are derived from the EU Reference Scenarios 2016 (Capros et al., 2016).

For the BEV scenario, the electricity demand (i.e. charging profile) from the previous chapter 2 is added to the electricity demand of CH. It is important to note that BEV are only added additionally in CH, in the EU the regular penetration of electro-mobility as stipulated by the above mentioned sources is assumed. Figure 9 shows these electricity demand projections for CH and the EU: The upper figure shows the CH electricity demand with and without BEV, while the lower figures show the total EU electricity demand including electricity for road transportation.

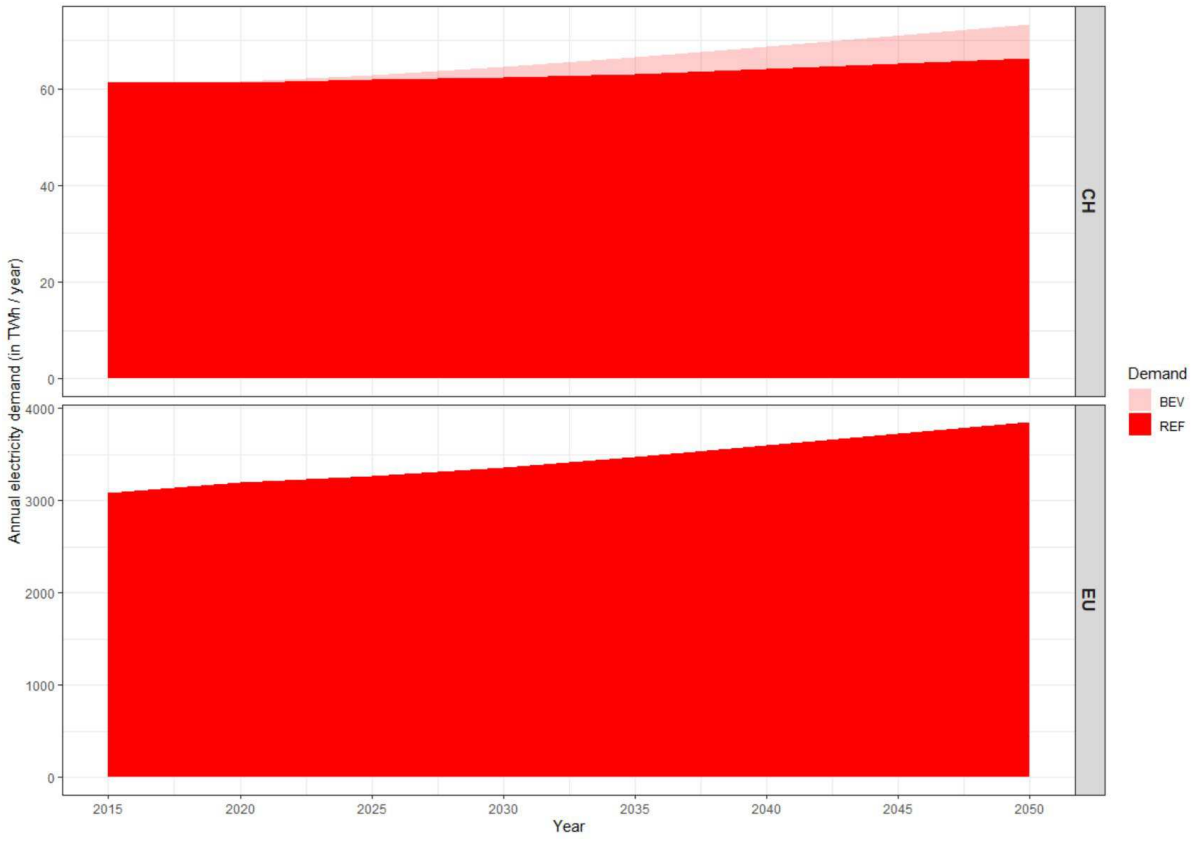

Figure 9 Annual electricity demand from 2015 to 2050 in the EU (lower subplot) based on Reference Scenarios 2016 (Capros et al., 2016)] and CH (upper subplot) based on scenario "BAU" of SES2050 (Prognos, 2012) with and without the additional annual electricity demand of BEV (only for CH).

3.2.2. Electricity Supply

The trajectories of transformation of the electricity supply system in a region are largely influenced by its renewable resources potentials and the local policies that influence the development or phase-out of generation technologies. The main sources of the information on resource potentials are the NREAP (National renewable energy action plans and progress reports data portal), ENTSO-E's TYNDP (Ten-Year Network Development Plan) and technology roadmaps from IEA as well as studies conducted by European Commission's JRC. The data obtained from the aforementioned sources are complemented by several other region- or technology-specific studies and data sources (Pattupara, 2016).

The phase-out of nuclear power plants (NPP) is scheduled to follow the current trajectories in Germany and Switzerland, with a complete phase out by 2023 and 2034 respectively. In France, the targeted 50% reduction in electricity produced by NPP is assumed to be achieved by 2035. For the Eastern European region, the installed capacity of NPP is assumed to increase up to 20 GW in 2050, which includes a capacity of 0.9 GW that is under construction in present day, and additional planned capacities of 14.2 GW. To this end, each NPP is successively removed from the overall NPP supply at its planned phase-out year. In order to have a continuous NPP production in EUSTEM for the years between the modelled years (2020, 2025, 2030, etc.) a linear phase-out transition is implemented.

3.2.3. Electricity Storage

Rapid growth in intermittent renewable generation technologies necessitates deployment of electricity storage technologies to exploit their full potential. Apart from pumped hydro storage (PHS), three additional storage technologies – lithium-ion batteries, lead-acid batteries, and advanced adiabatic Compressed Air Energy Storage (CAES) – are implemented in EUSTEM. There is no restriction on deployment of these storage technologies in EUSTEM.

3.2.4. Cross-border transmission interconnections

EUSTEM is capable of endogenously investing in transmission interconnections between the regions and distribution grids within each region. In this study, the maximum allowable investments in cross-border interconnections are limited by the Net Transfer Capacity (NTC) development projections for 2020 and 2030 by ENTSO-E.

3.2.5. Decarbonization scenarios

EUSTEM has two decarbonization approaches: a reference (“Ref”) and a low-carbon (“LC”) one:

- In **“Ref”**, electricity demand for Switzerland is adopted from SES2050; and for the EU regions, the 2016 reference demand is used (see Fig. 6). A set of existing EU policies are included, too. For example, the binding target of the EU's 2020 climate and energy package are applied, which include the planned reduction of GHG emissions from the energy sector by 20% until 2020 compared to 1990 levels. The GHG emission levels are then assumed to stay constant post-2020.
- In **“LC”**, the EU total GHG emissions are reduced by 80% until 2050 compared to the 1990 levels. This ambitious target is translated to a reduction in GHG emissions from the electricity sector of -31.5% by 2020 (Ref, LC), -60% by 2030 (LC), and -95% by 2050 (LC) of the 1990 levels. In addition to a larger expansion of renewable electricity technologies also carbon capture and storage (CCS) with fossil power plants (e.g. gas and coal) is implemented.

3.3. Evolution of CH and EU electricity system

3.3.1. Generation mix

3.3.1.1. Annual supply

Figure 10 shows the evolution of the CH- and EU-wide electricity generation mix (including imports) from 2015 to 2050 with and without BEV for the two decarbonization scenarios “Ref” and “LC”. Also shown are corresponding electricity demands subdivided by the total demand (including the additional demand of BEV and the base demand), as well as the demand of storage (pump-hydro storage HYD_PUMP and stationary batteries STG_BAT) and exports.

At this absolute scale, a difference between the generation mix with and without BEV cannot be seen easily for both CH and EU as the additional electricity demand of BEV, even in 2050, accounts for less than 5% of the total CH electricity demand, while also the CH electricity demand is less than 1% of the total EU electricity demand.

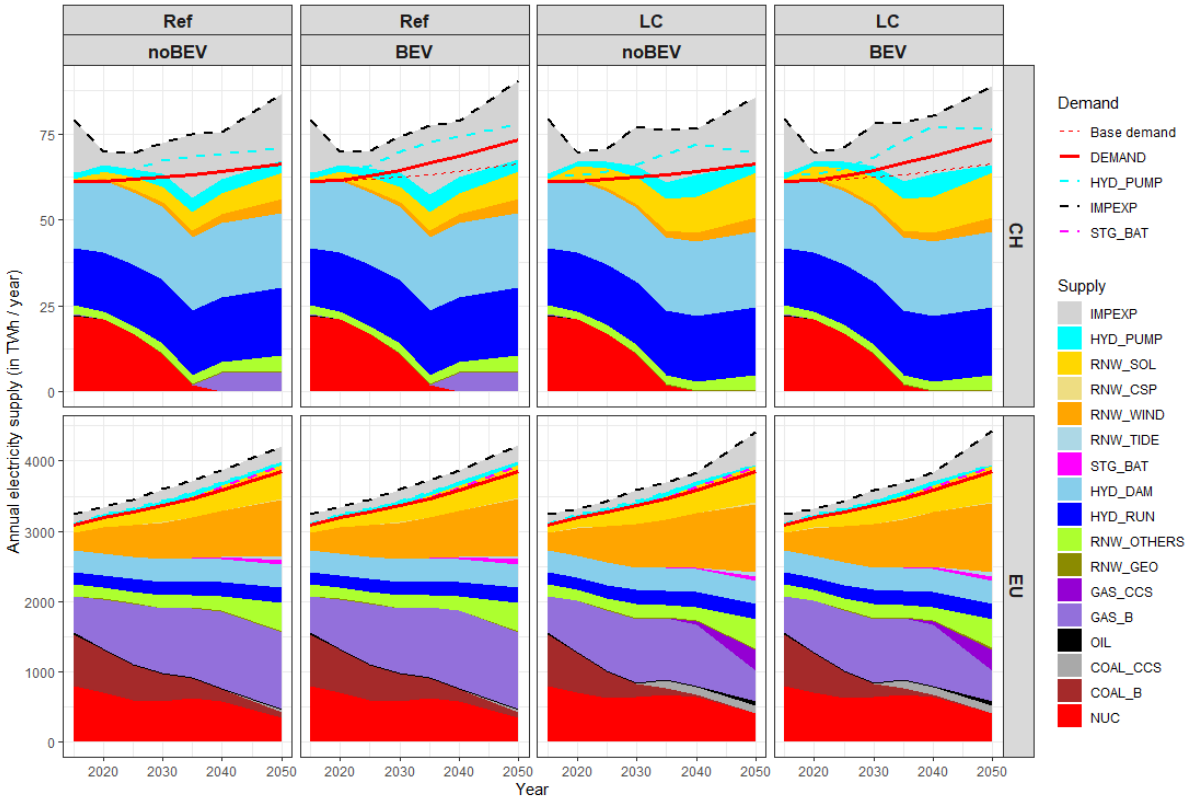

Figure 10 Evolution of the technology mix in CH and EU with and without BEV for decarbonization "Ref" and "LC".

However, in Figure 10 differences in the technology mix between the two decarbonization scenarios "Ref" and "LC" can be seen. These differences are also shown in Figure 11 in detail**.** A main characteristic of "Ref" in CH is that electricity from newly built combined-cycle gas turbine (CCGT) power plants (GAS_B) is introduced as of 2035, when nuclear power (NUC) is phased out, while in "LC", more PV (RNW_SOL) is installed. In the EU, the main difference between "Ref" and "LC" is that in "LC", gas and coal power plants are equipped with Carbon Capture and Storage (CCS) and more wind (RNW_WIND) is installed. The additional installation of other renewables (incl. PV), in turn, is less pronounced.

In terms of demands (lines in Figure 10), especially in 2030 for CH, in "LC" a much larger amount of electricity is exported (IMPEXP) than in "Ref", this is due to the additional PV supply of +3.3 TWh compared to "Ref", which produces large amounts of (surplus) electricity at noon that can only be exported, as domestic demand at that time of the day is lower than supply (see Figure 13).

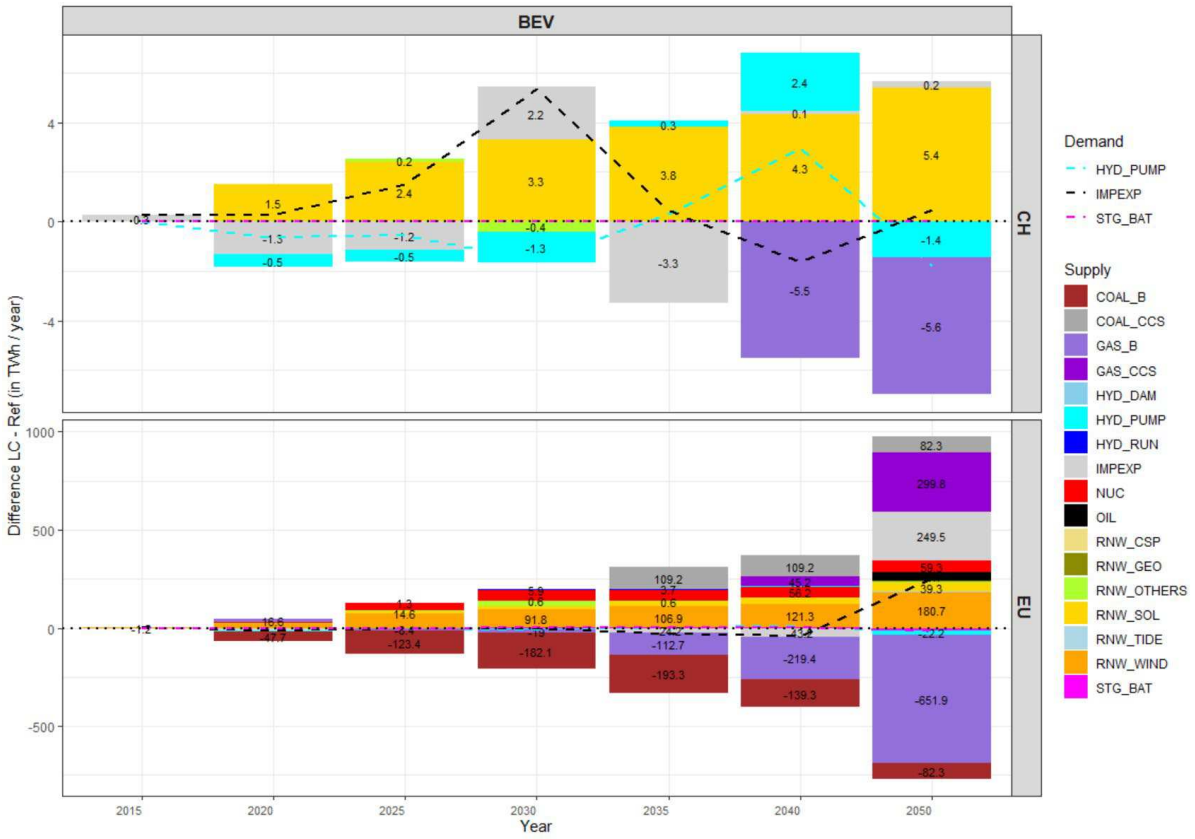

Figure 11 Difference in the supply and demand in CH and EU between “LC” vs. “Ref” with BEV.

A representation of the differences in the mix of electricity generation and demands with and without BEV based on Figure 10 is displayed in Figure 12. According to Figure 12, the additional electricity needed for BEV in CH is mainly imported (grey IMPEXP bar), while exports are simultaneously reduced (black dashed IMPEXP line). In turn, the domestic CH electricity generation only increases slightly in “Ref”, with an additional 0.2 TWh of PV supply to cover the additional electricity demand of BEV of up to 7 TWh in 2050. In LC”, due to readily available low-carbon imports from the EU, no additional domestic electricity is generated in CH for BEV at all in all years. However, pumped-hydro storage (HYD_PUMP) is used more prominently (see section 3.2.3). The additional imported electricity from the EU in “Ref” is - based on the least cost optimization of EUSTEM - mainly supplied by an increased GAS_B (+2.3 TWh until 2040) and OIL (+2.4 TWh in 2050) supply. In the “LC” scenario, an increased RNW_WIND (+3.9 TWh in 2050) supply is deployed along with GAS_B (including CCS) in order to meet the additional electricity demand of BEV in CH.

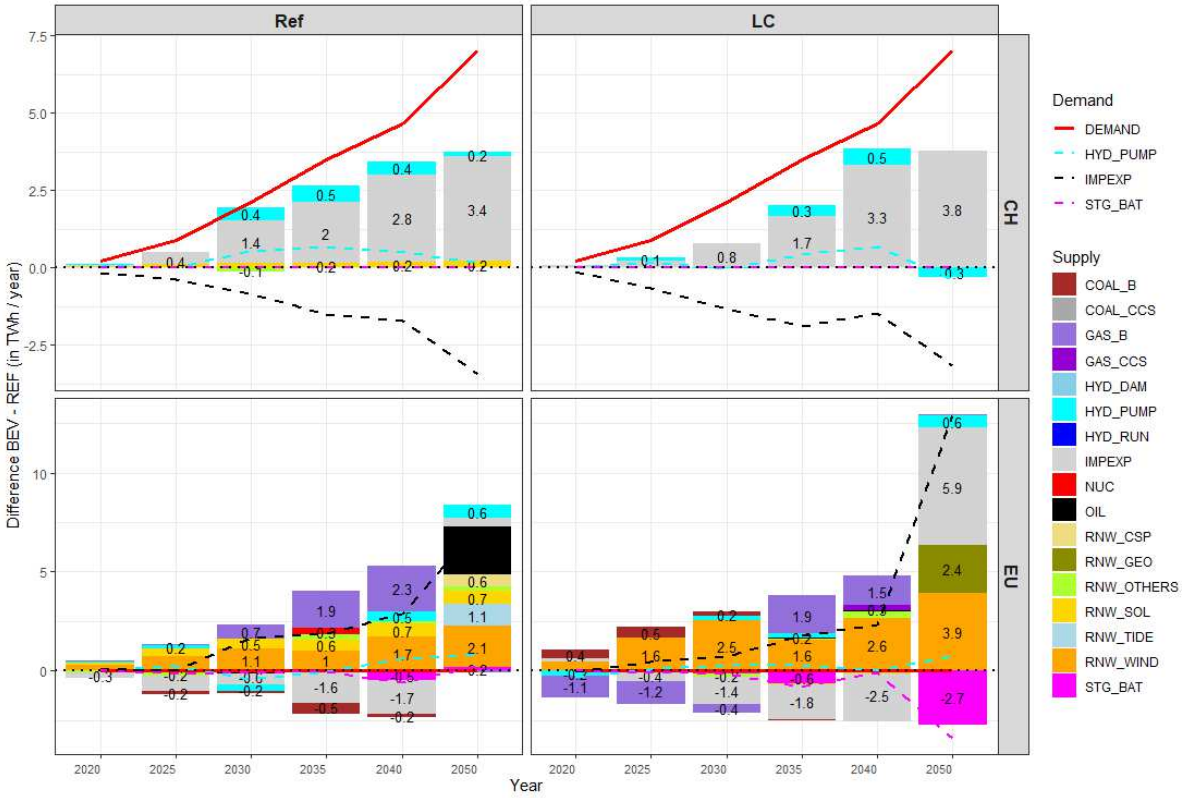

Figure 12 Difference in the supply and demand in CH and EU between scenarios “BEV” and “noBEV” in the “LC” and “Ref” decarbonization scenario.

3.3.1.2. Hourly supply

Figure 13 and Figure 14 shows the hourly demand and supply profiles of a typical (average) day of scenario “LC” in 2050 divided by seasons and weekdays for CH and EU, respectively. For CH, on weekends, abundant PV electricity at noon is pumped by means of PHS and shifted to the evening hours, when it is most exported and needed to cover the additional BEV demand. On weekdays, PHS turbination occurs only in winter mainly in the evening, while PHS pumping only occurs in summer at noon.

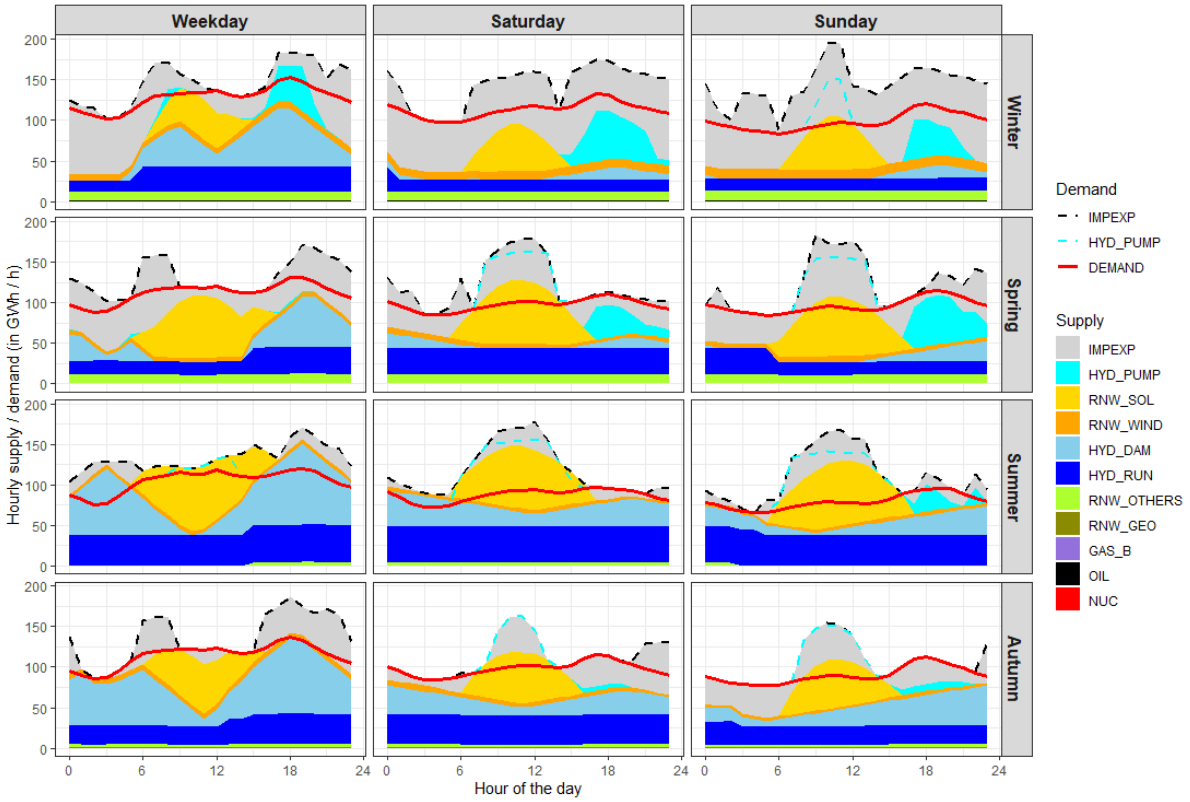

Figure 13 Typical days of 2050 in CH for scenario “LC” with BEV.

Similar trends can be observed in Figure 14 for the EU hourly supply and demand profiles. Regarding wind supply (RNW_WIND), this mainly occurs in winter (at night), while PV supply is complementary large in summer (at noon). Again, PHS (HYD_PUMP) and stationary batteries (STG_BAT) are used to shift abundant PV supply from noon to the largest demand hours in the evening.

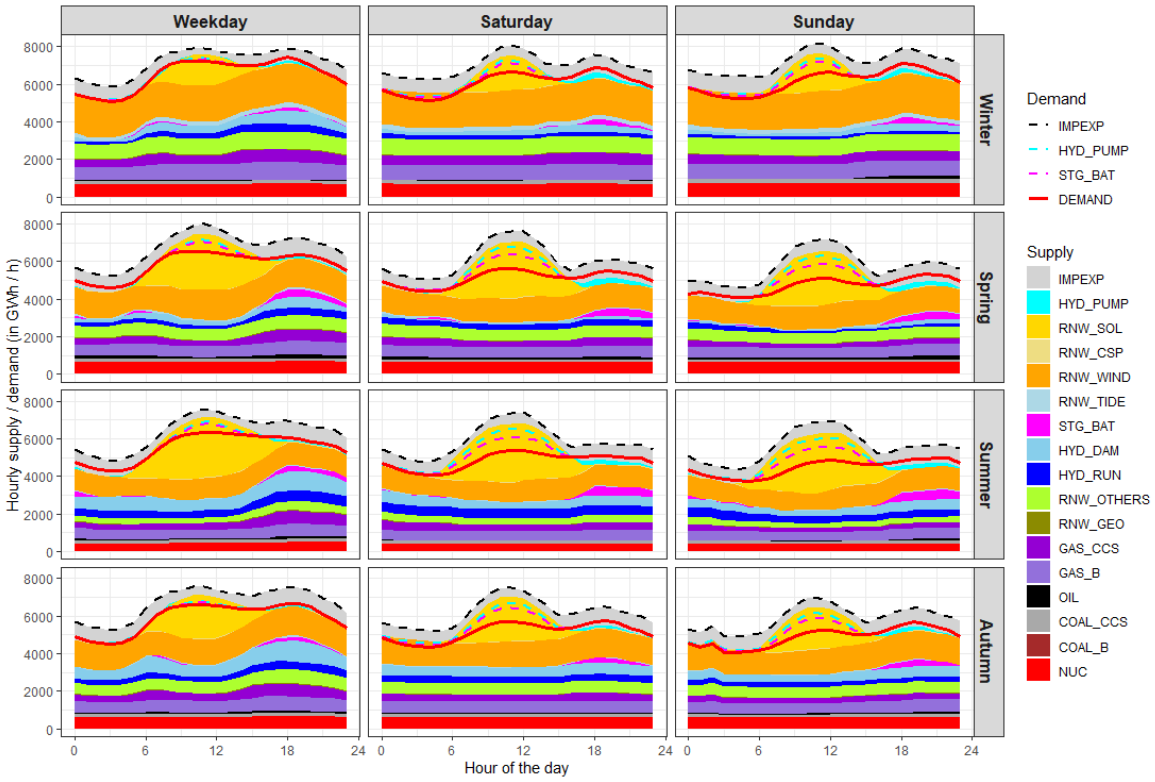

Figure 14 Typical days of 2050 in the EU for scenario “LC” with BEV.

3.3.2. Use of electricity storage

The use of pumped-hydro storage (PHS) in the “Ref” and “LC” scenarios is shown in Figure 15 with and without BEV divided by seasons. Generally, electricity (water) is pumped up in summer and autumn, while it is re-generated in winter and spring. This implies seasonal storage by PHS. No seasonal difference can be seen between "BEV" and "noBEV". However, there are differences between “LC” and “Ref”. In “LC”, PHS is used more to store renewable electricity, while in “Ref” it is less used due to more base load electricity from “GAS_B”. For both “LC” and “Ref”, a substantial reduction in the use of the PHS from 2040 to 2050 is observed (especially for “LC” with less pumping in summer and less turbinating in winter), while it is gradually increasing for the years before.

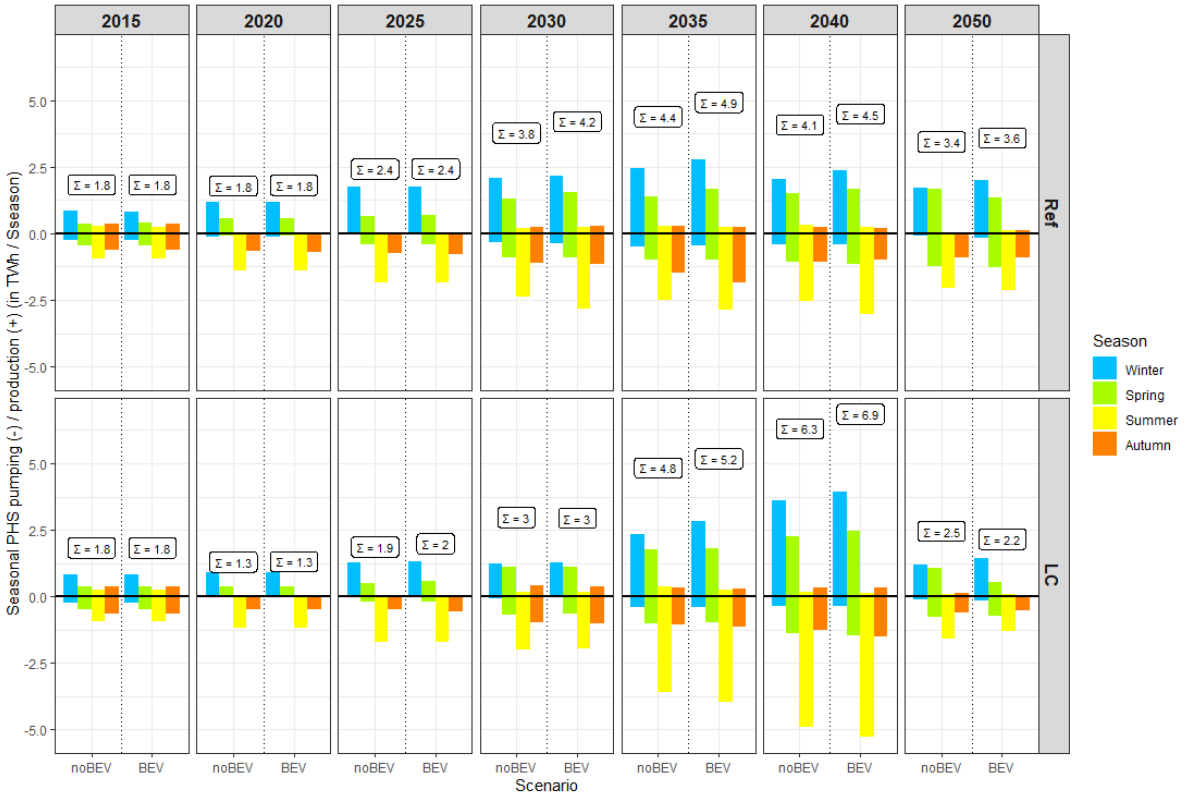

Figure 15 Use of pumped-hydro storage (PHS) in CH for “BEV” and “noBEV” for the reference (“Ref”) and low-carbon (“LC”) decarbonization scenario.

3.3.3. Imports and exports

Figure 16 shows the imported and exported electricity of CH with and without BEV for the two scenarios “LC” and “Ref”. For both “LC” and “Ref”, the amount of net imported electricity increases with "BEV" compared to "noBEV". With BEV, a substantial larger amount of electricity is imported, while less is exported, irrespective of the decarbonization scenario.

Figure 16 Seasonal imports and exports of CH for “BEV” and “noBEV” for the reference (“Ref”) and low-carbon (“LC”) decarbonization scenario.

GHG content of imported and domestic electricity supply

3.3.4. Hourly GHG content of imported electricity

The hourly GHG intensity of imported electricity is displayed in Figure 17 for a typical day in each season and all years as well as both scenarios “Ref” and “LC”. Additionally also the annual mean (horizontal line including label) is shown. A distinction between weekends and weekdays is not made. In this respect, the GHG intensity of imported electricity is just the GHG content of the produced electricity in the EU according to the GHG intensity of each technology in section 3.3.1 and the overall supply from above. Due to the higher share of renewables (mostly wind and PV as well as CCS) in “LC”, the GHG intensity is lower than in “Ref”. The gap between “LC” and “Ref” increases with the years as more renewables and CCS are installed. Generally, the GHG intensity drops at noon due to a large share of PV, this is even more pronounced in “Ref”, while “LC” also features a large share of wind, which typically produces low-carbon electricity in winter at night. This way, the annual average in the GHG intensity of imported electricity in CH decreases from 319 g CO_2-eq/kWh in 2015 to 133 g CO_2-eq/kWh in “Ref” and 73 g CO_2-eq/kWh in “LC” in 2050. Maximum and minimum hourly values in 2050 range from 49 g CO_2-eq/kWh at noon in summer in “LC” to 161 g CO_2-eq/kWh at night in spring in “Ref”. On the EU level, the influence of additional BEV demand in CH is negligible.

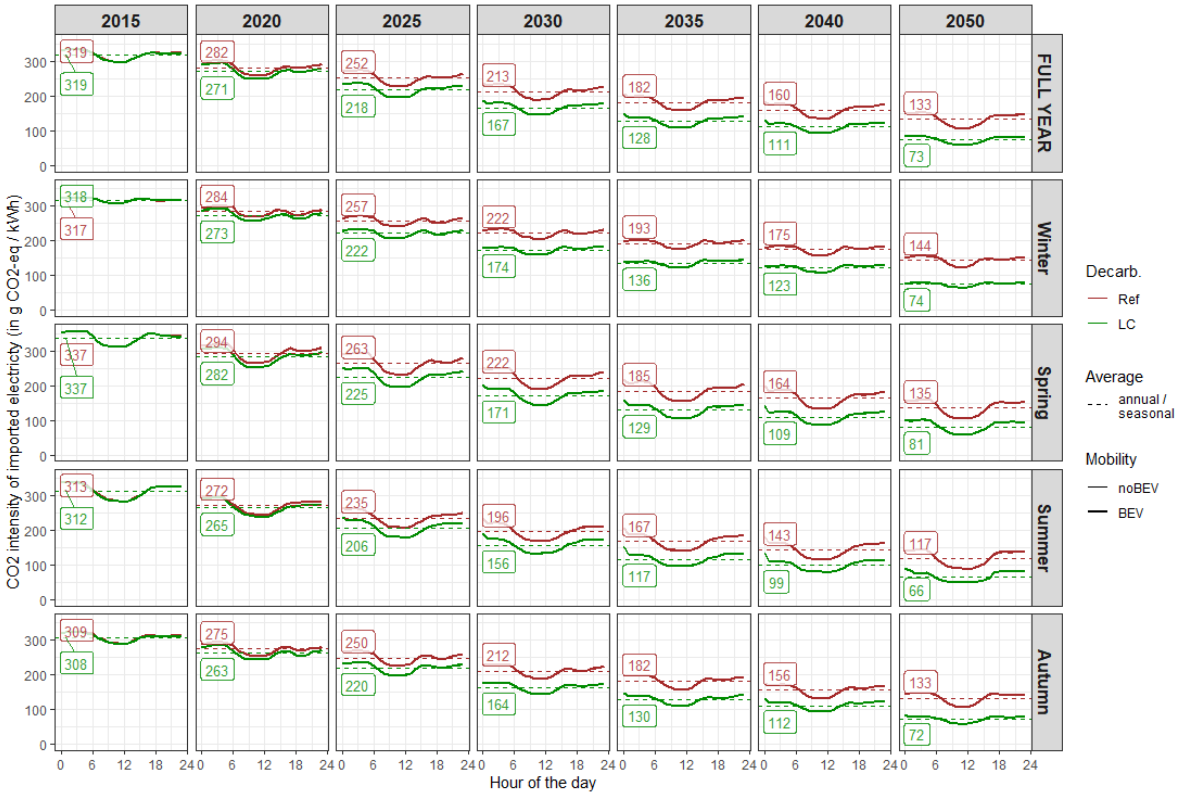

Figure 17 Hourly CO_2 intensity of EU electricity (imports) for both decarbonization scenarios “LC” and “Ref”.

3.3.5. Hourly GHG content of CH electricity supply

A corresponding hourly representation of the GHG intensity of domestically produced electricity in CH is shown in Figure 18. The increase in the GHG intensity at noon is mainly due to increased PV supply, which has a higher GHG intensity (see section 4.2) than hydro (and until 2035 nuclear), which are the major domestic electricity suppliers in all other hours of the day. Due to their low GHG intensity, the annual average of the domestic electricity supply remains constantly low between 12 g CO_2-eq/kWh and 15 g CO_2-eq/kWh for all years in “LC” and until 2035 in “Ref” (shut-off year of the last Swiss nuclear power plant). In 2040 and 2050 in “Ref”, in particular in winter and spring, the influence of additionally deployed domestic CCGT power plants (GAS_B) increases the hourly (and annual) GHG intensity (mainly at night). The hourly influence of BEV demand can mainly be seen in the “Ref” case in 2040 and 2050 (thin vs. thick lines), when they are charged in the evening and more electricity that is domestic is produced from CCGT power plants. In all other years, the influence of the additional BEV demand is negligible. Moreover, as the additional electricity demand of BEV is mostly covered by imports, their effective influence on the GHG intensity of electricity must include both domestically produced and imported electricity (from the previous section).

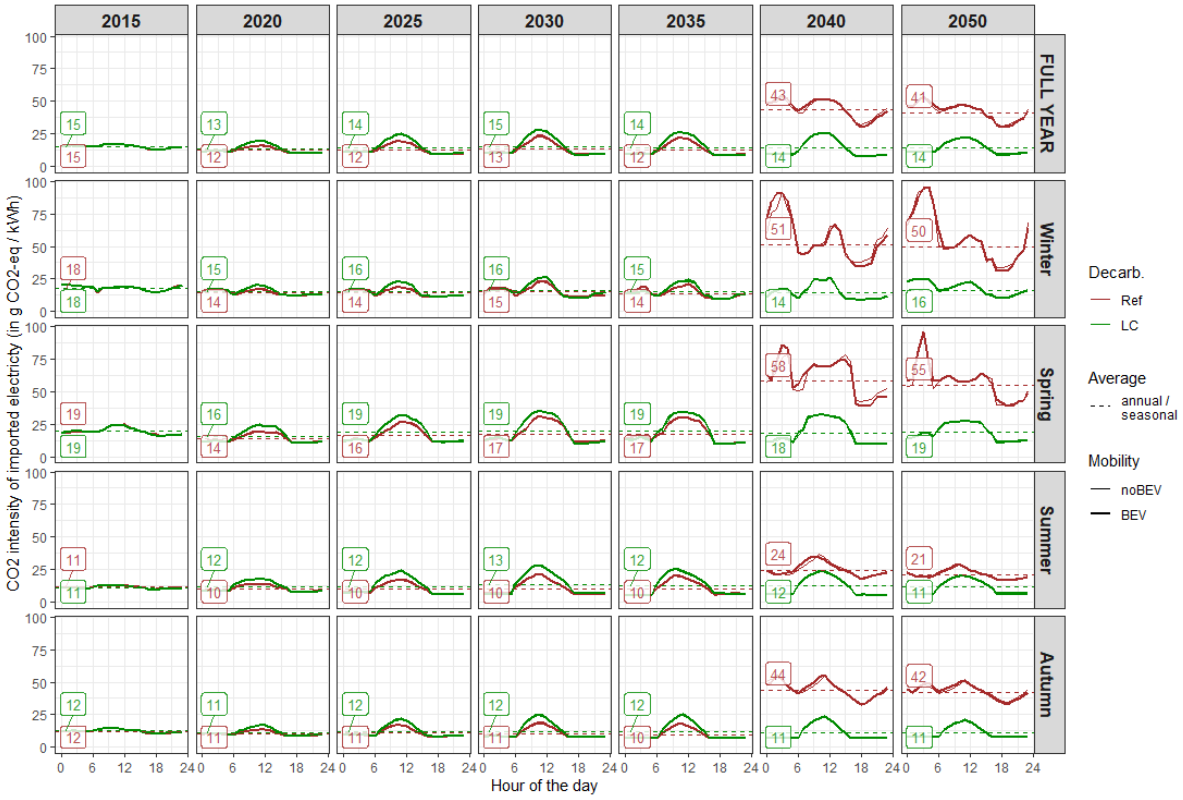

Figure 18 Hourly CO_2 intensity of CH electricity production (only CH) for both decarbonization scenarios “LC” and “Ref”.

4. Life Cycle Assessment (LCA): electricity, fuels and vehicles

4.1. Introduction

While the environmental performance of conventional gasoline, diesel and natural gas vehicles in terms of GHG emissions is mainly determined by the amount of exhaust CO_2 emissions, these are zero for battery electric vehicles (BEV) and fuel cell electric vehicles (H2-FCEV). However, their production and fuel supply chains can cause substantial amounts of GHG emissions (Cox et al., 2020; Knobloch et al., 2020) . In case of gas vehicles fueled with synthetic natural gas (SNG-V), exhaust CO_2 emissions are (almost) the same as for conventional natural gas vehicles, but depending on the source of CO_2 used for SNG production (methanation), these emissions are (partially) compensated by either extraction of CO_2 from the atmosphere, or reduction of CO_2 emissions of (industrial) point sources (Müller et al., 2020; Zhang et al., 2020, 2017). A fair comparison of different powertrain and fuels must therefore rely on Life Cycle Assessment (LCA) taking into account the entire life cycle of vehicles (including production, use, and end-of-life) with associated material and energy supply chains.

For all three EBM powertrains considered in this study, the GHG intensity of electricity in the power grid at the time when the power for mobility purposes (either for battery charging, or for electrolysis) is supplied by the grid is one of the determining factors concerning the GHG emissions per driven km of each vehicle technology. Additionally, GHG emissions tied to conventional and electricity based vehicle technologies and associated processes such as vehicle production, fuel supply, and infrastructure requirements need to be determined at the LCA level as well.

In this chapter, LCA based specific GHG emissions of different fuel supply and vehicle technologies are provided. In this respect, fuel supply does not only concern electricity produced in Switzerland and abroad, but also conventional natural gas, gasoline and diesel, H2 and SNG. These GHG emission factors are based on previous analysis (Bauer et al., 2017; Cox et al., 2020; Zhang et al., 2017), performed by some of the authors of this report as well as the ecoinvent LCA database[2] (Wernet et al., 2016), as detailed in the subsequent sections.

GHG emissions are the only environmental aspect analyzed in this study. However, it must be emphasized that GHG emissions are not the only concern from the environmental perspective in the mobility context: local and regional air pollution with associated impacts on human health and ecosystem quality, resource demand, noise and other aspects would need to be considered in a more comprehensive assessment (Hirschberg et al., 2016; Infras, 2020; Ricardo, 2020). Quantifying such impacts, however, partially requires methods beyond traditional LCA and is out of scope of this analysis.

4.2. Electricity

Impacts on climate change are represented by overall (systemic) GHG emissions. GHG intensities of electricity supply are provided in units of kg of GHG equivalents (CO2-eq) per kWh of electricity produced at the power plants from a life-cycle perspective taking into account production, use and disposal of the power plants. However, transmission and distribution of electricity is not taken into account. System aspects such as potentially required back-up technologies are also not considered, since these depend on the actual layout and composition of the electricity supply system.

GHG emissions are quantified using global warming potentials for a time horizon of 100 years according to IPCC (2013). For the years 2015 and 2020, if not stated otherwise, GHG intensities are estimated based on the LCA database ecoinvent. The system model "allocation, cut-off by classification" is used.

[2] www.ecoinvent.org

In this system model, recommended for attributional LCA, environmental burdens related to recycling processes are allocated to the user of the secondary materials and scrap materials are free of environmental burdens. For 2025 to 2050 extrapolations considering expected future technology development according to Bauer et al. (2017) are performed.

4.2.1. Domestic supply

The specific GHG emissions (intensities) of electricity produced by power plants in Switzerland and assumptions made for their derivation are listed in Table 2.

Table 2 Specific GHG emissions (intensities) from 2015 to 2050 of electricity produced by power plants in Switzerland. The full transition from 2015 to 2050 can be seen in Figure 19.

Technology (EUSTEM terminology)	**GHG intensity (2015 - 2050) (in g CO2-eq/kWh)**	**Comments / assumptions**
Gas (baseload) (GAS_B)	423 - 360	not available in Switzerland, therefore Combined cycle gas turbine (CCGT) power plants from Germany are taken as an approximation
Pumped-hydro storage (PHS) (HYD_PUMP)	6 (only infrastructure related emissions)	GHG intensity of PHS depends on the GHG intensity of the electricity used for pumping; the fixed part of GHG emissions is equal to those of dam hydro power plants (i.e. 6 g CO2-eq/kWh)
Dam Hydro (HYD_DAM)	6	reservoir in alpine region; assumed to stay constant over time
Run of River (HYD_RUN)	3	assumed to stay constant over time
Nuclear (NUC)	10	pressure water reactor; assumed to stay constant over time
Geothermal (RNW_GEO)	26	deep geothermal; assumed to stay constant over time
Other Renewables (RNW_OTHER)	72 - 50	interpreted as woody biomass (e.g. wood chips) for combined heat and power (CHP) generation; 6667 kW; state-of-the-art 2014
Waste (RNW_WASTE)	4	from municipal waste incineration plants (MWIP) to generic market for electricity, medium voltage; assumed to stay constant over time
Solar PV (RNW_SOL)	71 - 30	3 kW_p slanted-roof installation, multi-Si, laminated, integrated
Wind (RNW_WIND)	17 - 15	1-3 MW turbine, onshore
Oil (OIL)	690 - 650	heat and power co-generation, diesel, 200 kW electrical, SCR-NOx reduction

The evolution of specific life-cycle GHG emissions (intensities) per electricity generation technology, as implemented in this analysis, are shown in Figure 19 from 2015 to 2050.

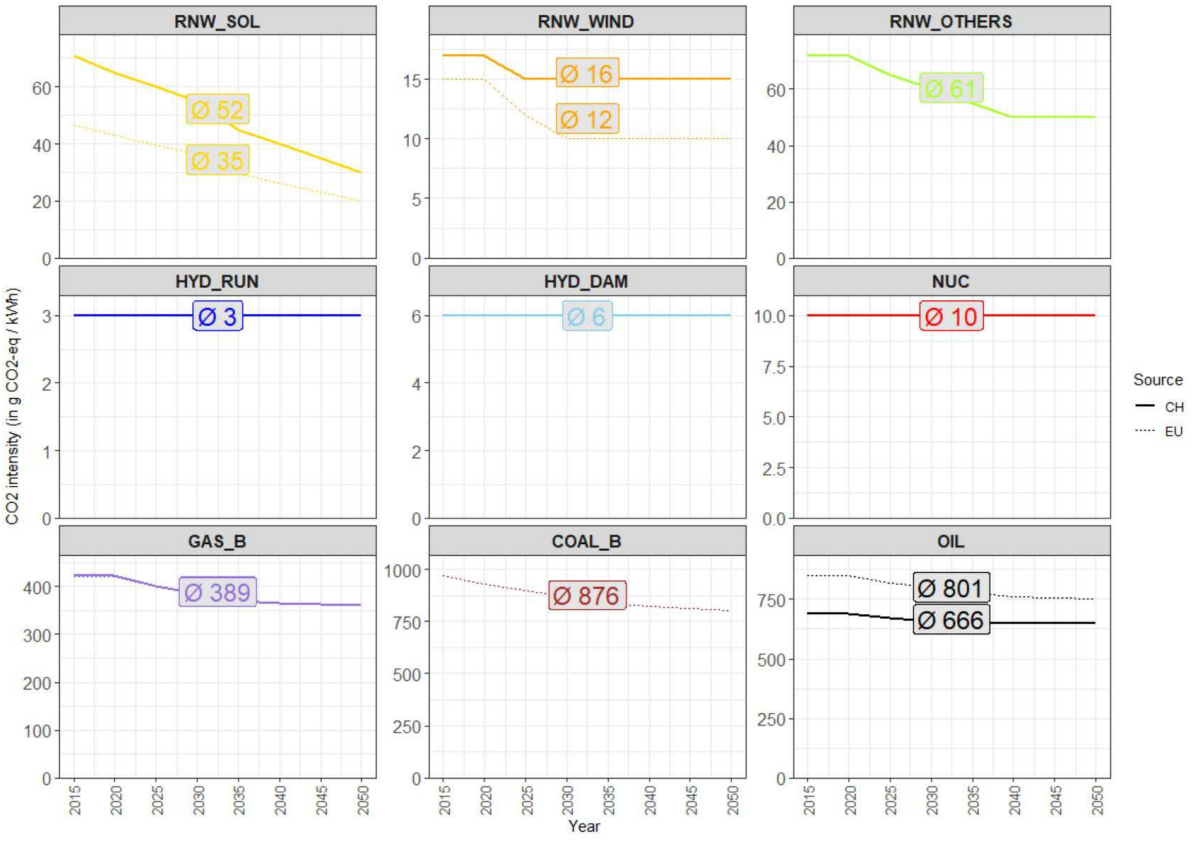

Figure 19 Specific life-cycle GHG intensities of electricity generation technologies in Switzerland from 2015 to 2050

4.2.2. Imported electricity

For electricity imported into Switzerland, the GHG content is estimated based on the specific GHG emissions per power generation technology in the EU-28 (not including Estonia, Latvia, and Lithuania). Additional technologies to those also present in Switzerland (see Table 2 and Figure 19) are shown in Table 3 along with their underlying assumptions. These additional technologies are baseload coal (lignite and hard coal), flexible gas, concentrated solar power (CSP), wave and tidal power (marine) plus gas and coal with carbon capture and storage (CCS).

For those technologies present in both Switzerland and the EU, there is only a difference in the GHG emission for wind, oil and PV: wind in the EU is mostly from off-shore turbines or from on-shore turbines at locations with higher wind speeds than in Switzerland, while in Switzerland it is exclusively from on-shore turbines; oil in Switzerland is only used for combined heat and power (CHP) generation, while in the EU it is also used in oil power plants; eventually for PV it is assumed that GHG intensities in the EU are 1/3 lower than in CH due to higher yield in southern countries.

Table 3 *Specific GHG emissions (intensities) for 2015 and 2050 of power plants in the EU-28 (not including EE, LV, LT). The full transition from 2015 to 2050 can be seen in Figure 19. Technologies with the same GHG intensity as in Switzerland can be found in Table 2 and Figure 19.*

Technology	**GHG intensity (2015 - 2050) (in g CO2-eq/kWh)**	**Comments / assumptions**
Coal Baseload	970 - 800	based on Bauer et al. (2017); coal assumed to be lignite
Hard Coal Baseload	850 - 785	-
Coal CCS	80 - 70	based on Bauer et al. (2017)
Gas CCS	100 - 80	based on Bauer et al. (2017)
Gas CHP	500 - 475	based on Bauer et al. (2017)
Gas Flexible	450 - 400	based on Bauer et al. (2017)
Solar CSP	44 - 15	solar tower power plant, 20 MW
Marine	50	Electricity from tidal and wave power plants; not available in the ecoinvent database; rough estimate from Bauer et al. (2017)
Solar PV	47 - 20	assumed to be 1/3 lower than in CH due to higher yield
Wind	15 - 10	1-3 MW turbine, offshore
Oil	850 - 750	Oil power plant in Germany; rough extrapolation for 2025 onwards

In order to estimate the hourly GHG content of imported electricity to Switzerland, it is assumed that it is equal to the GHG content of the overall electricity mix produced in the EU. In other words, there is a common market for electricity in the EU, while Switzerland can only import electricity from all EU countries simultaneously and proportionally to their overall production. This overall EU production is provided by EUSTEM (see chapter 3) at an hourly time resolution for typical (average) days with respect to seasons and weekdays for the years 2015 to 2050. Thus, the hourly GHG content is only calculated for such typical days. This means the actual daily and hourly dynamics of volatile renewables such as PV and wind are averaged out. Nonetheless, this averaged GHG content in each hour of these typical days features typical production patterns of these volatile renewables with a high production in summer at noon for PV and higher production for wind in winter (during the whole day).

In order to account for the GHG content of electricity imported to Switzerland, two scenarios are used:

1. **“LC” (EUSTEM):** In this scenario, the hourly GHG content of imported electricity is taken from the corresponding scenario in chapter 3. It is calculated based on the specific GHG intensity of all technologies in the EU supply mix of the low-carbon (LC) scenario implemented in EUSTEM. In this scenario, a substantial share of renewables as well as fossil power plants with carbon-capture-and-storage (CCS) are contained in the EU supply mix.
2. **“CCGT”:** In addition to the “LC” scenario, we exogenously establish a second scenario in which only (import) electricity from combined-cycle-gas-turbine (CCGT) power plants is available. This scenario is in line with the assumed GHG content of imported electricity in Rüdisüli et al. (2019) and can be regarded as the “best case” for fossil imports. The GHG content of “CCGT” is assumed constant throughout the year, yet will decrease from 423 g CO2-eq / kWh to 360 g CO2-eq / kWh from 2015 to 2050, respectively. Moreover, instead of importing electricity, an

alternative option would be to build new Swiss CCGT (Prognos, 2012). Thus, this “CCGT” scenario represents this variant, too.

The hourly GHG intensity of imported (“LC” or “CCGT”) and domestically produced (“CH”) electricity is displayed in Figure 20 for a typical day in each season and all years. A distinction between weekends and weekdays is not made. For domestic production, a distinction between the 13 TWh and 52 TWh PV scenarios is made. Due to the increasing share of renewables (mostly wind and PV) and CCS in the “LC” scenario, the gap between the GHG intensity of “LC” and “CCGT” import electricity increases with every year. In the “CCGT” scenario, the GHG intensity is constant throughout the year, but drops from 423 g CO2-eq / kWh in 2015 to 360 g CO2-eq / kWh in 2050. In the “LC” scenario, there is a clear seasonal and diurnal variability of the GHG intensity. Regarding the seasonal variability, GHG intensities are highest in winter and lowest in summer. Regarding the diurnal variability, in all seasons, the GHG intensity drops at noon due to increased PV supply and increases at night due to more conventional-thermal generation. This nightly increase, however, decreases with larger shares of wind generation, which typically produces low-carbon electricity at night and in winter. This way, the annual average GHG intensity of imported electricity in “LC” decreases from 319 g CO2-eq / kWh in 2015 to 73 g CO2-eq / kWh by 2050. Due to the large share of low-carbon electricity generation technologies, the average GHG intensity of the domestic (CH) supply mix is low between 12 and 21 g CO2-eq / kWh throughout all years, seasons and PV expansion scenarios. The highest diurnal GHG intensities in “CH” occur at noon due to an increased contribution of domestic PV generation with a relatively higher GHG intensity compared to nuclear and hydro (see Table 2 in supplementary materials).

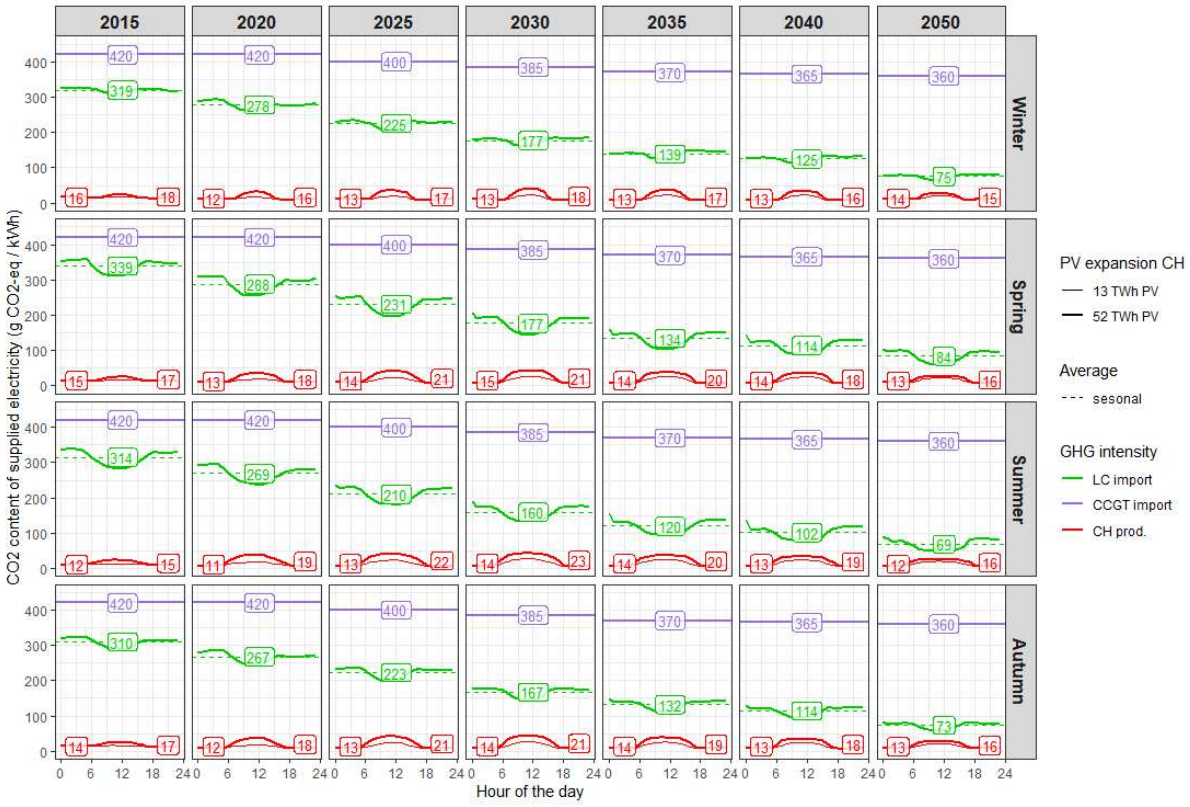

Figure 20 Hourly GHG intensity of imported (“LC” and “CCGT” scenario) as well as domestically produced (“CH”) electricity divided by seasons and years. Seasonal averages are given in labels. For “CH” production, a distinction between the two PV expansion scenarios (13 and 52 TWh PV) is made.

4.2.3. Systemic and specific GHG emissions

The impacts of EBM on GHG emissions in the energy system (including both the electricity and NG grid) is investigated both with respect to overall (systemic) GHG emissions (in Mt CO2-eq / year) and specific GHG emissions of EBM powertrains only (in g CO2-eq / km travelled). While, the overall GHG emissions are obtained by summing all direct and indirect GHG emissions in the model in Figure 27 over one year, specific GHG emissions of EBM are obtained by means of a short-term marginal electricity mix approach. This approach assigns all additional GHG emissions to meet an additional (marginal) demand to that additional consumer (e.g. BEV). In other words, it refers to the rate at which GHG emissions would change with a small change in the energy demand (Mandel and McCormick, 2016). This implies running the model twice; once with and once without that additional demand and then calculating the differences in terms of GHG emissions. Despite its intuitive and differentiated accounting of additionally consumed renewable energy, which could otherwise also be used elsewhere to reduce fossil energy (Schmidt, 2020), the notion of “additional” demand and “marginal” GHG emissions may be controversial (Pareschi et al., 2017; Schram et al., 2019), as a proper definition and ranking of “additional” energy demands (in particular if there are several such as from the mobility and heating sectors, etc) may be ambiguous.

4.3. Natural gas from the grid

The GHG content of NG from the grid highly depends on the admixture of biomethane generated from biogenic matter. In 2020, the biomethane content in the NG grid was about 20% (VSG, 2020). According to the Association of the Swiss Gas Industry (VSG), the NG grid is supposed to be "GHG neutral" by 2050 (VSG, 2020). This can be achieved by increasing the share of biomethane, using power-to-gas processes with low-carbon electricity for SNG production, and by blending H2 into the NG grid. Within this study, we conservatively assume a linear increase of biomethane in the NG grid from 20% in 2020 to 50% by 2050. This biomethane can either be produced in Switzerland, or imported.

For fossil NG, we assume a GHG intensity of 224 g CO_2-eq/kWh_gas (combusted), whereof 199 g CO_2-eq/kWh_gas directly originate from the combustion. For biomethane, the combustion is regarded as “GHG neutral” (0 g CO_2-eq/kWh_gas), however, the pre-processing of biomethane accounts for about 61 g CO_2-eq/kWh_gas (Stolz and Frischknecht, 2019). Hence, in 2020 with a biomethane share of 20%, NG from the grid has a GHG intensity of 202 g CO_2-eq/kWh_gas, which linearly decreases to 154 g CO_2-eq/kWh_gas by 2050 (see Figure 21). Alternative to an increased biomethane content in the NG grid also an increase in SNG from renewable foreign sources may be possible.

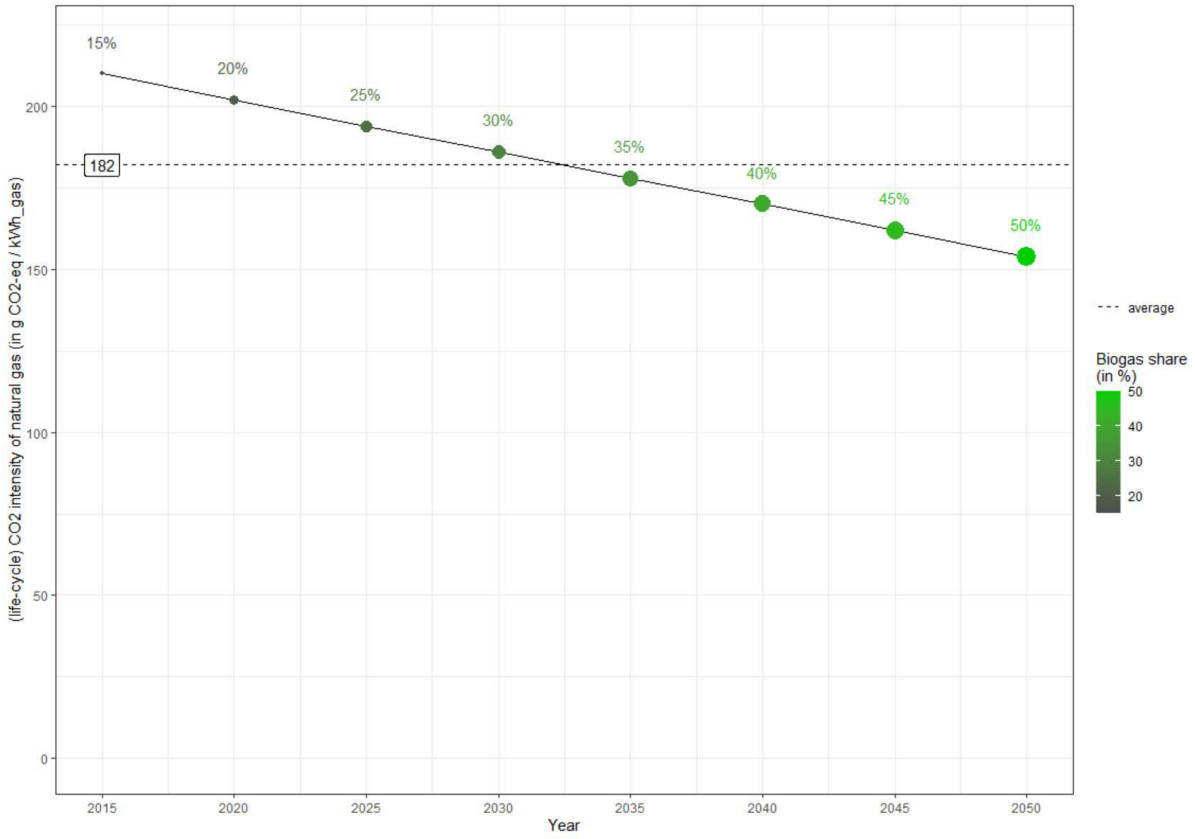

Figure 21 Life cycle GHG content of NG from the grid from 2015 to 2050 with increasing shares of biomethane from 15% in 2015 to 50% in 2050.

4.4. Conversion processes

The life-cycle assessment of H_2 generation via electrolysis is relatively simple, while it is much more complex for SNG production due many technology options and system variations. This entails various potential sources of CO_2 (direct air capture, capture from cement, fossil power or waste incineration plants or from biomethane upgrading) and different methanation processes (catalytic, microbiological) (Teske et al., 2019). In this context, multi-functionality of processes generating CO_2 to be used as feedstock for methanation needs to be considered (Müller et al., 2020; Zhang et al., 2017).

4.4.1. Hydrogen and SNG production

The associated life-cycle GHG emissions to build, operate, and discard ELYSE and METH infrastructure are included in the indirect GHG emissions of the corresponding H2-FCEV and SNG-V powertrains, as provided by the LCA study of Cox and Bauer (2018) and based on the original analysis of Zhang et al. (2017). In this analysis, METH is fed with CO_2 captured from ambient air (so-called “Direct Air Capture”, DAC). This assumption reduces complexity, as multi-functionality of processes generating CO2 feedstock do not need to be taken into account.

4.4.2. Steam Methane Reforming (SMR)

For SMR to produce H2 from NG, indirect GHG emissions of 50 g $CO_{2,eq}$/kWh_H_2 are assumed according to Antonini et al. (2020). These indirect GHG emissions of SMR are assumed to stay constant over time. In turn, for the used NG, the GHG intensity from above with increasing amounts of added biomethane are taken.

4.5. Fossil and EBM powertrains

LCA data of vehicle production are important, since different powertrain technologies will exhibit different production related GHG footprints; in this context, batteries and fuel cells for BEV and H_2-FCEV, respectively, are the most important components that deserve special attention. Different end-of-life strategies for vehicles must also be addressed, since recycling or secondary applications of e.g. batteries and fuel cells might reduce their life-cycle impacts substantially.

Direct and indirect GHG emissions associated with EBM and fossil powertrains are taken from the study on the LCA of current and future passenger cars in Switzerland of Cox and Bauer (2018), which build upon the analysis of Cox et al. (2020).

4.5.1. Conventional mobility (diesel, gasoline)

The specific LCA (direct and indirect) GHG emissions of fossil ICEV linearly decrease between 2018 and 2040 from 294 to 195 g CO2-eq/km for gasoline and from 234 to 167 g CO_2-eq/km for diesel, respectively. This reduction is due to power trains that are more efficient, light-weighting and mild hybridization. Before 2018 and after 2040, GHG emissions are, for the sake of simplicity, assumed to remain constant (see Figure 22). By assuming a constant ICEV composition of 60% gasoline and 40% diesel vehicles from 2015 until 2050 in the reference scenario (“non-EBM”) and their corresponding share in the total CH mileage in Figure 4, the total GHG emissions of this ICEV fleet (red area in Figure 4 with ICEV instead of an EBM fleet can be estimated.

4.5.2. Indirect emissions of EBM

For the novel EBM powertrains BEV, H_2-FCEV and SNG-V, only the indirect (“grey”) GHG emissions are needed, as the fuel related GHG emissions associated with their primary fuel “electricity” are calculated within the supply chain model of EBM fuels in Figure 27 (Chapter 5). These indirect GHG emissions of EBM include - amongst others - the construction of the vehicle and on-board fuel storage devices (e.g. batteries, pressurized H2 and SNG tanks, etc.) as well as other infrastructure such as ELYSE and METH plants. For more information on these indirect GHG emissions of EBM, refer to Cox et al. (2018; 2020) and Zhang et al. (Zhang et al., 2017). The evolution of these indirect GHG emissions of powertrains from 2015 to 2050 is displayed in Figure 22). Again, a stagnation of the GHG emissions after 2040 is assumed in order to be in line with the anticipated S-shaped curve of technology improvements (see section 2.3.1).

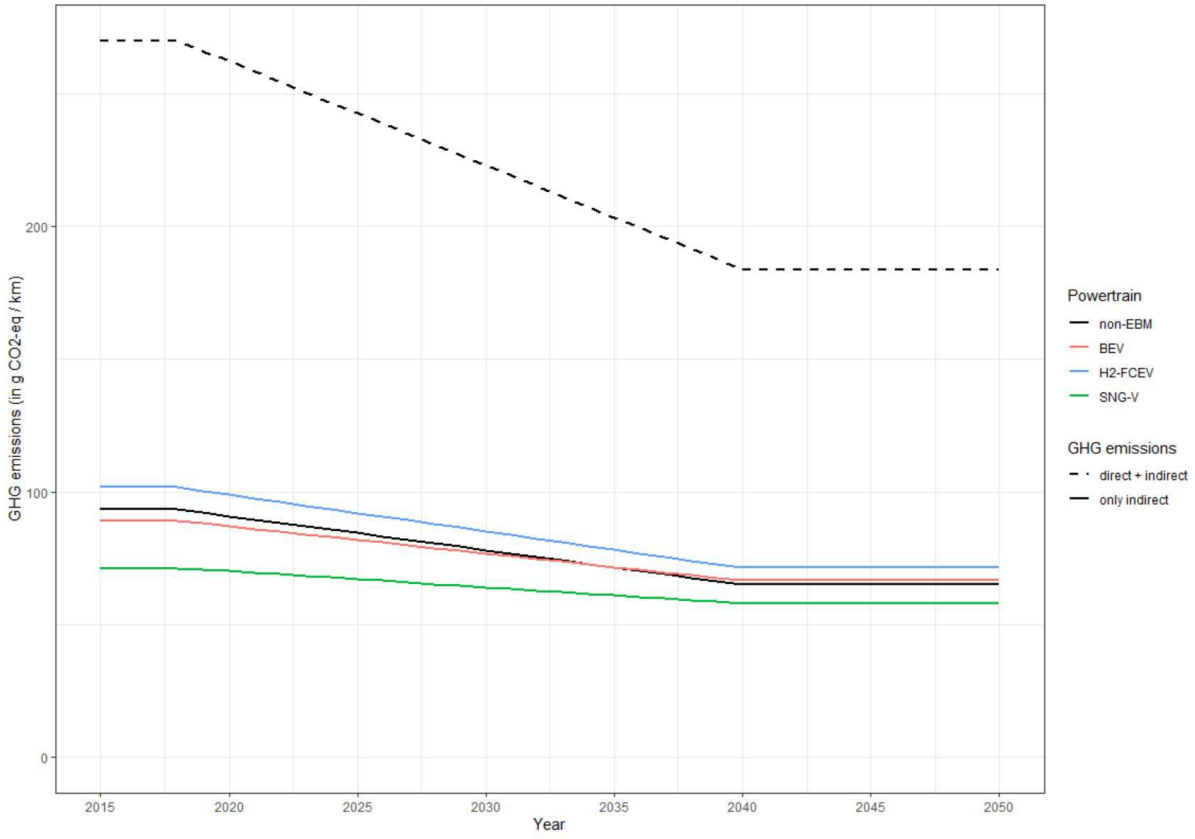

Figure 22 Assumed evolution of the indirect (“grey”) GHG emissions of EBM powertrains from 2015 to 2050 based on Cox and Bauer (2018). As a comparison also the indirect and overall (direct + indirect) GHG emissions of a

5. Dynamic mobility demand and effective GHG content of mobility

5.1. Introduction

This chapter deals with the modelling of the supply chain of the different EBM fuels. It targets to identify the possibilities of time-shifted fuel production and electricity supply. Furthermore, the corresponding systemic GHG emissions of the three EBM (BEV, H_2-FCEV, and SNG-V) and a reference "non-EBM" fleet are evaluated according their end-energy demand derived in chapter 2, the evolution on the Swiss and European electricity generation mix derived in chapter 3 and the life-cycle (LCA) GHG emission factors derived in chapter 4.

5.2. Methodology

5.2.1. Supply chain model of EBM fuels

In order to model the supply chain of EBM fuels at an hourly time resolution with respect to GHG emissions imposed by EMB , the "open energy modelling framework" (oemof) is used (Hilpert et al., 2018). Oemof is a mixed-integer-linear-programming (MILP) software to flexibly describe energy systems. In oemof, the energy system is represented as a graph with nodes and edges. While edges represent energy flows, nodes are subdivided into buses and components. In a bus, all input and output flows must be balanced at any time. Components are sources (e.g. power plants), sinks (e.g. electricity demand) and transformers (e.g. electrolyzers). Sinks and sources may have fixed or variable values. Variable inputs and outputs are used as "slack variables". Additionally, there are storage nodes. A schematic representation of the supply chain model used in this study and its implementation in oemof can be found in Figure 23.

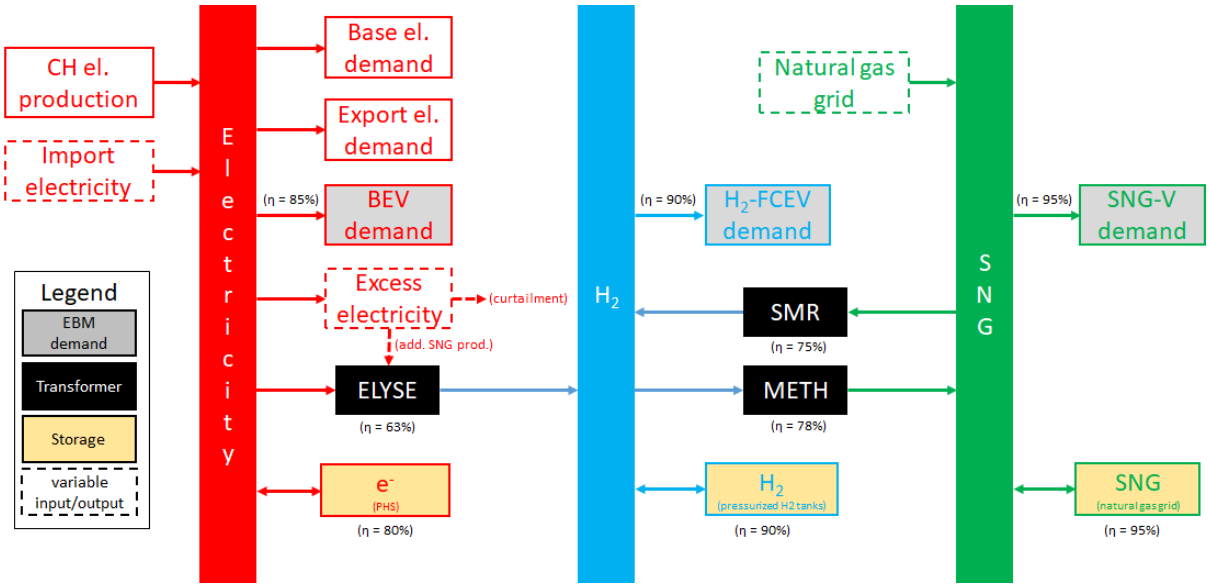

Figure 23 *Scheme of the model used in this study to investigate the supply chain of EBM fuels with respect to GHG emissions implemented in oemof.*

The model in Figure 23 is composed of three buses: an electricity, a hydrogen (H_2) and a synthetic natural gas (SNG) bus. The inputs to these buses come from various electricity supply sources in Switzerland (CH) and abroad (import) as well as from the natural gas (NG) grid. Sinks are the base electricity demand, the exported electricity and the end-energy (fuel) demand of BEV, H_2-FCEV and SNG-V. Moreover, there is a (slack) excess electricity sink, from which excess electricity is either curtailed (lost) or converted to additional SNG by means of sector coupling via electrolysis (ELYSE) and methanation (METH) for further use in other energy sectors (e.g. heavy-duty transportation, process heat, chemicals, etc.). Besides ELYSE and METH, there is also a steam methane reforming (SMR) energy transformer node to produce H_2 from synthetic and grid NG. Contrarily, the re-electrification of H_2 or SNG is not possible due to economic and regulatory reasons (Teske et al., 2019). All buses are linked to energy storage nodes, which are pumped-hydro storage (PHS) for electricity, generic pressurized tanks for H2 as well as the existing NG grid for SNG.

In the following sections, all inputs and outputs as well as other characteristics (e.g. constraints and boundary conditions) of the fuel supply chain model are described in more detail.

5.2.2. EBM scenarios

The model surrounds three main scenarios, in which a certain share of the total Swiss passenger car fleet is substituted by one of the EBM powertrains BEV, H_2-FCEV or SNG-V according to their penetration in the future Swiss passenger cars fleet (see chapter 2). In a fourth, reference scenario “non-EBM”, a share of 60% gasoline and 40% diesel ICEV is kept in the passenger car fleet instead of EBM. In this case, the legislative targets for average GHG emissions of newly registered passenger cars cannot be fulfilled. This “non-EBM” scenario is used to benchmark the GHG mitigation potential of EBM against a reference fossil-fuels based mobility.

5.2.3. Electricity supply

5.2.3.1. General

Electricity can be supplied from either imports (EU) or domestic (CH) electricity generation. While domestic electricity is a fixed input, imports are modelled as a slack variable to balance - along with other slack variables - all supply and demand in the energy system subject to given constraints and the objective of GHG optimization. The composition of both the domestic and imported electricity mix is obtained from chapter 3 by means of the technology-rich, bottom-up, cost optimization model EUSTEM and its low-carbon (LC) scenario for the years 2015 to 2050 (see Figure 10).

For the import composition, hourly profiles of typical (average) days for all seasons are used (see chapter 3). For the domestic production, actual hourly production profiles of 2015 are taken for each technology as reference and linearly scaled to the annual electricity supply of EUSTEM-LC for all years 2015 to 2050.

In the following, the determination and sources of these domestic hourly production profiles are described in detail.

5.2.3.2. Nuclear (NUC)

Swissnuclear (2020), the association of the Swiss nuclear power plant (NUC) operators, provides the operation hours and outages (including reasons) of every NUC in Switzerland. As in 2015 the availability of all Swiss NUC was only 76%, they produced only 22.1 TWh as compared to previous years with about 25 TWh and an availability of above 85% (BFE, 2015). This was primarily due to extraordinary outages of the nuclear power plants (NPP) in Beznau and Leibstadt. Therefore, to have a NUC production profile with a regular availability, the individual operation hours of each NPP from 2010 to 2014 were used and averaged. If they were operational, it was assumed that they produced at their nominal (installed) capacity. Eventually, these individual production profiles were aggregated to obtain the overall NUC production profile of Switzerland (see Figure 25).

The planned phase-out of these NPP is modelled with a given service life of 50 years, thus the corresponding shutdown years are 2019, 2023, 2028, and 2034 for the NUC Mühleberg, Beznau 1 + 2, Gösgen and Leibstadt, respectively.

5.2.3.3. Photovoltaics (RNW_SOL)

The website “rewables.ninja” (Pfenninger and Staffell, 2016) provides the hourly capacity factors of PV in Switzerland based on solar irradiance and ambient air temperature data of the SARAH satellite. These capacity factors are linearly scaled to the annual PV supply of EUSTEM-LC from 2015 (1.1 TWh) to 2050 (13.1 TWh). The corresponding PV production profile of 2015 can be seen in Figure 25.

In addition to the annual PV supply provided by EUSTEM-LC, which is roughly the PV expansion stipulated by the renewable variant “E” in the SES2050 (Prognos, 2012), also two exogenous PV expansion scenarios with a 2.5- and 4-times larger PV production are implemented in order to investigate the influence of a higher PV expansion in Switzerland. For 2050, these two exogenous PV expansion scenarios yield 32 TWh and 52 TWh (see Figure 24), which is roughly between the estimated Swiss PV potential of suitable roofs by Prognos et al. (2020) and by “sonnendach.ch” (Nordmann, 2019; Portmann et al., 2016), respectively. In these exogenous PV scenarios, the annual supply of all other CH and EU electricity generation technologies remains unchanged as provided by EUSTEM-LC (see Figure 10).

It must be noted that these two additional PV scenarios are not based on any least-cost optimization with given demands, etc. as performed by EUSTEM. Instead, they are introduced completely exogenously since one of the objectives in the SES2050 is to substitute roughly 25 TWh of nuclear power by renewables (mainly PV) by 2035. Therefore, Switzerland must already now establish a national PV expansion strategy with predefined targets of installed PV capacities to be ready, when NPP disappear from one day to the other. Such a policy target may for example be to produce 32 or 52 TWh of PV electricity by 2050 without exactly knowing (modelling) the additional electricity demand of or other energy sectors (e.g. heat pumps for electric heating, etc.). Therefore, this approach does not assume a free and open market, where the growth and competition of demand and supply would occur in parallel, as in reality policy makers may not depend and wait on such a free market to eventually settle at a demand and supply equilibrium, but may rather set an annual PV expansion rate in order to reach a predefined expansion target by a certain year (e.g. 2050). This approach is in agreement with Jochem et al. (2015) who claim that renewable power plants (such as PV) are constructed neither due to economic reasons alone, nor because of a strategically good allocation in terms of the electricity demand, but rather because of regulations, politics, and regional potentials.

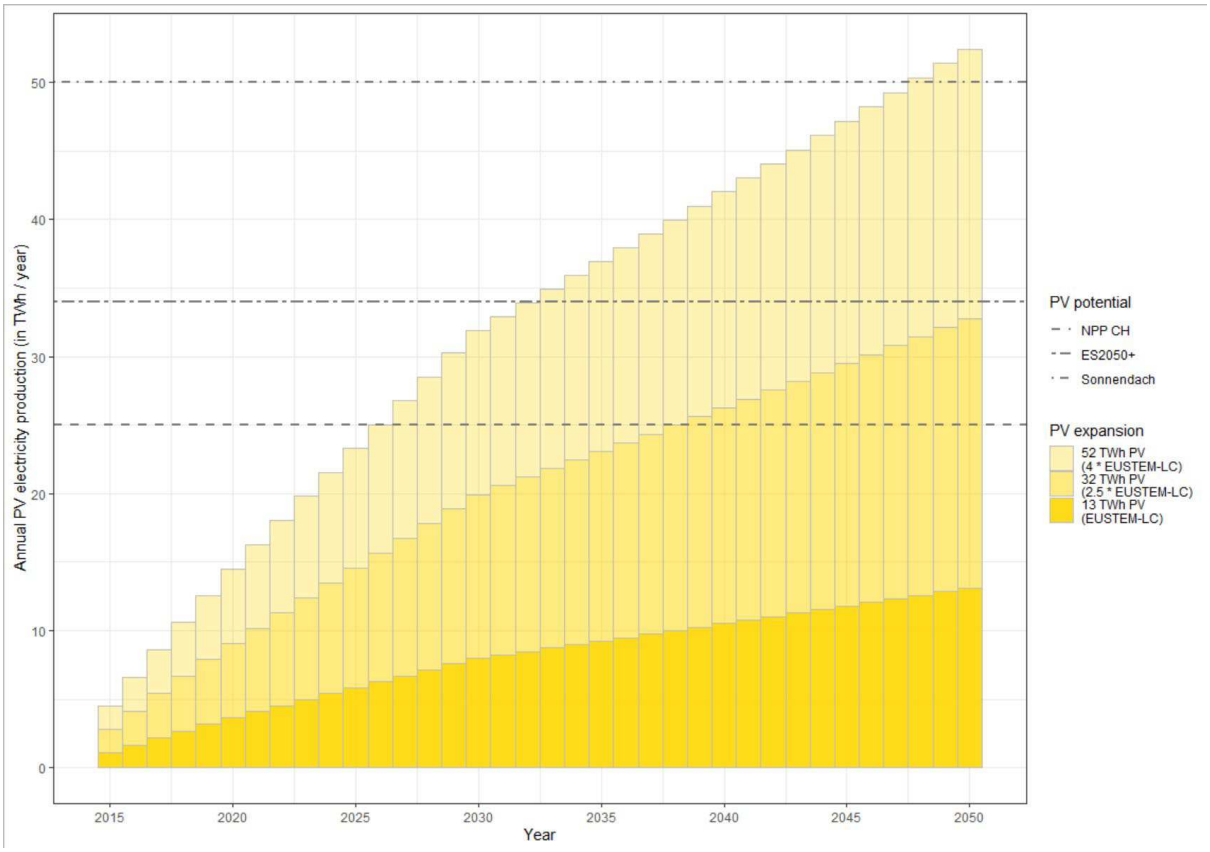

Figure 24 The three PV expansion scenarios used in this study with their annual production from 2015 to 2050. Only the lowest PV expansion scenario with 13 TWh in 2050 is based on a least-cost optimization by EUSTEM-LC, the other two PV scenarios are exogenously defined as multiples of the EUSTEM-LC expansion.

5.2.3.4. Wind (RNW_WIND)

Hourly capacity factors of wind electricity in Switzerland are provided by the website “renewables.ninja” based on the current on-shore wind turbine fleet in Switzerland and wind data from the MERRA-2 satellite (Staffell and Pfenninger, 2016). These capacity factors are linearly scaled to the annual wind production of EUSTEM-LC from 2015 (0.1 TWh) to 2050 (4.1 TWh). The corresponding wind production profile of 2015 can be seen in Figure 25. No exogenously defined larger wind expansion (as with PV) is assumed as the currently estimated potential and acceptance of wind power in Switzerland is limited.

5.2.3.5. Run-of-River (HYD_RUN)

The hourly production profile of run-of-river (HYD_RUN) hydropower plants is estimated from the summed HYD_RUN production at each Wednesday of a year reported by the SFOE [BFE2020_ElStat_Webpage]. This daily Wednesday production is then uniformly distributed over the entire week and adjusted such that the monthly and annual production of HYD_RUN is met. Finally, the hourly profile is smoothed by a LOESS filter (Garimella, 2017) with a Gaussian kernel spanning 20 days. The corresponding HYD_RUN production profile of 2015 can be seen in Figure 25.

5.2.3.6. Conventional-thermal (GAS_B / RNW_OTHERS)

In 2015, conventional-thermal power plants, mainly municipal waste incineration plants (MWIP) and gas-powered combined heat and power (CHP) plants, constituted about 3.1 TWh of renewable and fossil electricity in Switzerland. Their hourly production profile is estimated by uniformly distributing and adjusting Wednesday production sums reported by SFOE to an hourly resolution, similar to the

approach used with HYD_RUN (see above). As the Wednesday sums of SFOE also contain PV and wind electricity, their share is first subtracted with the aid of the hourly PV and wind profiles for above. The resulting hourly production profile of conventional-thermal is eventually split into ⅚ "Other Renewables" (RNW_OTHERS) and ⅙ "Gas power plants" (GAS_B) such as given in the annual supply of EUSTEM-LC. The corresponding RNW_OTHERS and GAS_B production profile of 2015 can be seen in Figure 25.

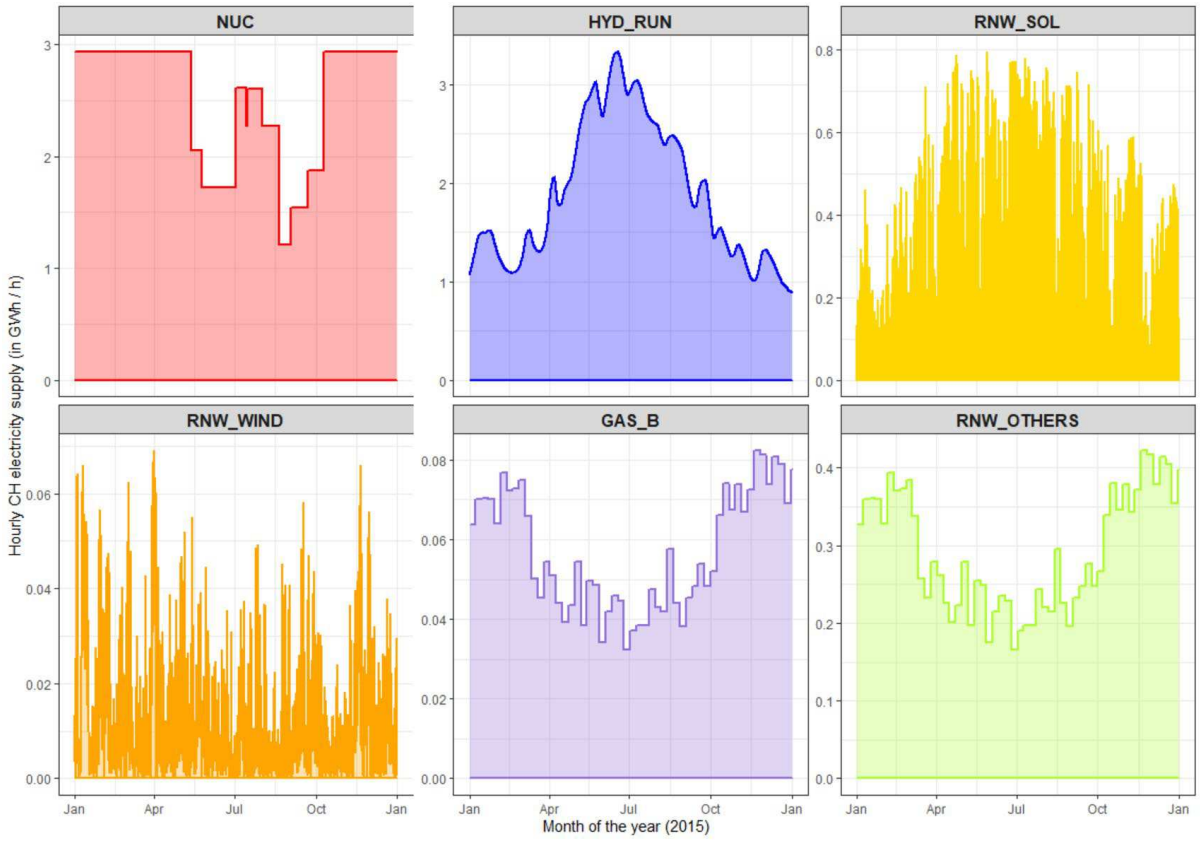

Figure 25 Actual hourly electricity supply of inflexible electricity generation technologies in the reference year 2015, which is linearly scaled to the annual supply of EUSTEM-LC for the years 2015 to 2050.

5.2.3.7. Dam storage (HYD_DAM)

All of the above-mentioned electricity generation technologies (nuclear, run-of-river, PV, wind and conventional-thermal) are inflexible in the dispatch of their electricity production. In other words, they cannot shift their production to times with higher demand and thus higher prices on the electricity market - mostly due to physical, economical and/or legal constraints. On the other hand, dam storage hydropower plants (HYD_DAM) are flexible in this respect as they can shift - within certain limits - their production to times of higher electricity demands and prices.

Therefore, the production of HYD_DAM is modelled individually for each year given the corresponding inflexible supply mix and electricity demand. As a proxy for electricity prices on the electricity market, the residual load is used (Dillig et al., 2016; Von Roon and Huber, 2010). The residual load is the momentary difference between the electricity demand and the inflexible electricity supply. It is positive for hours with deficits (i.e. demand larger than supply) and negative for hours with surplus (i.e. supply larger than demand). In this study, only flexibility on the demand side (e.g. demand response) is assumed for H2-FCEV and SNG-V, yet not for BEV and other electricity consumers, as in order to be GHG-efficient they should shift the production of their fuels via ELYSE mainly to hours with surplus renewable electricity.

Especially in summer, also HYD_DAM is partially forced to inflexibly produce electricity due to high natural inflows and limited storage capacities in their intermediate retention reservoirs. This inflexible share of HYD_DAM is heuristically modelled according to Beer (2018): First, the hourly HYD_DAM production profile is obtained by subtracting from the 2015 total electricity production in the control block Switzerland provided by Swissgrid (2018) all (inflexible) hourly production from above (see Figure 25). For NUC, the actual 2015 profile with 76% availability as reported by Swissnuclear (2020) (not the averaged profile from Figure 25) is used. The remaining profile after this subtraction is roughly the hourly HYD_DAM production. Then, this HYD_DAM profile is linearly scaled to the annual HYD_DAM supply of EUSTEM-LC. Next, a running minimum filter with a centered window of 7 days is applied to the profile, while assuming that this running minimum is the inflexible HYD_DAM production. This inflexible HYD_DAM production is then added to the other inflexible production profiles of all other technologies to calculate - along with the corresponding demand (see section 5.2.5) - the residual load for every hour in every year.

In a subsequent step, the remaining (i.e. flexible) hourly HYD_DAM production is summed for every consecutive time window of 5 days within a year. The number of 5 consecutive days is chosen heuristically such that only short-term production shifts within 5 days are allowed. HYD_DAM may theoretically also retain electricity for longer durations (e.g. seasonally), however, to be economically profitable, they are filled in spring (and summer) from snowmelt and precipitation such that they are full in autumn and can profitably produce electricity throughout winter. Consequently, they must stick to a seasonally inflexible generation schedule, which, however, is flexible within a couple of days (to weeks). Therefore, in the model within these 5 consecutive days, HYD_DAM can shift its available electricity to the most profitable hours, i.e. the hours with the largest residual loads (deficits). To this end, the residual load profile is first made non-negative by shifting (translating) it such that the most negative value (i.e. the largest surpluses) becomes zero and consequently all other values are positive. In a next step, this shifted residual load is squared in order to give higher weights to hours with large deficits. Eventually, the shifted and squared residual load is normalized to 1 and the summed HYD_DAM production is linearly redistributed according to this normalized residual load, while not exceeding the maximum installed turbination power of 8.1 GW. These steps are iteratively repeated until all HYD_DAM production is adequately redistributed within these 5 consecutive days. With this heuristic approach, the annual production and seasonal storage scheme of HYD_DAM is intrinsically maintained and the obtained profile has a smooth and realistic shape.

5.2.4. Natural gas supply

Natural gas (NG) from the grid is used as an additional energy source in the model to fuel SNG-V and H_2-FCEV (via SMR), if its impact on the overall (systemic) GHG emissions is less than the one of corresponding synthetic fuels from electricity (via ELYSE and METH). This may occur if the GHG content of electricity is higher than the one of grid NG, which is especially the case if grid NG contains a substantial share of low-carbon biomethane (see chapter 4). In this study, no H2 distribution infrastructure (grid, trucks, etc.) is implemented, although this is also a viable option as the European Hydrogen Backbone Initiative shows (Wang et al., 2020).

5.2.5. Base electricity demand

The base electricity demand is the end-use electricity demand (including losses) in Switzerland without the additional demand of and pumps of pumped-hydro storage (PHS), etc. The end-use electricity demand (without losses) in the control block Switzerland is reported at a quarter-hourly time resolution by Swissgrid (2020). In 2015, this end-use electricity consumption was 56.8 TWh. In order to be at a consistent temporal resolution with other datasets, the reported 15-min end-use consumption is aggregated to an hourly time scale (see Figure 26). Next, the hourly profile is linearly scaled to the annual base electricity demand (including losses) from 2015 to 2050 provided by EUSTEM-LC. The evolution of this base electricity demand in EUSTEM is based on the scenario “BAU" of the SES2050 (Prognos, 2012) (see Figure 26).

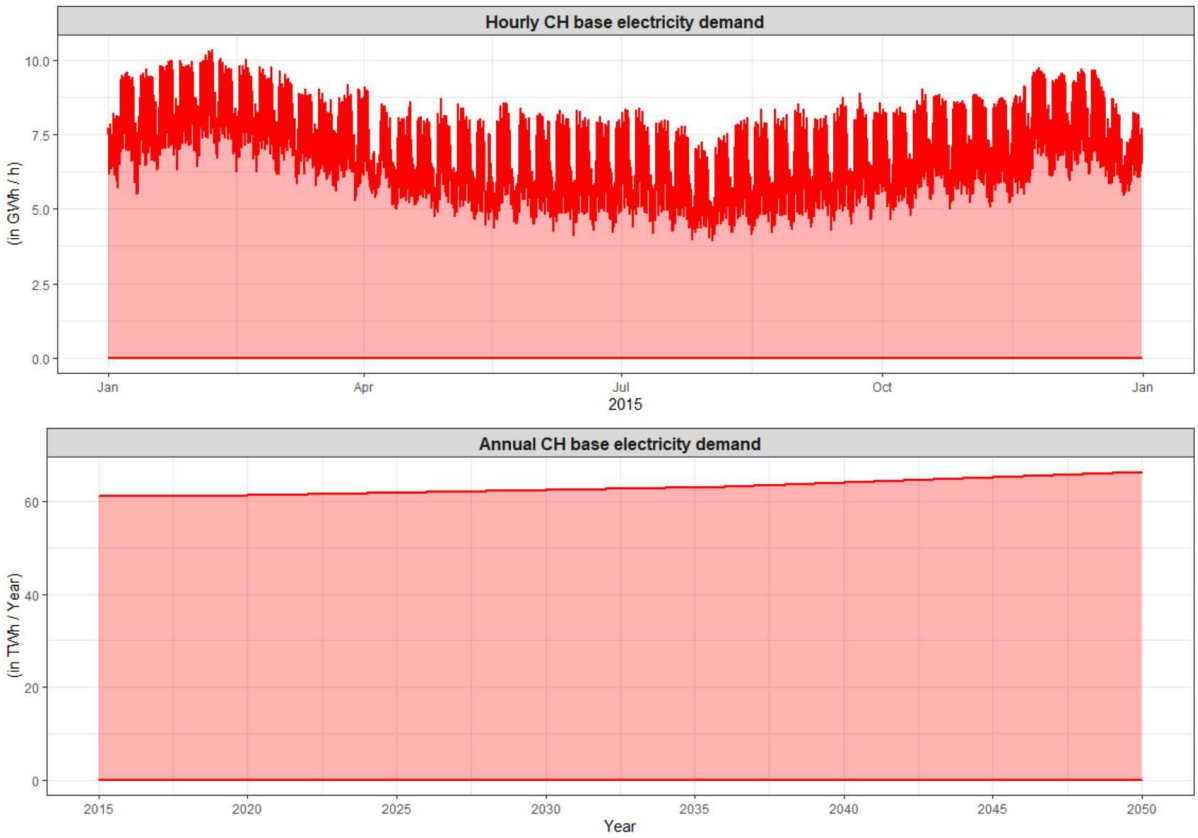

Figure 26 Hourly and annual CH base electricity demand from Swissgrid (2020) and EUSTEM-LC (according to scenario “BAU” in SES2050 (Prognos, 2012)), respectively.

5.2.6. End-energy demand of EBM

The hourly end-energy demand of each EBM powertrains (BEV, H_2-FCEV, SNG-V) is derived from their annual end-energy demand (see chapter 2) as well as the Swiss mobility survey “Mikrozensus Mobilität und Verkehr (MZMV)” (BFS, 2020b) and the methodology described in Pareschi et al. (2020).

5.2.7. Export electricity demand

The exported electricity from Switzerland is modelled as an additional demand (sink) in the fuel supply chain model in Figure 23. It is taken as the net export of the EUSTEM-LC model. The net export is only the positive hourly differences of the total (gross) exports minus the gross imports of each hour in each typical (average) day per year and season. No distinction between weekdays and weekends is made. This hourly net export demand from EUSTEM-LC (without BEV) can be seen in Figure 27 (red thick solid line) - along with the gross and net imports/exports - for the exemplary years 2015, 2035 and 2050 and all seasons. This net export demand is used with all EBM, PV expansion (see section 5.2.3.3) and import GHG content scenarios (see section 4.2.2) in this study. Figure 27 also shows the total annual net exports for the exemplary year in the winter column. Other years (not displayed) range between 2.6 TWh (2040) and 6.8 TWh (2030) per year. It must be noted that in the fuel supply chain model in Figure 23 only the net export is a-priori set as a fixed input from EUSTEM-LC, net imports are modelled dynamically as a slack variable for every hour of the year by means of the oemof optimization.

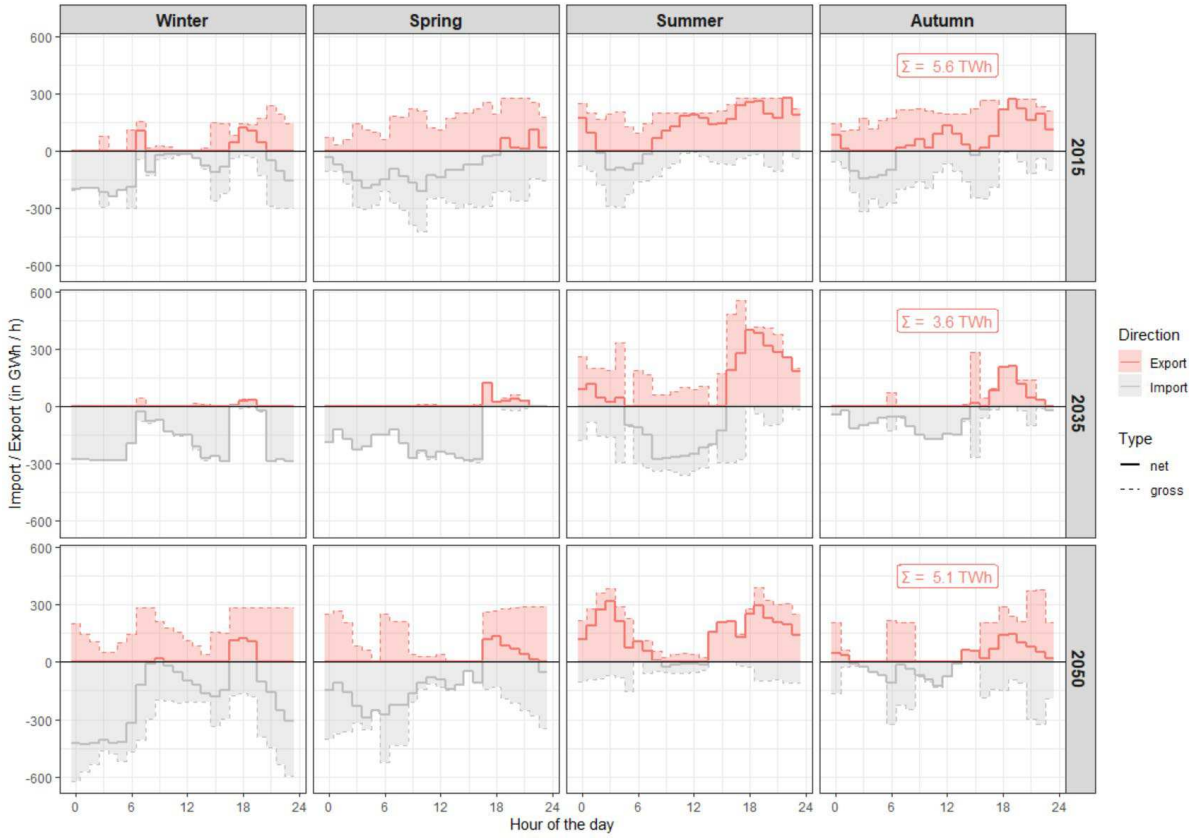

Figure 27 Hourly net and gross exports / import from EUSTEM-LC for the exemplary years 2015, 2035 and 2050 in all seasons. The annual total net exports are shown as labels in the “Winter” column. NOTE: In the model in Figure 23 only the net exports are exogenously set as an input, while the net imports are modelled endogenously within the optimization.

5.2.8. Energy conversion technologies

5.2.8.1. Electrolysis (ELYSE)

The electrolysis (ELYSE) implemented in the fuel supply chain model in Figure 23 an efficiency of 0.63 (LHV). Additionally, there is a compression efficiency of 0.9 to compress H_2 to 700 bar. Thus, the overall (electricity-to-tank) efficiency to produce H2 from electricity via ELYSE to be used with H2-FCEV is 0.57 (LHV). This overall efficiency is in line with Cabalzar (2019).

The installed ELYSE capacity (in GW_el) is taken as the maximum hourly surplus electricity that could be used by the ELYSE per year. This way, all excess electricity (red dotted “sector coupling” arrow in Figure 23) can be converted (see section 5.2.10).

5.2.8.2. Methanation (METH)

The conversion efficiency of the methanation (METH) in the fuel supply chain model in Figure 23 is 0.78 (LHV). Furthermore, there is a compression efficiency of 0.95 to compress SNG to 250 bar. Thus, the overall (electricity-to-tank) efficiency to produce SNG via ELYSE and METH to be used with SNG-V is 0.47 = 0.63 * 0.78 * 0.95 (LHV). This overall efficiency is in line with (Teske et al., 2019).

The installed capacity of the METH is the same as the installed capacity of the ELYSE. This way, all excess electricity (red dotted “sector coupling” arrow in Figure 23) can instantaneously be converted to H2 and all H2 can instantaneously be converted to SNG.

For METH, no limiting availability of GHG is assumed. Teske et al. (2019) showed that on a national-scale in Switzerland there is always enough GHG from industrial sources such as cement plants and municipal waste incinerator plants (MWIP) available for METH. On a regional scale, such a GHG limitation from industrial sources may occur, however, then also the use of atmospheric GHG is an option.

5.2.8.3. Steam Methane Reforming (SMR)

For Steam Methane Reforming (SMR), which is used to produce H2 from grid NG for H2-FCEV, the net efficiency is 0.77 (LHV) (Antonini et al., 2020). Additionally, a supply storage efficiency of 0.95 is assumed (Ligen et al., 2018). Along with the efficiency of 0.90 to compress H_2 to 700 bar, an overall (methane-to-tank) efficiency of 0.65 (LHV) to produce H2 via SMR to be used with H2-FCEV is obtained.

As the installed SMR capacity (in GW_H_2), the annual maximum hourly demand of H_2-FCEV is taken. This way, the full demand of H2-FCEV can be met with grid and synthetic NG via SMR at any time.

5.2.9. Energy storage

5.2.9.1. General

In this study, only energy stationary fuel storage, not on-board fuel storage, is considered. The three implemented energy supply storage nodes (PHS, generic pressurized H_2 tanks and NG grid) in the fuel supply chain model in Figure 23 have several common characteristics: (1) the initial storage level (state-of-charge, SOC) is always set to 50% of their maximum storage capacity, (2) at the end of each year the SOC must be at 50% again and (3) there are losses (round-trip-efficiency).

5.2.9.2. Electricity storage

In the fuel supply chain model in Figure 23, electricity can be stored with PHS. EUSTEM-LC provides annual values for the installed charging (pumping) and discharging (turbining) capacity as well as the totally stored electricity for both of these technologies. The maximum charging (pumping) and discharging (turbining) power of electricity storage is 3.76 GW_{el} (for all years). This value is about the projected installed PHS capacity in Switzerland, if all pending PHS projects (Linth-Limmern, Nant de Drance, etc.) are completed.

The round-trip-efficiency of PHS is assumed to be globally 80%. According to Piot (2014), the total available storage capacity of all current and future PHS in Switzerland is about 300 GWh. This capacity is based on the limiting amount of upstream or downstream water resources. In order to restrict the oemof optimization from using PHS also for seasonal electricity storage, which in reality is not economically and ecologically sound, the storage capacity of PHS is set to the maximum daily surplus electricity in scenario "non-EBM" with a PV expansion according to EUSTEM-LC. With this assumption, only short-term storage up to a couple of days is possible. Consequently, the storage capacity of PHS must be predefined for every year. As a constraint, this storage capacity must increase monotonically from year to year, that is, it cannot decrease in a subsequent year, although the corresponding maximum daily surplus amount can.

5.2.9.3. H_2 storage

5.2.9.3.1. Short-term storage

For short-term (days to weeks) H_2 supply storage, generic pressurized H_2 tanks at 700 bar are used. They may be located at the fueling station or at the ELYSE site. Their charging and discharging power is assumed unlimited. Their storage capacity is the maximum daily demand of H_2-FCEV. This way, at least one day of H_2-FCEV demand can be met only from short-term H_2 storage. The round-trip storage efficiency is assumed 90% (Schaber et al., 2004).

5.2.9.3.2. Seasonal storage

As especially in summer more H_2 can be produced from abundant excess (PV) electricity via ELYSE than can immediately be consumed by H_2-FCEV, it is assumed that this excessively produced H_2 can be stored seasonally in the NG grid as SNG produced by METH. In times of insufficient (renewable) surplus electricity to produce enough H_2 for H_2-FCEV (e.g. in winter), this stored SNG can be converted back to H2 via SMR. This route of seasonal H_2 storage is chosen, if despite the additional loss in METH and SMR, features less GHG emissions than using NG from the grid (e.g. in winter).

In turn, H_2 cannot be stored seasonally directly in the NG grid by admixture, although recent studies show that an admixture of more than the current legal limit of 2% (H_2) would be technically feasible [Lambert2018].

5.2.9.3.3. SNG storage

For SNG supply storage, the existing NG grid is used. Therefore, both the charging and discharging power as well as the total storage capacity are assumed unlimited. This way, SNG can easily be stored and shifted seasonally. The round-trip storage efficiency is assumed 95%.

5.2.10. Excess electricity

5.2.10.1. General

Excess electricity occurs if the momentary electricity supply is larger than the momentary electricity demand. There are two (extreme) cases how such excess electricity is treated in the fuel supply chain model in Fig. 1: (1) Curtailment and (2) production of additional SNG by power-to-gas (ELYSE-METH). Additional exports are not allowed as the export demand is already set a-priori (see section 5.2.7) and as it is assumed that in a future energy system with a large expansion of PV and wind, situations of excess electricity will occur almost everywhere and almost at the same time due to similar transcontinental weather (climate) conditions as well as limited transmission capacities (Zappa et al., 2019). This simultaneous excess electricity situation is partly already the case today as negative electricity prices on the electricity markets show (De Vos, 2015; Götz et al., 2014). Additional short-term electricity storage with PHS and new batteries (incl. vehicles-to-grid) is neither an option, as the main discrepancy between electricity demand and supply is seasonal, thus by storing (with losses) additional noon excess electricity and shifting it to evening/night hours with supply deficits would only alleviate the situation marginally (Rüdisüli et al., 2019). Teske et al. (2019) showed there is not enough overall electricity demand to substantially consume large amounts of future (PV) excess electricity in summer, and seasonal electricity storage is neither an economically nor an ecologically viable option. Therefore, remaining excess electricity must either be curtailed (lost) or an additional electricity consumer (e.g. power-to-gas) - ideally with a seasonal energy storage potential - must be found in the energy system.

5.2.10.2. Curtailment

In this case, excess electricity is lost (curtailed) as there is no additional electricity demand and no additional seasonal energy storage. This is the reference case for the scenarios "BEV" and "non-EBM", as additional power-to-gas infrastructure such as ELYSE and METH are not available a-priori. In other words, they must additionally be built (and paid back).

5.2.10.3. Additional SNG production (power-to-gas)

In this case, excess electricity is converted to additional SNG via power-to-gas (ELYSE-METH) to substitute grid NG in other energy sectors (e.g. heavy-duty vehicles, heating, chemical industry, etc. Another, albeit highly inefficient option would be the re-electrification of SNG via gas power plants (CCGT). This is the reference case for the scenarios "H_2-FCEV" and "SNG-V" as ELYSE and METH are already available in such an energy system in order to meet the end-energy demand of these powertrains. It must be noted that this additional use of SNG in other energy sectors is not explicitly modelled in this study, we just assume that it may be used elsewhere and just quantify the amounts of excess electricity and producible SNG available for such additional use.

5.3. Results and discussion

5.3.1. Hourly fuel supply and electricity demand of EBM

The mean hourly electricity demand per season of each EBM powertrain in 2050 for each PV and GHG import scenario is displayed in Figure 28. For BEV, the hourly electricity demand is given exogenously by the analysis described in section 2.3.2 with the highest demand in the evening and at night (see Figure 7). In turn, for H2-FCEV and SNG-V primarily surplus electricity produced at noon in summer is used, in particular with a large domestic PV expansion and "LC" imports. With the lowest domestic PV expansion (13 TWh), this seasonal variation cannot be seen, however, the same diurnal variation occurs. With CCGT imports, less electricity is used compared to "LC". Instead, more grid NG (and SMR)

is used as this has a lower GHG impact than using high-carbon CCGT electricity to produce SNG and H2.

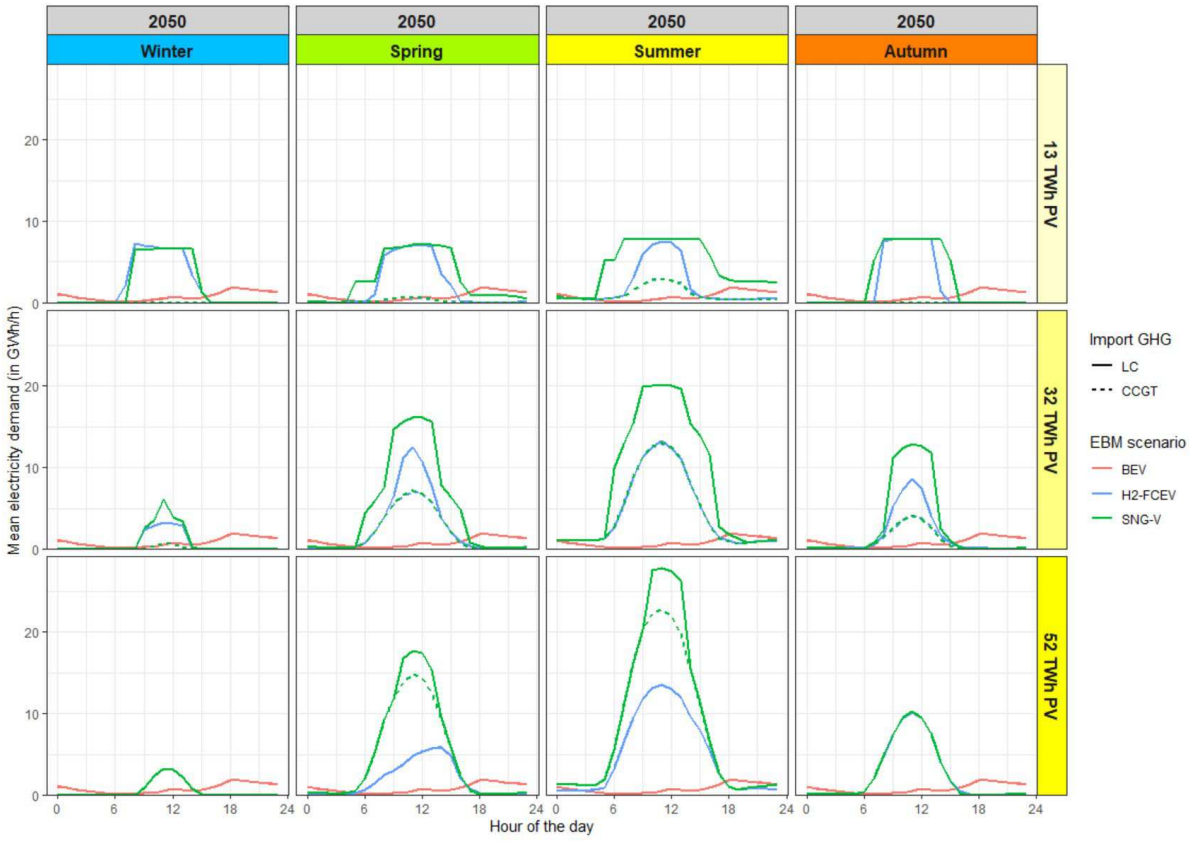

Figure 28 Mean hourly electricity demand for each EBM powertrain and season in 2050.

5.3.2. Annual fuel supply and electricity demand of EBM

5.3.2.1. BEV

Figure 29 shows the amount and origin of electricity needed to meet the demand of BEV in all PV (13 TWh, 32 TWh, and 52 TWh) and import GHG scenarios (LC and CCGT). All electricity either stems from additional imports or from domestic (excess) electricity. Both sources can increasingly be exploited by using short-term electricity storage (i.e. PHS) to shift them to the actual hours of BEV demand. With LC imports and 13 TWh PV, mainly import electricity (5.6 TWh, including PHS losses[3]) is used, whereof 1.1 TWh are shifted by means of PHS. With more PV in Switzerland and LC imports, it is an increasing amount of domestic electricity (mainly from PV) that is used (and shifted by PHS). With CCGT imports, no imports are shifted by PHS, as the additional losses in PHS need to be offset by even more additional high-carbon imports.

[3] 4.2 + 1.1/0.8 = 5.6 (LC / 13 TWh PV)

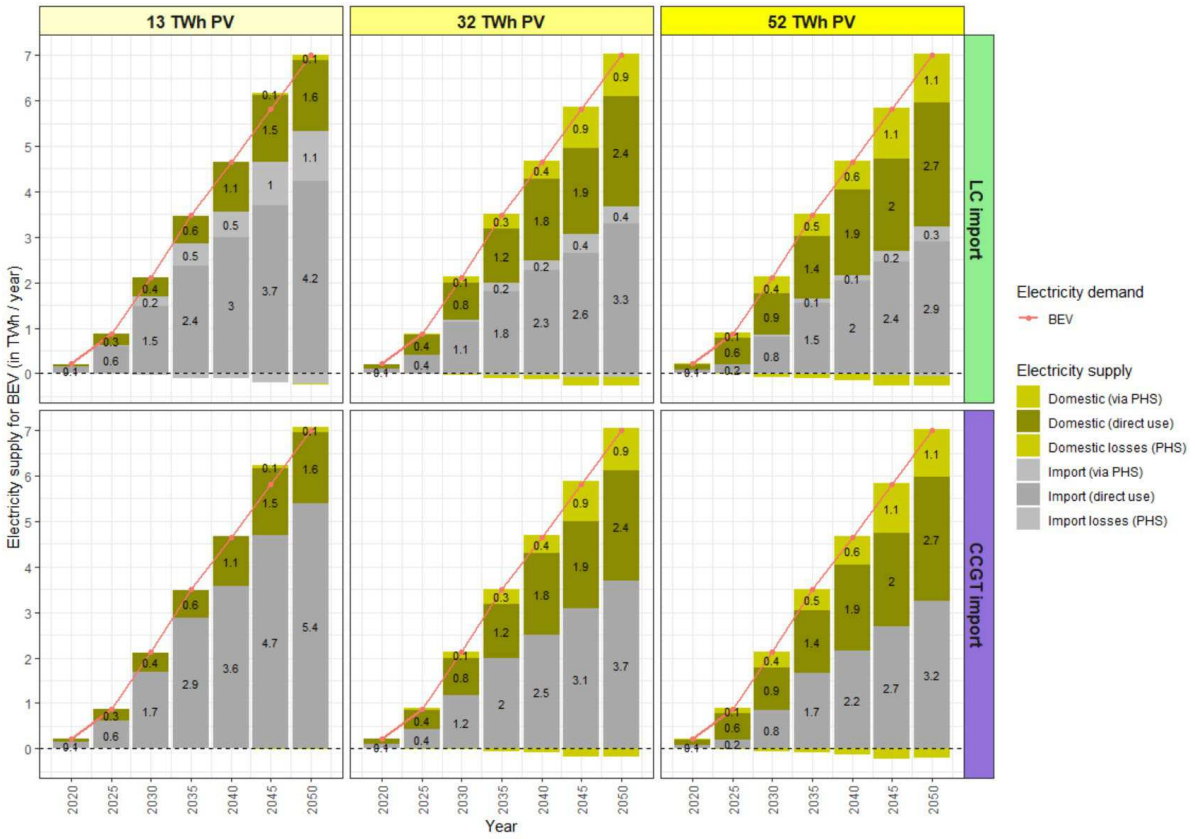

Figure 29 Origins of electricity (import and domestic) to meet the end-energy (electricity) demand of BEV (red line) in all PV expansion and import GHG scenarios. Additionally, the share of electricity shifted by PHS and associated losses (negative values) are displayed.

5.3.2.2. H_2-FCEV

In Figure 30, the H_2 supply for H_2-FCEV is displayed for all PV and import GHG scenarios along with corresponding losses in all conversion steps ELYSE, METH and SMR. H_2 is primarily produced from electricity and grid NG via ELYSE and SMR, respectively.

Grid NG is only used, if import electricity has a high-carbon footprint (CCGT) and PV expansion in CH is low (13 TWh), since in this case, H_2 from grid NG via SMR features less GHG emissions than H_2 produced from non-renewable electricity. In all other cases, H_2 is primarily produced from electricity via ELYSE and directly used thereafter. With increased PV expansion in Switzerland, also the route of seasonal storage of H_2 as SNG is used more often, despite the additional losses of the two additional conversion steps (METH and SMR).

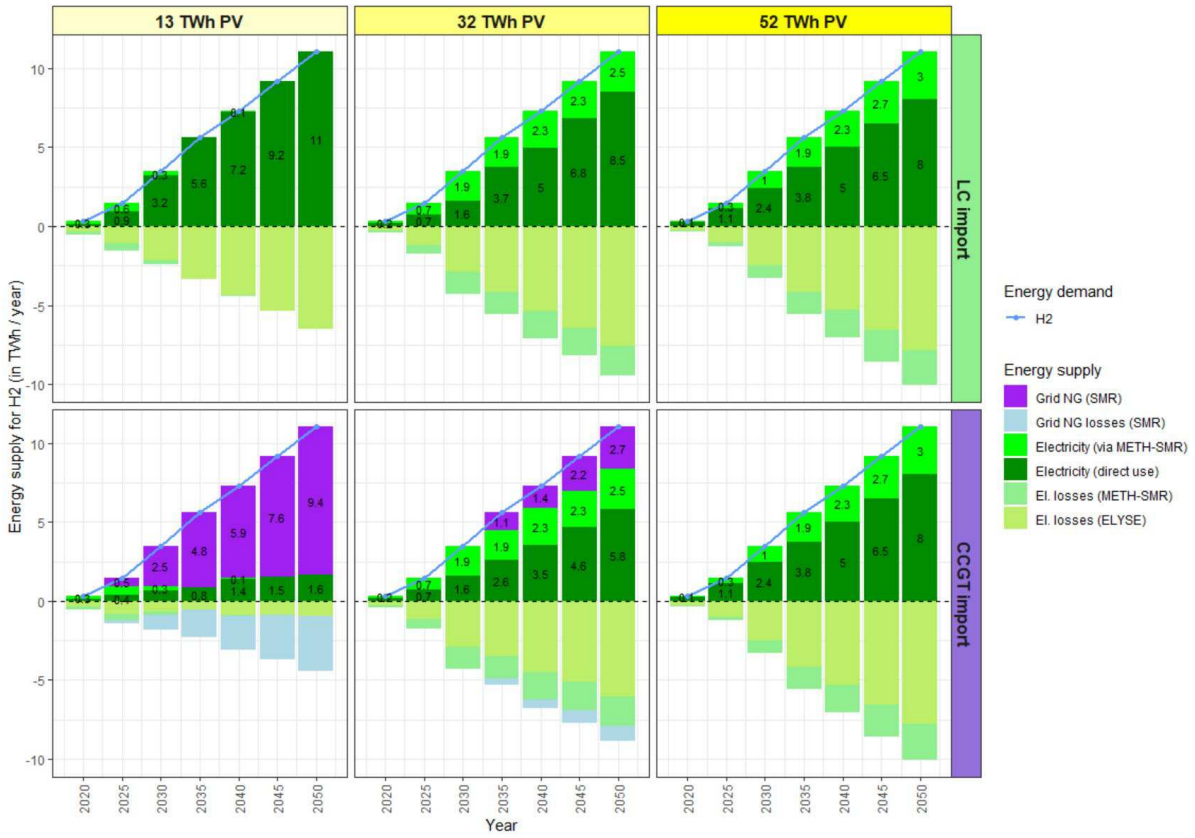

Figure 30 a1be23c6c5064cebb701c091ebdffc36: Supply routes of H2 (i.e. direct use from ELYSE, seasonal storage via METH-SMR and use of grid NG via SMR) to meet the end-energy (H2) demand of H2-FCEV (blue line) in all PV expansion and import GHG scenarios. Additionally, associated losses (negative values) within the conversion steps ELYSE, METH and SMR are displayed.

In Figure 31, the origin of electricity used for ELYSE divided by imports and domestic (excess) electricity is shown along with the amount of electricity shifted by PHS. Import electricity is primarily used for ELYSE in the “LC” scenario with a low PV expansion in CH. In this case, no seasonal storage of H2 as SNG is employed (see Figure 30) as throughout the year (i.e. also in winter) enough low-carbon import electricity is available. The more PV is installed in CH - or if only high-carbon (“CCGT”) imports are available - the more domestic excess electricity from PV in summer is used. In these cases, in summer, H2 is produced by ELYSE in excess (i.e. more than can within short terms be used by H2-FCEV), and then converted further to SNG (via METH) to be seasonally stored in the NG grid. In winter, when there is a lack of renewable electricity, the seasonally stored SNG is reconverted to H2 via SMR. Short-term electricity storage via PHS is used - to a lower extent - with import electricity in the “LC" scenario with 13 TWh PV and 32 TWh PV.

Depending on the PV expansion and import GHG scenario, the total amount of electricity needed to fuel H2-FCEV in 2050 via ELYSE varies between 2.6 TWh TWh and 21.1 TWh per year.

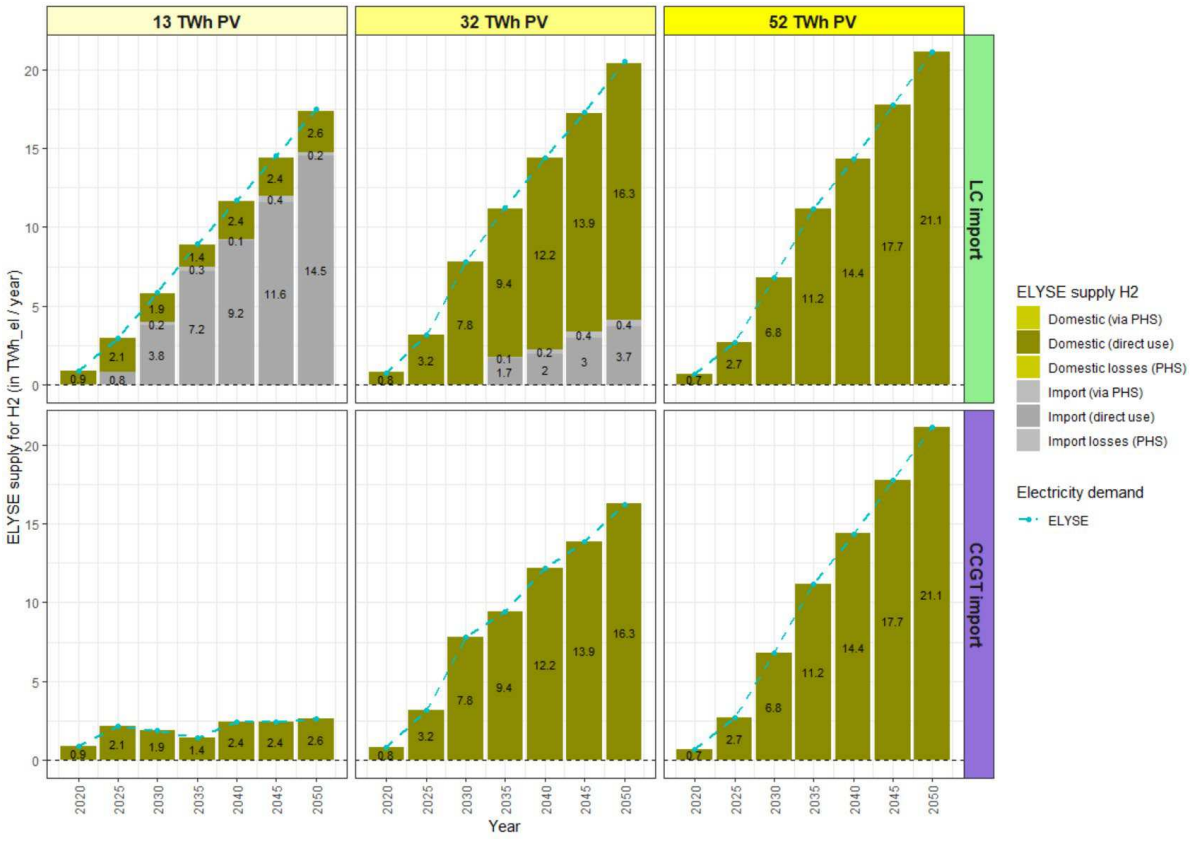

Figure 31 Origin of electricity (import and domestic) used in the ELYSE step to produce H2 for H2-FCEV. Additionally the share of electricity shifted by PHS and associated losses are displayed.

5.3.2.3. Synthetic Natural Gas Vehicles (SNG-V)

Figure 32 depicts the SNG supply for SNG-V for all PV and import GHG scenarios along with corresponding losses in the ELYSE-METH (eta = 0.47) step. No losses are assumed, if grid NG is directly used. Grid NG is primarily used, if import electricity has a high-carbon intensity (CCGT) and PV expansion in CH is low (13 TWH), as in this case, grid NG features less GHG emissions than SNG produced from (non-renewable) electricity. This is in particular the case with a large content of biomethane in the NG grid. Only in the scenario with a high PV expansion in CH (52 TWh) and LC imports, SNG is exclusively produced from 18.1 TWh electricity.

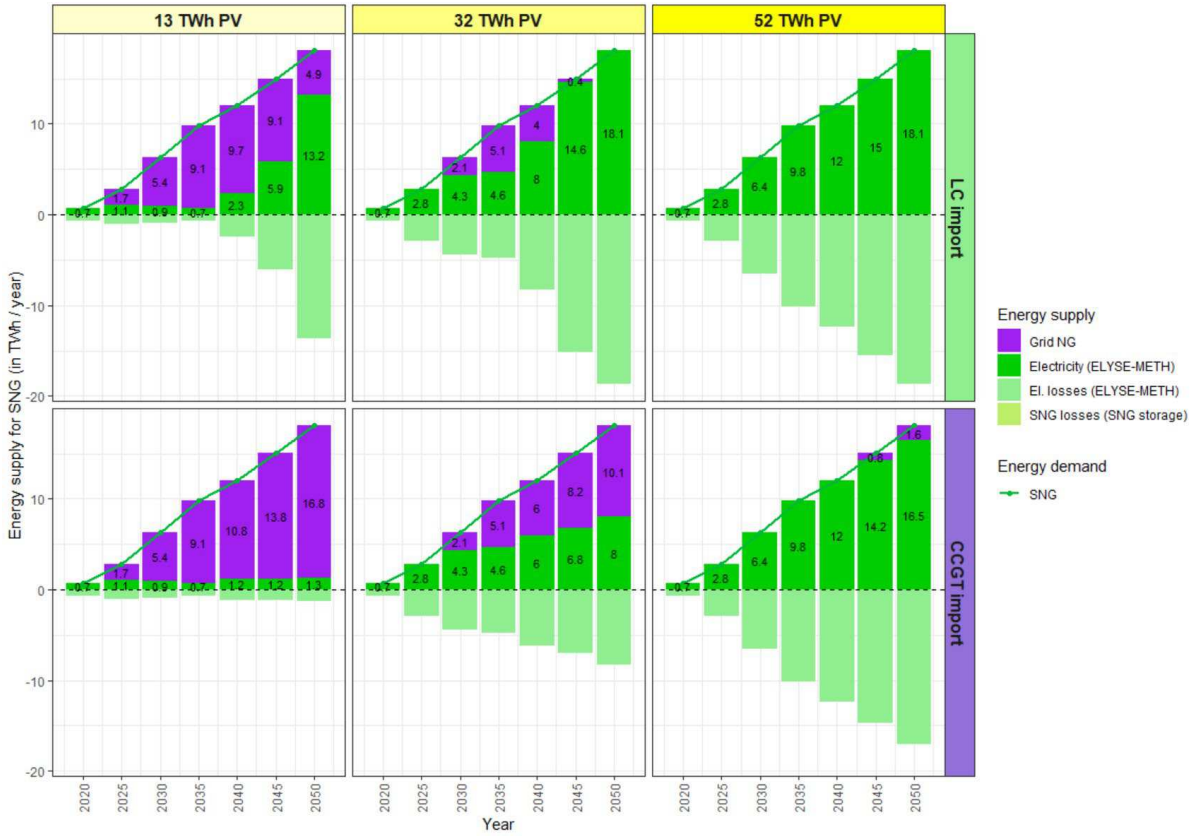

Figure 32 Supply routes of SNG (i.e. from electricity via ELYSE-METH and direct use of grid NG) to meet the end-energy (SNG) demand of SNG-V (green line) in all PV expansion and import GHG scenarios. Additionally, associated losses (negative values) within the conversion step ELYSE-METH are displayed.

In Figure 33, the origin of the electricity used for ELYSE-METH divided by import and domestic (excess) electricity is shown. Import electricity is - as in other EBM scenarios - primarily used in the “LC” import scenario with a low PV expansion in CH. The more PV is installed in CH, the more domestic excess electricity, which mainly occurs in summer, is used. With high-carbon (CCGT) imports, grid NG rather than import electricity is used along with gradually more domestic excess electricity as PV expansion increases. In these cases, in summer, SNG is produced in excess and seasonally stored in the NG grid. In winter, when there is a lack of (renewable) electricity, the seasonally stored SNG is used again to meet the SNG-V demand. Short-term electricity storage via PHS is used - to a lower extent - with import electricity in the “LC" scenario and decreasing PV expansion.

Depending on the PV and import GHG scenario, the total amount of electricity needed to fuel SNG-V in 2050 varies between 2.6 TWh and 36.8 TWh per year.

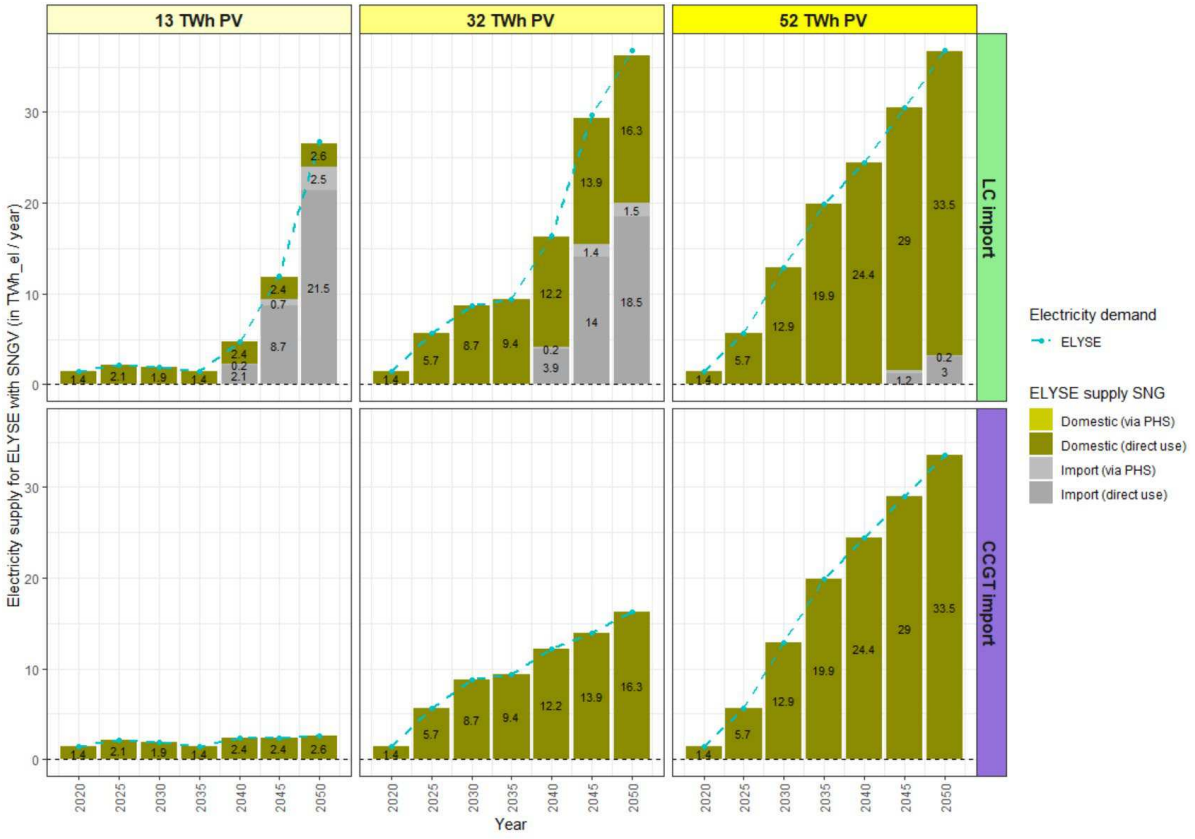

Figure 33 Origin of electricity (import and domestic) used in the ELYSE-METH steps to produce SNG for SNG-V. Additionally the share of electricity shifted by PHS and associated losses are displayed.

5.3.3. Impact on the electricity system

5.3.3.1. Imported electricity

In Figure 34, the totally required import electricity is shown for all PV expansion, import GHG and EBM scenarios (including “non-EBM” as dark-shaded bars and numbers below the bars). The additional import electricity demand of EBM compared to “non-EBM”, as provided in the previous section, is annotated on top of the bars. Already in the “non-EBM” scenario, a substantial amount of electricity must be imported. Depending on the year and PV expansion, this amount is between 1 TWh (in 2020 and 2025 with the highest PV expansion scenario) and 14 TWh (in 2040 with the 13 TWh PV expansion and LC imports).

In 2050, compared to “non-EBM” and depending on the PV and import GHG scenario, BEV need between +3 and +6 TWh, H_2-FCEV between +0 and +15 TWh and SNG-V between +0 and +25 TWh of additional import electricity. While BEV need additional import electricity in both import GHG scenarios, H_2-FCEV and SNG-V only in the “LC” scenario, as in the “CCGT” scenario they can use PV excess electricity and/or grid NG (see above).

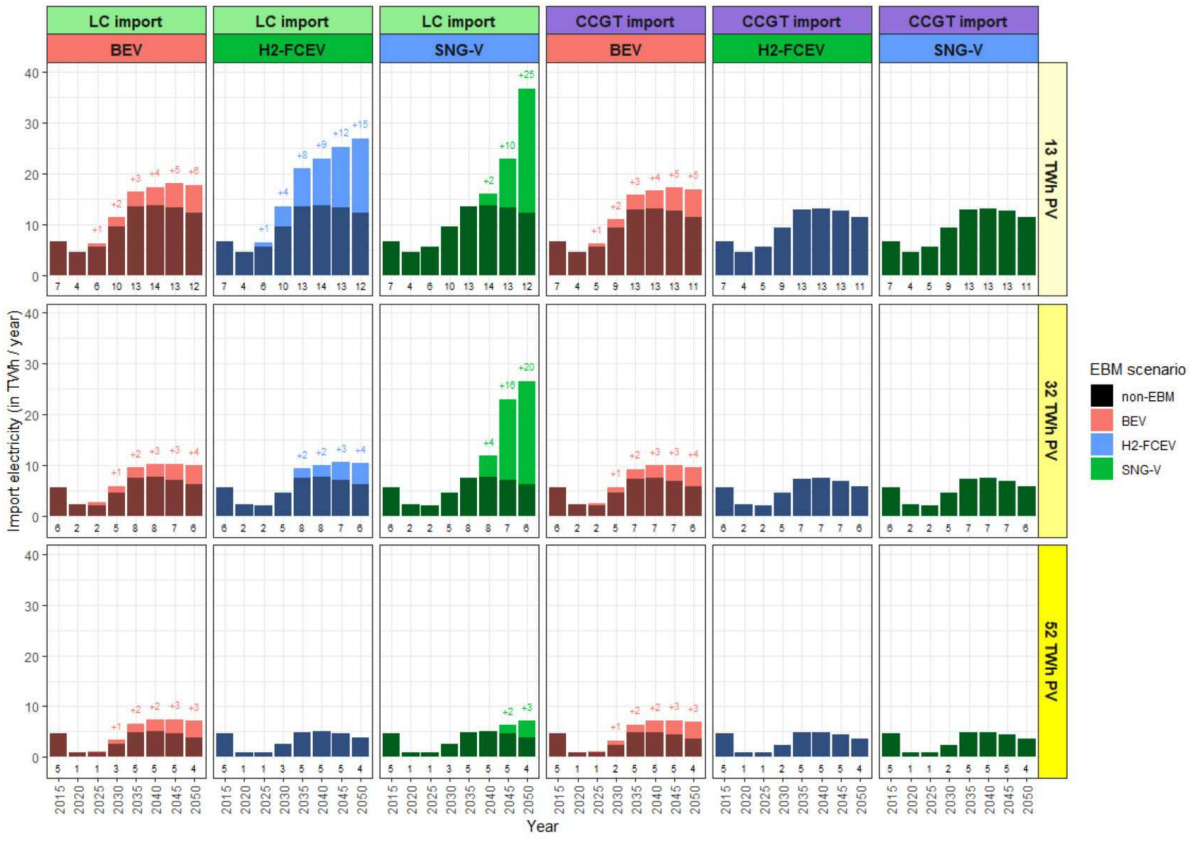

Figure 34 Required import electricity for the different EBM, PV and import GHG scenarios. As a comparison, also the required import electricity in the "non-EBM" scenario is displayed as black-shaded bars and numbers below the bars. The additional import electricity compared to "non-EBM" is shown as numbers above the bars.

5.3.3.2. Excess electricity

Figure 35 displays the annual excess electricity in all PV expansion, import GHG and EBM scenarios (including "non-EBM" as black-shaded bars and numbers below the bars). This excess electricity can be converted to other energy carriers (e.g. SNG via power-to-gas) or must be curtailed. Depending on the PV expansion, in "non-EBM" excess electricity amounts to less than 3 TWh in the lowest PV scenario (13 TWh PV) and more than 34 TWh in the highest PV scenario (52 TWh PV). Depending on the EBM scenario, this excess electricity can be reduced substantially with H_2-FCEV and SNG-V due to their capability of seasonally storing this excess electricity as SNG. With BEV, due their overall lower fuel demand and no seasonal fuel storage, a large amount of this excess electricity remains in the energy system. In other words, in the BEV (and non-EBM) scenario with a high PV expansion more than half of the annually produced PV electricity (yellow dashed line in Figure 35) is excess electricity.

In order to put these amounts of excess electricity into context with energy demands in other sectors, heavy-duty (HD) vehicles (i.e. vans, trucks, cargo trains, etc.) currently consume about 12 TWh of fossil energy (mainly diesel) (BFE, 2019). With state-of-the-art TTW efficiencies and the conversion losses of ELYSE-METH in this study, this would result in an equivalent electricity demand of about 17 TWh and 29 TWh for HD-H_2-FCEV and HD-SNG-V, respectively. Figure 35 shows that in all PV expansion scenarios with BEV, there would be enough excess electricity to (at least partially) fuel such HD vehicles. However, this would mean that in addition to an infrastructure for BEV (e.g. charging stations, grid reinforcements, etc.) also a power-to-gas infrastructure with ELYSE (and METH) must be installed.

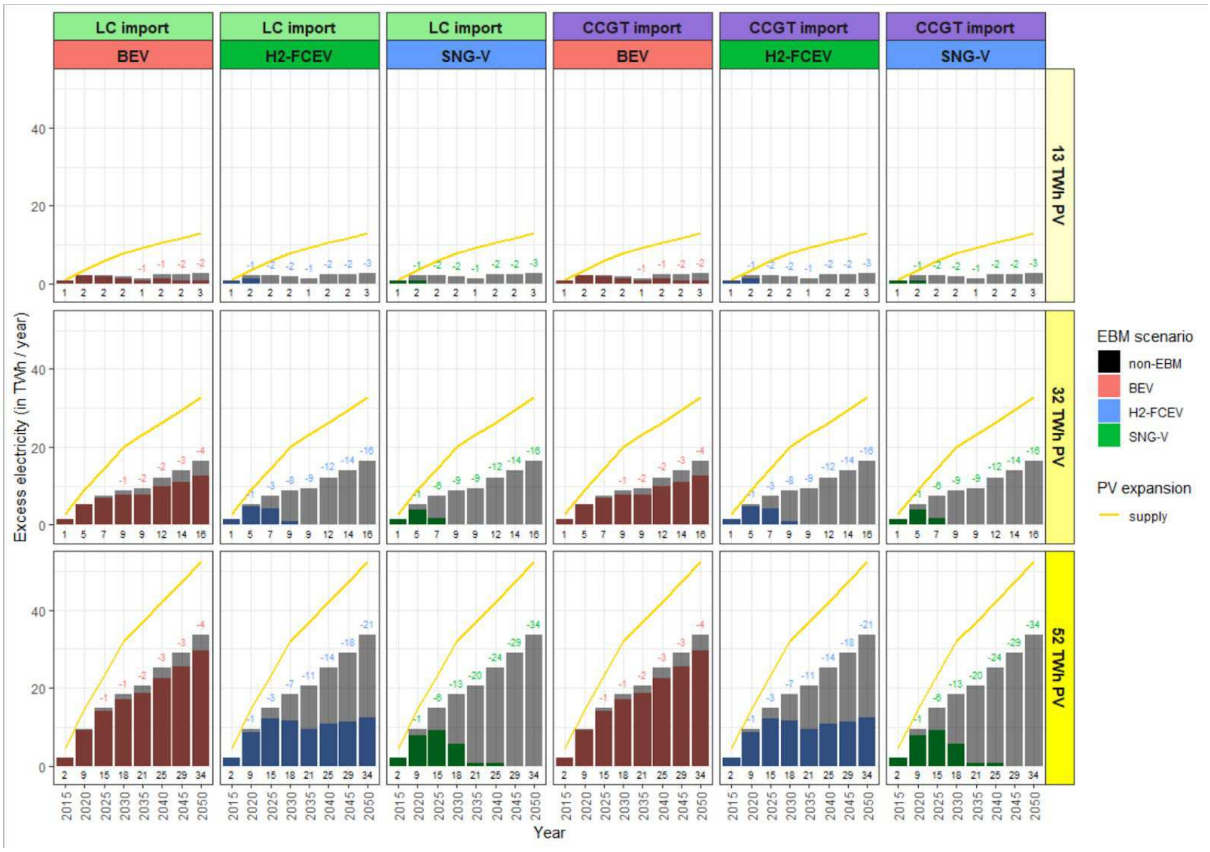

Figure 35 Annual excess electricity (bars) and annual PV production (yellow line) for all EBM, PV and import GHG scenarios (see Fig. 523d59a6b8114e77a38bbc244a0376f8 for more details).

5.3.3.3. Installed ELYSE capacity

Figure 36 shows the needed ELYSE capacity to convert all excess electricity to H_2 (and subsequently SNG). For H_2-FCEV and SNG-V, also the already installed ELYSE capacities to meet their fuel demand are shown. In the H_2-FCEV and SNG-V scenario, the additional ELYSE capacity to convert all excess electricity to H_2 is small compared to the already needed capacities. In contrast, with BEV, the additionally required ELYSE capacity would be almost equal to the one needed in the H_2-FCEV and SNG-V scenario, that is, in 2050, 7 GW_{el} and 35 GW_{el} in the 13 TWh and 52 TWh PV scenario, respectively. There is no difference between the “LC” and “CCGT” import GHG scenario. For comparison, the totally installed pump capacity of PHS in CH is 3.8 GW_{el} (incl. the currently commissioned PHS projects in Linth-Limmern and Nant de Drance).

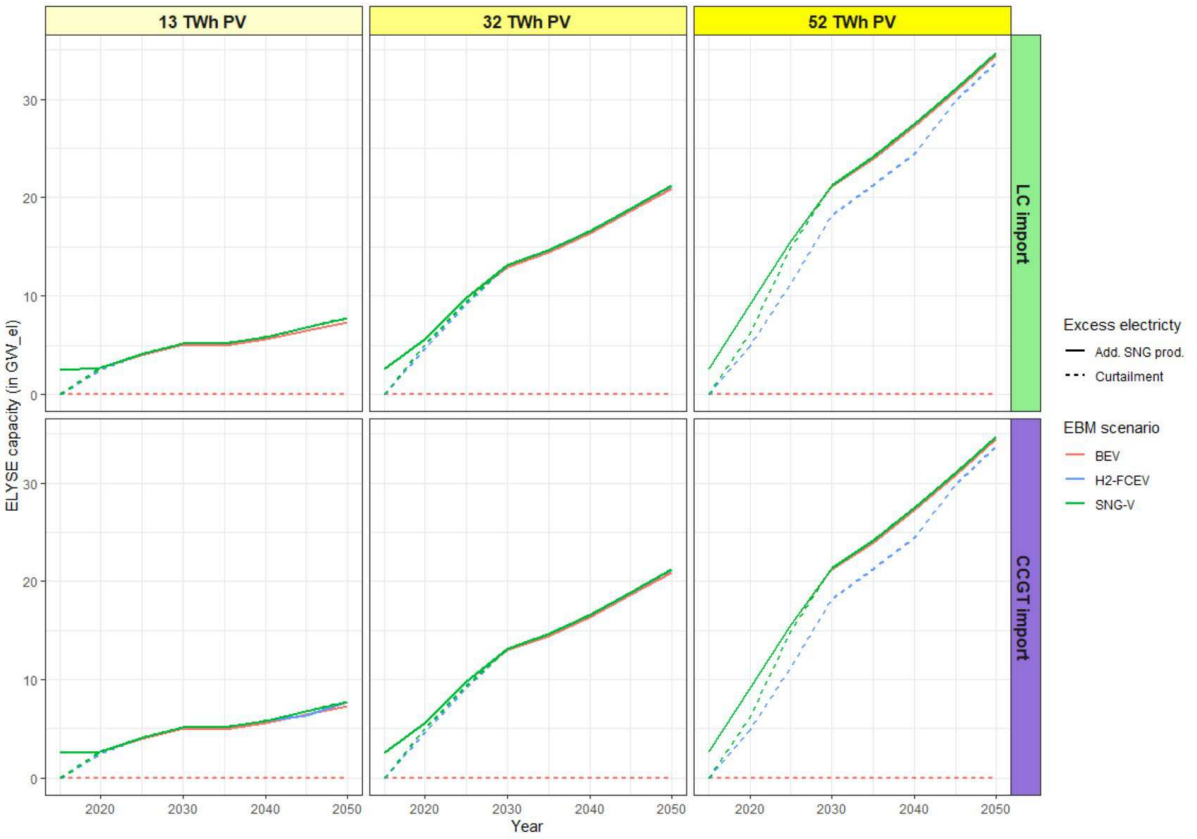

Figure 36 Required ELYSE capacity (in GW_el) to meet EBM demand (dotted lines) and to avoid curtailment of excess electricity (solid lines) with all PV expansion and import GHG scenarios.

The corresponding equivalent full load hours (eqFLH) of the ELYSE operation with the capacities from Figure 36 are displayed in Figure 37. Moreover, Figure 38 shows all hours with excess electricity ordered by their magnitude for the exemplary year 2050. In the “CCGT” scenario, eqFLH are all below 1000 h since there is a steep decrease in the ordered magnitudes of excess electricity in Figure 38. With H_2-FCEV and SNG-V in the “LC” import and 13 TWh PV scenario, in turn, ELYSE can operate at full load for a substantial amount of time (especially after 2040), thus increasing the eqFLH to more than 2000 h. However, in order to be economically viable, the eqFLH of ELYSE should be at least 4000 h [Teske et al., 2019]. Higher eqFLH can be attained by lowering the installed ELYSE capacity, however, at the expense of not converting all excess electricity (i.e. more curtailment) or by first temporarily storing excess electricity (e.g. with PHS or batteries), however, at the expense of additional storage losses and required storage (charging) capacities as large as the required ELYSE capacities in Figure 36.

In a subsequent step, this temporarily stored excess electricity could then be constantly fed to the ELYSE at a lower installed capacity and consequently higher eqFLH. Such economical and technical aspects of ELYSE operation, which generally increase systemic GHG emissions, as well as the build-up of parallel infrastructure for both BEV and additional SNG production for HD vehicles have to be assessed in a follow-up techno-economical study.

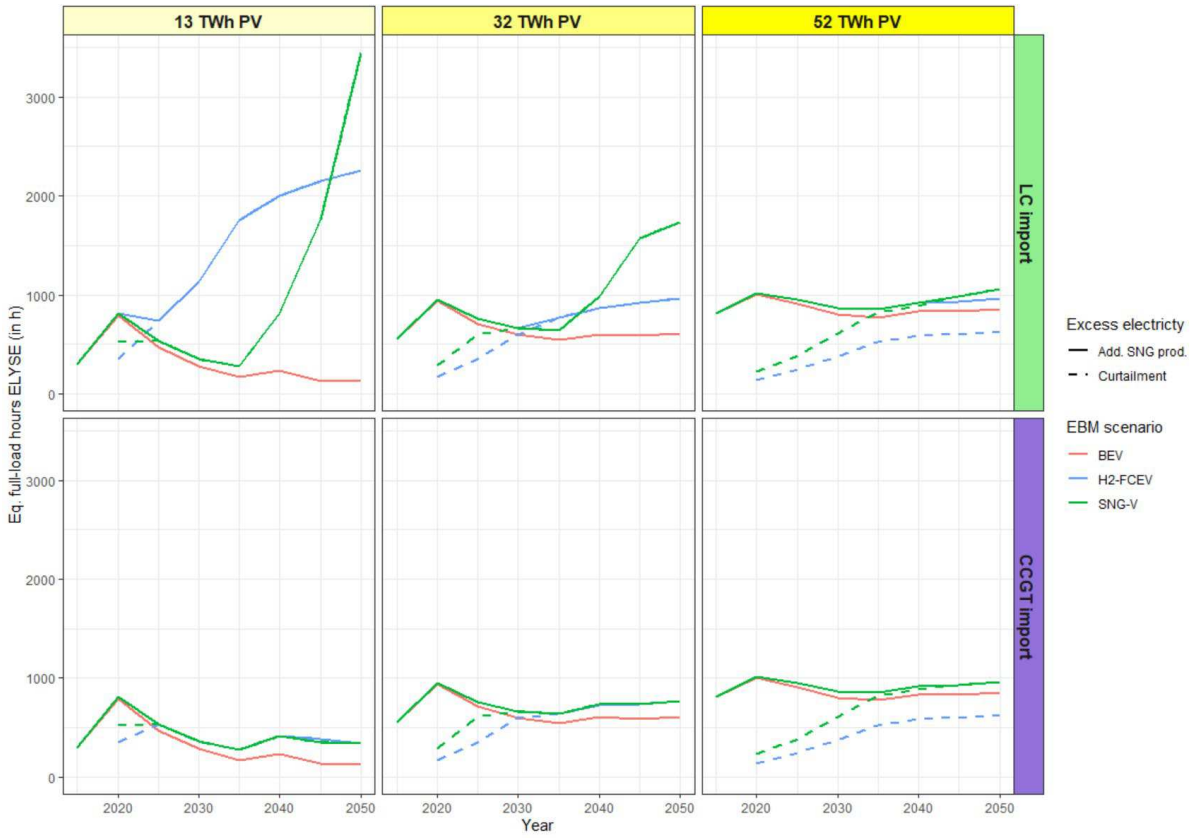

Figure 37 Equivalent full load hours (eqFLH) of ELYSE operation in the different PV and import GHG scenarios. The dashed lines are for operation only, while the solid lines include a full conversion of all excess electricity by ELYSE (add. SNG production) in order to fully avoid curtailment in all scenarios.

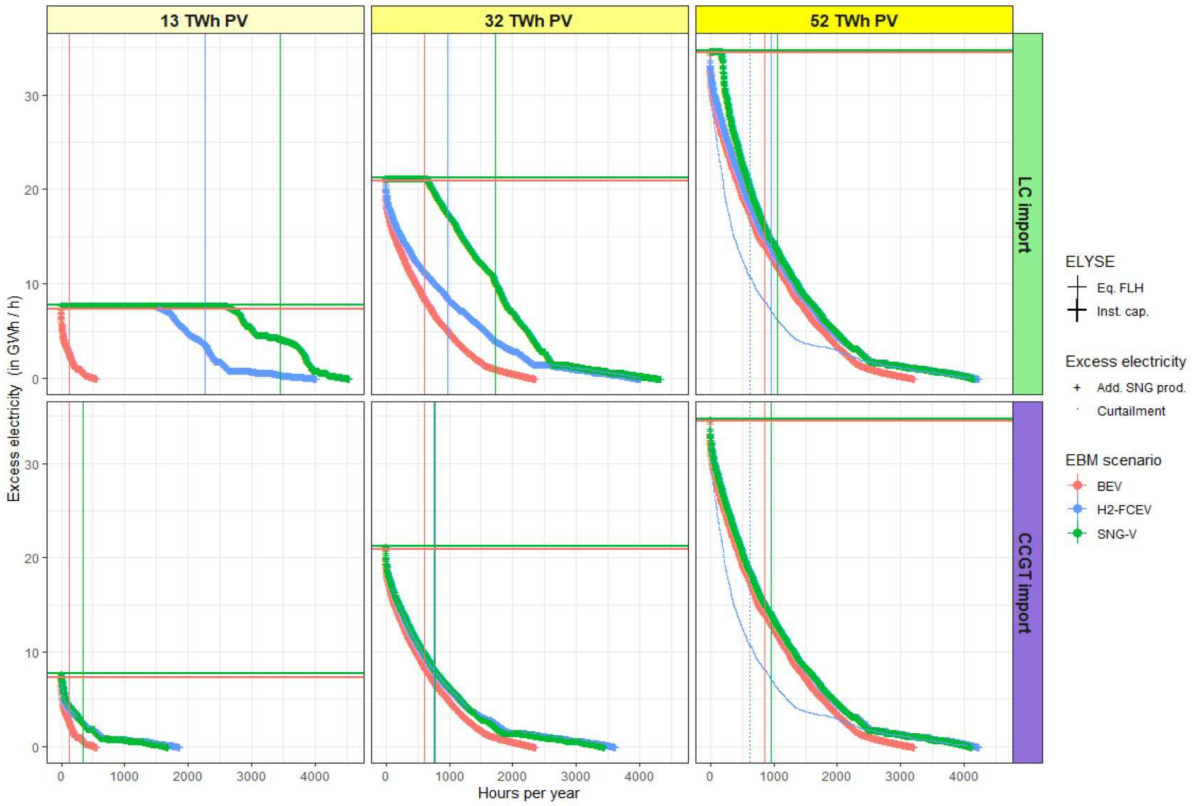

Figure 38 Ordered excess electricity by their magnitude in 2050 for all PV and import GHG scenarios. Vertical lines are the eq. FLH from Fig. 0f6fd098053c4aeb8cc3ad4eb6fe3546; horizontal lines are the installed ELYSE capacities from Figure 36 for full conversion of all excess electricity (no curtailment).

5.3.3.4. Short-term electricity storage

From an economical and ecological point of view only short-term storage of electricity is viable, as costs (CAPEX and OPEX) as well as (indirect) GHG emissions to construct and operate the storage device decrease per unit of stored electricity, in other words, if they are distributed over as many storage cycles as possible - provided the lifetime (amortization) of the storage device is mainly affected by age and less by the number of storage cycles.

Figure 39 shows how short-term electricity storage (i.e. PHS) is used in all scenarios and years in comparison to the “non-” scenario. With BEV, compared to “non-”, substantially more electricity (mainly from PV) is stored in PHS, in particular with “LC” imports and large PV expansions to shift renewable electricity from noon hours (supply peak) to evening/night hours (demand peak). With plenty of renewable electricity available in the system at noon (either from domestic or abroad production), this day-night shift is more GHG-efficient than importing (high-carbon) electricity at night despite the additional losses incurred by «round-trip-efficiency» of PHS (80%). An optimization of this situation could only be achieved by demand response (i.e. «noon charging» of BEV). This influence of demand response (demand side management) shall be addressed in a further study.

With H_2-FCEV and SNG-V, a reduction in the use of PHS - compared to “non-” - is observed with “LC” imports and for all PV expansion scenarios in almost all years. This is because in these cases, low-carbon electricity can at almost any time directly be converted to H2 and afterwards be stored as H2 (or SNG) more efficiently than in PHS. With H_2-FCEV and SNG-V as well as high-carbon (“CCGT”) imports, PHS is used almost as in “non-”, since in this case H_2 and SNG are primarily produced from grid NG (see Figure 31 and Figure 32).

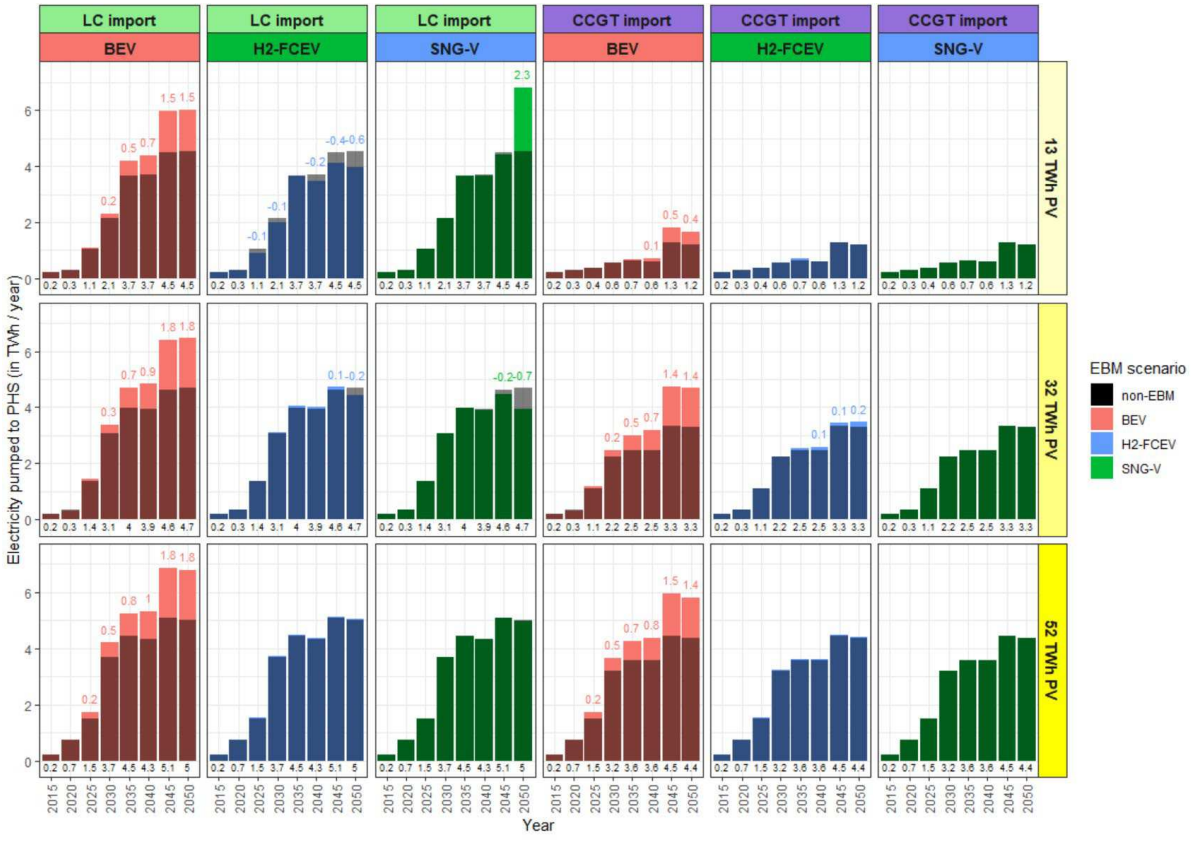

Figure 39 Amount of electricity stored with PHS for the different, PV and import GHG scenarios. As a comparison also the stored electricity in PHS in the “non-” scenario is displayed as black-shaded bars and numbers below the bars. The additional import electricity compared to “non-” is shown as numbers above the bars.

5.3.3.5. Dispatch of dam storage hydropower plants

Figure 40 shows how electricity generation from dam storage hydropower plants (HYD_DAM) is (on average) seasonally redistributed (shifted) according to the heuristic approach described in section 5.2.3.7, for all PV expansion scenarios with and without the additional electricity demand of BEV in the exemplary years 2015 (reference), 2035 and 2050. For H_2-FCEV and SNG-V, it is assumed that they primarily use remaining surplus electricity after HYD_DAM has been redistributed by this approach.

The validity of this heuristic approach with the residual load as proxy for electricity prices on the market and as the sole driver for HYD_DAM dispatch is shown by comparing the actual (original) HYD_DAM production profile and the modelled one in the reference year 2015. Except for the early morning (and noon in summer) hours, the approach correctly models the current dispatch characteristics of HYD_DAM.

Figure 40 also shows that an increased PV expansion shifts HYD_DAM production away from noon hours towards evening (and night) hours, when electricity demand is high and no competing PV supply is available. Particularly in the evening, the additional electricity demand of BEV (at about 6 p.m.) has a noticeable influence on this (modelled) HYD_DAM dispatch.

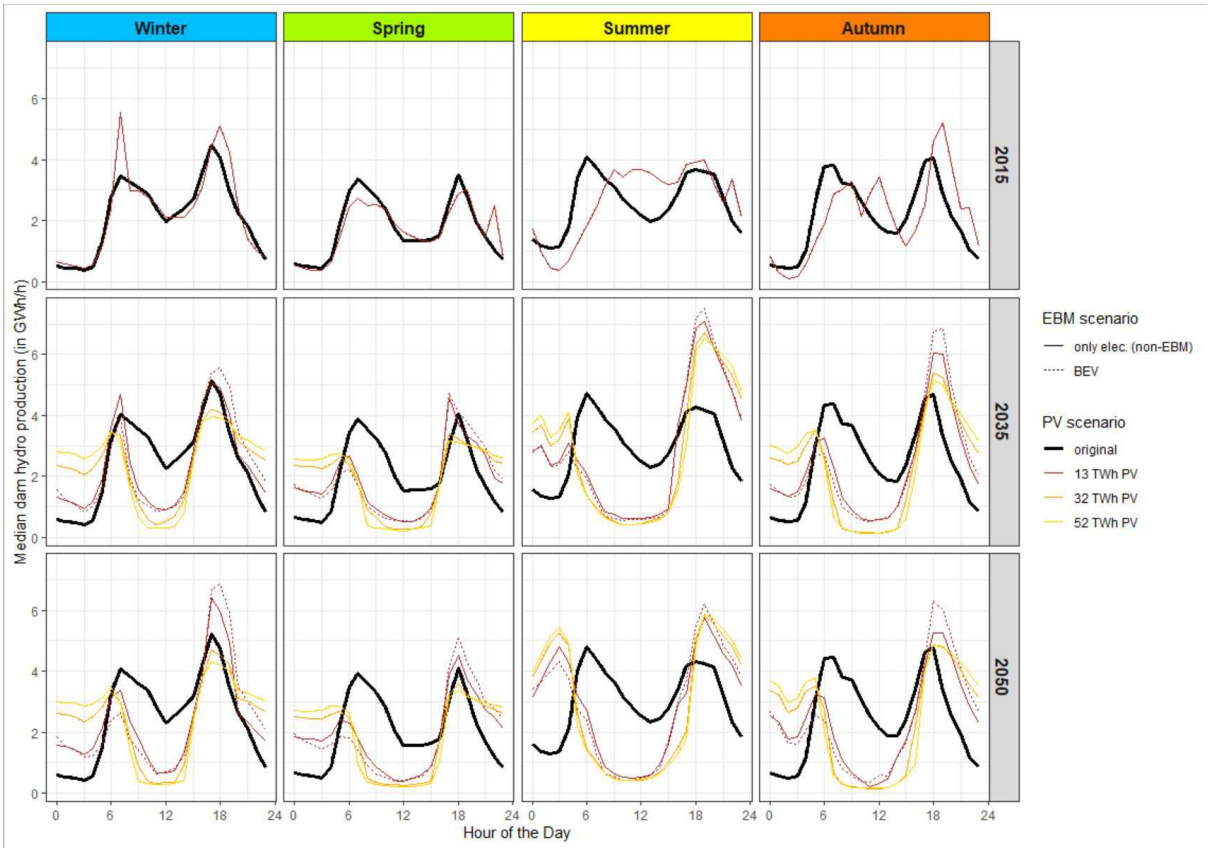

Figure 40 *Seasonal average redistribution of dam storage (HYD_DAM) electricity production according to the heuristic approach described in section 5.2.3.7 with the residual load as proxy for the electricity market in the exemplary years 2015 (reference), 2035 and 2050 as well as all PV expansion scenarios with and without BEV. The actual seasonal averaged HYD_DAM production in 2015 (original) is also shown for comparison.*

5.3.3.6. Seasonal and short-term H_2 and SNG storage

Figure 41 shows at a weekly aggregated time resolution for the exemplary year 2050, how much H_2 and SNG is weekly charged and discharged in the generic H_2 storage tank (short-term H_2 storage) and NG grid (seasonal SNG storage) as well as how much is converted by ELYSE, METH and SMR to produce H_2-FCEV and SNG-V in all PV expansion scenarios with "LC" imports. Only the "LC" import scenario is shown, as in the "CCGT" scenario, H_2 and SNG are primarily produced from grid NG, as this is more GHG efficient. Similar, albeit smaller, effects can also be observed in the "CCGT" scenario, however. For more information on this seasonal and short-term H_2 and SNG storage, refer to section 5.2.9).

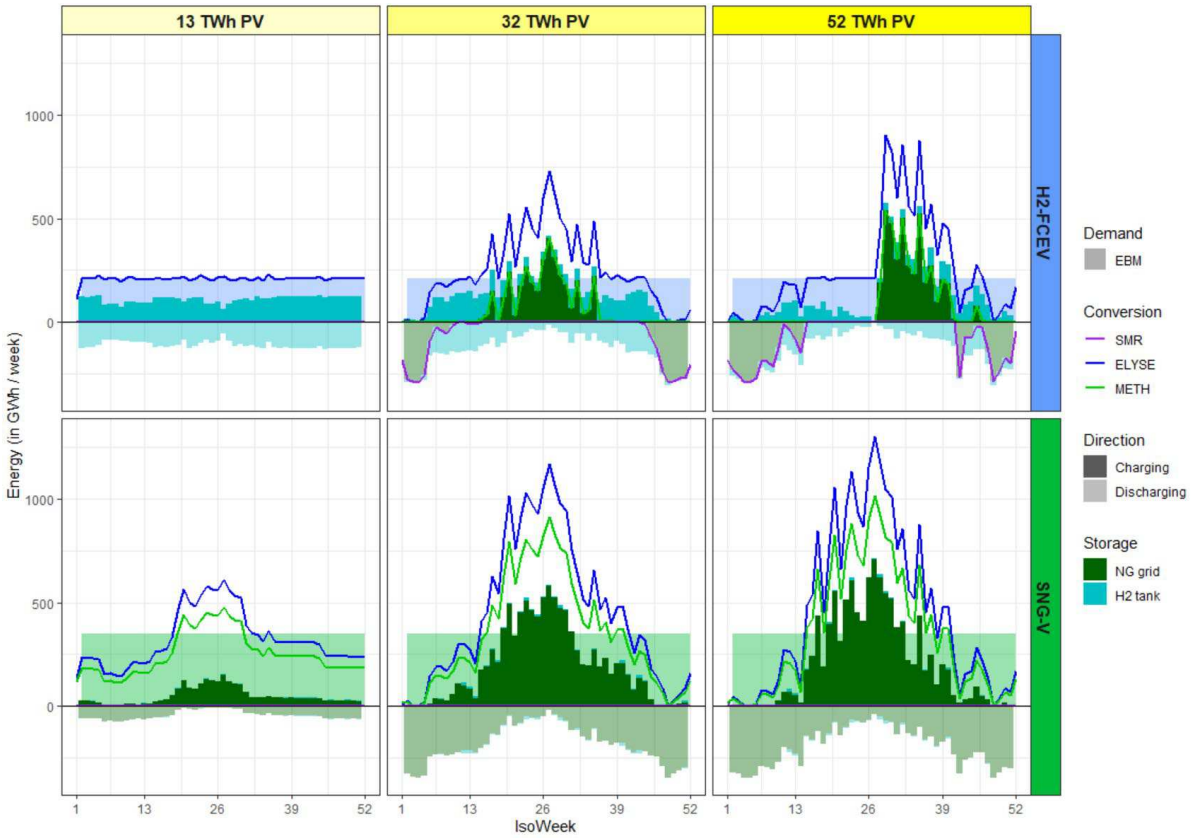

Figure 41 Weekly aggregated seasonal (NG grid) and short-term (H2 tank) storage with H2-FCEV and SNG-V for the exemplary year 2050 for all PV expansion scenarios and the "LC" import GHG scenario. Storage "charging" is displayed as positive values and "discharging" as negative values. As shaded areas, also the weekly end-energy demand of H2-FCEV and SNG-V is shown. The weekly operation of ELYSE, METH and SMR is shown as solid lines.

With H_2-FCEV and the lowest PV expansion, only short-term H_2 storage with a total (integral) of 5.8 TWh_{H2} (see Figure 42) is used. In the 32 TWh PV scenario, short-term H_2 storage is still used for 3.8 TWh_{H2} (integral), while in the largest 52 TWh PV scenario it decreases to 2.9 TWh_{H2} (integral). In turn, with larger PV expansion, the amount of H_2 seasonally stored as SNG (via METH) and reconverted via SMR increases from 3.4 TWh_{H2} to 4.1 TWh_{H2} in Figure 42.

This seasonal storage pattern can be seen in Figure 41, when in summer SNG is "charged" to the NG grid, while it is "discharged" again in winter along with SMR reconversion. With SNG-V and increasing PV production, seasonal storage becomes even more dominant with annual totals (integral) of 2.4 TWh_{SNG}, 9.9 TWh_{SNG} and 10.5 TWh_{SNG} seasonally stored in the NG grid for the three PV expansion scenarios in 2050, respectively (see Figure 42). Again, in summer, SNG is produced from low-carbon (renewable) excess electricity via ELYSE-METH and stored ("charged") in the NG grid, while it is

"discharged" in winter/spring, when low-carbon electricity is scarce Similar, albeit smaller, seasonal storage patterns with H_2-FECV and SNG-V can also be seen in other years in Figure 42.

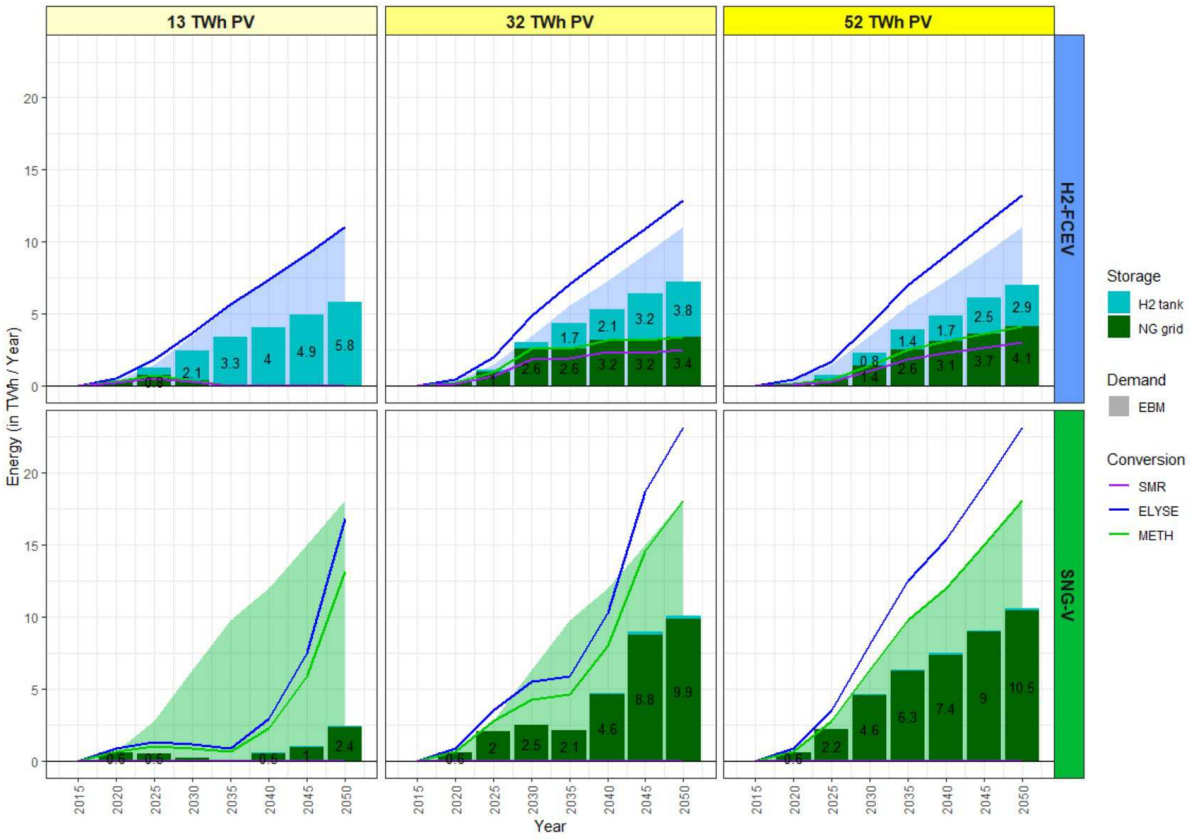

Figure 42 Total (integral) amount of fuel (H_2 and SNG) stored seasonally (NG grid) and short-term (H_2 storage tanks) for all years, all PV expansion scenarios and the "LC" import GHG scenario. The shaded areas represent the annual end-energy demand of H_2-FCEV and SNG-V. Solid lines are the annually produced end-energy by ELYSE, METH and SMR.

5.3.4. Greenhouse gas (GHG) emissions

5.3.4.1. Total (systemic) greenhouse gas (GHG) emissions

Figure 43 shows the overall (systemic) GHG emissions (including all life-cycle GHG emissions) associated with the three EBM (BEV, H_2-FCEV, SNG-V) and "non-EBM" powertrains for the three PV expansion and two import GHG scenarios ("LC" / "CCGT") for all years 2015 to 2050. A distinction between "additional SNG production" (three left columns) and "curtailment" (three right columns) of excess electricity is made (see section 2.3.10). Arrows indicate the additional GHG emissions of the EBM fleet added on top of the GHG emissions tied to the base electricity demand (dark grey area). GHG savings of the EBM against the reference "non-EBM" fleet are displayed as a light grey area along with their absolute numbers in 2050. GHG savings due to sector coupling ("add. SNG prod.") are displayed as a negative light blue area.

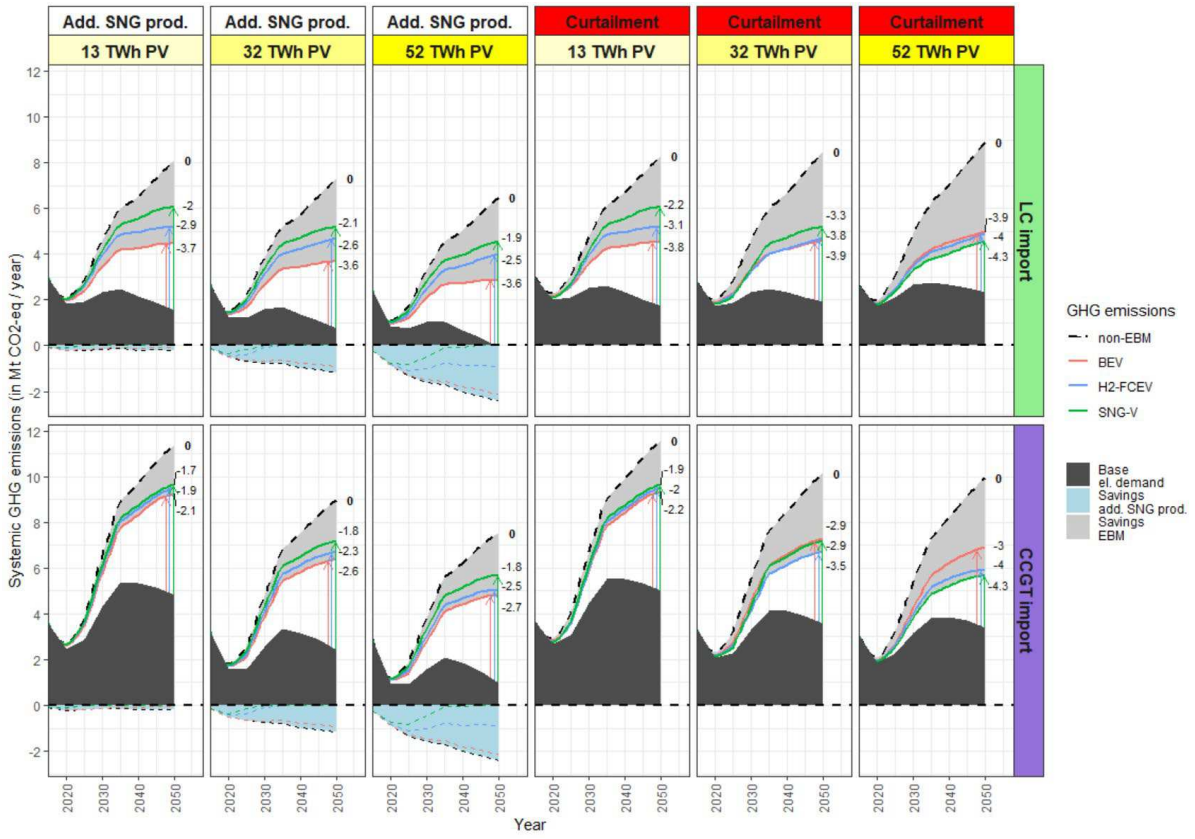

Figure 43 Overall (systemic) GHG emissions (in Mt CO2-eq / year) for all EBM (BEV, H_2-FCEV, SNG-V) and "non-EBM" powertrain scenarios in all PV expansion and import GHG scenarios. A distinction between "additional SNG production" and "curtailment" of excess electricity is made. The dark grey area shows the GHG emissions of the base electricity demand in the electricity sector (without mobility). The light grey area shows GHG savings of EBM powertrains against the "non-EBM" fleet. GHG savings due to "add. SNG prod." are displayed as a negative light blue area.

Irrespective of the PV expansion and import GHG scenario, all EBM powertrains always feature substantially lower GHG emissions than a corresponding "non-EBM" fleet. Systemic GHG savings of EBM compared to non-EBM range between -1.7 Mt $CO_{2\text{-eq}}$ ("SNG-V"; "13 TWh PV"; "CCGT"; "add. SNG prod.") and -4.3 Mt $CO_{2\text{-eq}}$ ("SNG-V; 52 TWh PV; LC; "curtailment") by 2050.

Regarding the three EBM powertrains individually, a clear distinction must be made between the scenarios and in particular with regard to excess electricity:

- **"Add. SNG prod.":** If additional SNG production from "excess" electricity due to a large PV expansion in Switzerland is possible and no curtailment occurs because there is enough additional demand for this SNG (e.g. heavy-duty transportation, process heat, etc.), BEV is in all scenarios the most GHG-efficient powertrain. The annual GHG reduction in 2050 with BEV compared to "non-EBM" in this case varies between -2.1 Mt $CO_{2\text{-eq}}$ ("BEV"; "13 TWh PV"; "CCGT"; "add. SNG prod.") and -3.7 Mt $CO_{2\text{-eq}}$ ("BEV", "13 TWh PV", "LC"; "add. SNG prod."). Within one GHG import scenario ("LC" or "CCGT"), GHG savings increase with an increasing PV expansion, in particular with CCGT imports. Without curtailment, also SNG-V and H_2-FCEV save at least -1.7 Mt $CO_{2\text{-eq}}$ ("SNG-V"; "13 TWh PV"; "CCGT"; "add. SNG prod.") against a corresponding non-EBM fleet.

- **“Curtailment”:** If there is substantial curtailment of excess electricity, H_2-FCEV and - with even more PV - SNG-V become equally or more GHG-efficient than BEV. This is in particular to case with high-carbon CCGT imports, where already in the 32 TWh PV case, scenarios with H_2-FCEV and SNG-V are slightly more GHG-efficient than BEV. This is mainly due to the fact that H_2-FCEV and SNG-V can either directly use the available excess electricity via ELYSE-METH or seasonally store it for times with otherwise only high-carbon electricity. Moreover, H_2-FCEV and SNG-V have the option to temporarily use grid NG, if electricity features higher GHG emissions. This increased flexibility in fuel supply and seasonal storability are assets of H_2-FCEV and SNG-V that BEV do not have and that result in equal to even lower systemic GHG emissions despite additional conversion losses and lower TTW powertrain efficiencies. Differences in terms of GHG mitigation between the three EBM technologies - given a scenario - are, however, typically small (i.e. less than 1 Mt $CO_{2\text{-eq}}$ by 2050). Therefore, with curtailment, only the extreme scenarios, namely “13 TWh PV” and “LC" as well as “52 TWh PV” and “CCGT”, show a clear superiority of particular EBM powertrains over the other(s), namely, BEV and SNG-V (and H_2-FCEV), respectively.

In reality, most likely a partial curtailment and additional SNG production (e.g. due to less installed ELYSE capacity in favour of more economical operation) would occur. Therefore, the two cases regarding the utilization of excess electricity can be seen as the two extremes with respect to systemic GHG emissions. These findings furthermore highlight the importance of using all excess electricity to reduce the allocated GHG impacts to BEV. In other words, a large BEV expansion in an energy system with large shares of PV is only more sustainable than other EBM powertrains, namely H_2-FCEV and SNG-V, if sector coupling (power-to-gas) is established alongside and if there are other energy sectors that can use this energy.

5.3.4.2. Specific GHG emissions

Specific GHG emissions of each powertrain are the difference between the GHG emissions tied to the base electricity demand (dark grey area) and the total systemic GHG emissions (lines) in Figure 4. In 2050, for all EBM powertrains, they are indicated by arrows and can be interpreted as short-term marginal GHG emissions. Given the total mileage of each powertrain, the specific GHG emissions of each powertrain per km travelled are obtained. This is shown in Figure 44 for all scenarios as well as a distinction between “Add. SNG prod.” and “Curtailment” of excess electricity (as in Figure 4). This representation of GHG emissions associated with each powertrains allows for more straightforward and more understandable comparison also with regard to legislative GHG emission targets in mobility.

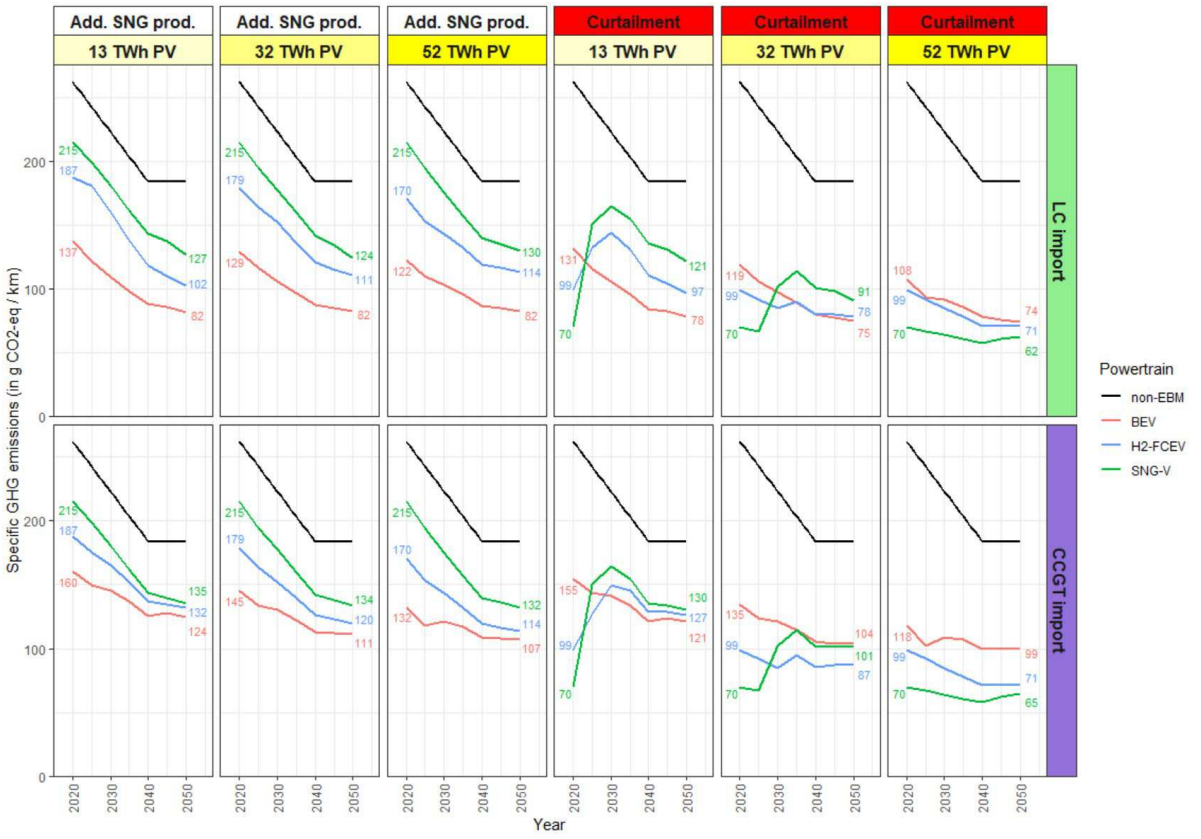

Figure 44 Specific life-cycle GHG emissions (in g $CO_{2\text{-eq}}$/km travelled) for all EBM (BEV, H_2-FCEV, SNG-V) and "non-EBM" powertrain scenarios in all PV expansion and import GHG scenarios. A distinction between "additional SNG production" and "curtailment" of excess electricity is made.

Depending on the year, PV expansion and import GHG scenario, these specific GHG emission range between 160 g $CO_{2\text{-eq}}$/km and 74 g $CO_{2\text{-eq}}$/km for BEV, 187 g $CO_{2\text{-eq}}$/km and 71 g $CO_{2\text{-eq}}$/km for H_2-FCEV and 215 g $CO_{2\text{-eq}}$/km and 62 g $CO_{2\text{-eq}}$/km for SNG-V, which is notably the lowest specific GHG emissions achieved by all EBM powertrains.

6. Impact of EV charging on low-voltage distribution grids: Methodology and Illustrative Simulations

6.1. Introduction

In this chapter, we tackle the problem of battery electric vehicle (BEV) penetration in low-voltage electric grids[4]. We present a Monte-Carlo-based method that sheds light on the effects that BEV charging has on grids' static security (i.e. nodal voltage magnitudes, branch current magnitudes and slack apparent power all within bounds). The method is illustrated on two real low-voltage networks situated in the western part of Switzerland (Rolle VD).

6.2. Monte-Carlo-based Load-Flow method

6.2.1. Concept

Load-flow Monte-Carlo simulations (LFMCSs) consist of carrying out a large number of load-flow computations with nodal active and reactive power injections randomly sampled from their respective probability density functions (PDFs) or cumulative distribution functions (CFDs) to output CDFs of network states[5]. In contrast to a traditional load-flow computation, that takes as input a deterministic vector of nodal power injections and outputs one vector of network states (i.e. complex nodal voltages in all nodes of the electrical grid), the aim of LFMCs is to output as many network states as the number of load-flow computations performed. The results are then used to create empirical CDFs of the network states and all other auxiliary electrical quantities that can be derived using the states[6]. Results of LFMCSs give an idea of the behavior of the electric grid quantities while taking account the stochasticity of the nodal power injections (i.e. stochastic renewable generation, EV loads and non-EV loads).

6.2.2. Method

Due to data scarcity, the idea of the developed method is to perform LFMCSs for every hour of a *representative* day. Representative days pertain to a specific season (i.e. winter, spring, summer and autumn) and day-type (i.e. workday or weekend/holidays).

To create the input PDFs/CDFs for the LFMCSs, the method needs hourly nodal injection profiles for every injection (i.e. active or reactive power injection) in the considered grid. Each hourly profile is first clustered into 4 seasons (i.e. $s \in${winter, spring, summer and autumn}), sub-clustered into day-type (i.e. $w \in${working days, weekend or vacation days}) then is sub-sub-clustered into hours of the day (i.e. $h \in${1,...,24}). Figure 45 illustrates the clustering.

[4] Note that, in this study, power grids are assumed balanced three-phase and are therefore modelled by their single-phase direct-sequence equivalent.

[5] We only mention power injections as we focus on low-voltage distribution grids and thus model all non-zero injection nodes as PQ-injection nodes.

[6] We assume here that the network topology and line parameters are known.

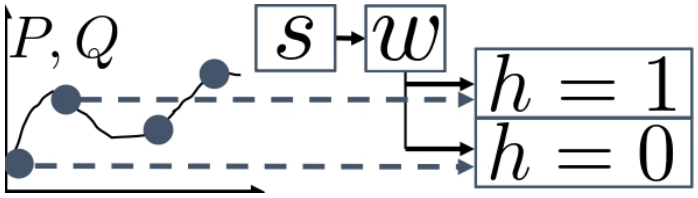

Figure 45 - Clustering illustration of a profile sampled hourly

After the clustering, the idea is to identify a PDF/CDF for each hour, of every day-type and season for every non-zero injection profile. Two options were considered to create the needed PDFs/CDFs:

1. Option 1 is based on non-parametric probability distribution identification. The empirical cumulative distribution function of the data of each sub-sub-cluster s_{w_h} is computed, and thus the needed CDFs are directly available.

2. Option 2 tries to quantify temporal correlation of data by fitting a multivariable distribution function over the 24 hours data contained in a sub-cluster s_w. Each random variable is, therefore, an hour of a sub-cluster. The fitting is repeated for every sub-cluster of every considered injection. In theory, the multivariable distribution can be either parametric or non-parametric but in practice, as our focus was not on function fitting, and we are using the MATLAB environment, we used a parametric approach, as non-parametric approaches were quickly non-tractable. The used PDF fitting method outputs a Gaussian Mixture Model (GMM). A GMM is a sum of multivariate Gaussian normal distributions (Reynolds, 2009). The number of Gaussian normal distributions is called the order of the GMM. On MATLAB, fitgmdist fits a GMM model to the inputted data. It has many options and needs as input arguments, at least, data and the GMM order. Seeing that fitgmdist has many input options, we implemented a *try-catch* function that tries to fit different GMM models with different orders and identification options until the *best-fit* (i.e. the one where the MATLAB algorithm converges with the least inferred probability error) is found. As an example, we considered the *shared covariance* identification option in our *try-catch* function. The *shared covariance* option, if set to TRUE, enforces that the same multivariate covariance matrix should be used for all the Gaussian distributions of the GMM. Indeed, that would entail that only the mean values would differ between the different terms of the GMM, which, in practice works well if the original data was close-to-normal and thus can be approximated with a single-order multivariate normal distribution. The implemented *try-catch* iterates over many options until convergence. The final output is the parametric expression of the multivariate PDF (and thus CDF) of a sub-cluster s_w belonging to an injection.

The choice between the two options is purely based on the datasets. The MATLAB function identifying the GMM models (fitgmdist) works well if the input data is large enough (i.e. number of measurements per random variable (here hour) should be larger than the total number of random variables (here 24)). Thus, a simple verification is done pre-identification to be sure that there is enough data for the *try-catch* function to converge.

The clustering and distribution identification process is repeated for all the profiles (i.e. all types (generation or load) of active and reactive power injections for all non-slack and non-zero injection nodes).

It is worth noting that hourly profiles should have *enough* (i.e. around one year hourly profiles) data for the clustering to be able to lead to meaningful distributions. The method to create the input PDFs/CDFs is schematically shown in Figure 46.

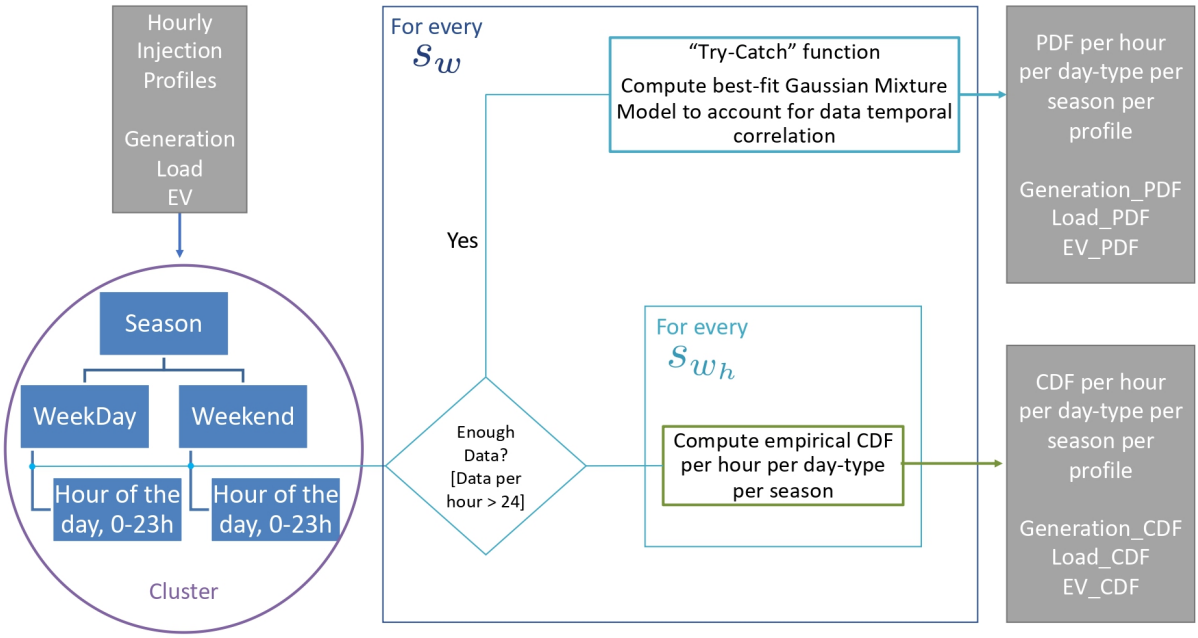

Figure 46 Schematic representation of the creation of the input CDFs

With the created distributions, LFMCSs are performed. Namely, for each hour of every day-type pertaining to a specific season, a large number (denoted by K) of load-flow computations (using the Newton-Raphson algorithm) is performed using injections that are randomly sampled from the created/inputted PDFs/CDFs.

After sampling all the PDFs/CDFs of all the injections of all nodes for a specific hour, day-type and season, a load-flow computation can be performed. As previously mentioned, this is done K times for every hour of every day-type and every season. Using the outputted states of all the load-flow computations (i.e. $|s|\ (=4)\ \times |w|\ (=2)\ \times |h|\ (=24)\ \times K = 192K$), we create CDFs of all the network states and auxiliary variables (e.g. branch currents, slack apparent power magnitudes, etc.) for every hour, day-type and season. The pseudo-code of the main algorithm used to perform the LFMCSs is shown in Figure 47.

```
For s = {Winter; Summer; Spring; Fall}
  For d = {Weekday; Weekend/Holiday}
    For h = {0,...,23}
      For r = 1,...,#ofRandomRealizations (=500)
        0. Initialize nodal injection vector
          P = zeros(n,1); where n is network size (multiplied by #of phases)
          Q = zeros(n,1); where n is network size (multiplied by #of phases)
        1. Generation,
          For n = nodes
            if n is Generation node
              Randomly sample Generation_CDF_P{s}{d}{h}{n} or Generation_PDF_P{s}{d}{h}{n} to get nodal active power injection, P_gen,n
              P(n) = P(n) + P_gen,n
              Randomly sample Generation_CDF_Q{s}{d}{h}{n} or Generation_PDF_Q{s}{d}{h}{n} to get nodal reactive power injection, Q_gen,n
              Q(n) = Q(n) + Q_gen,n
            end
          end
        2. Loads. Do as Generation but with Loads_CDF_P and Loads_CDF_Q to respectively sample P_load,n and Q_load,n and add them respectively to P(n) and Q(n)
        3. EV Loads Charging. Do as Generation but with EV_CDF_P and EV_CDF_Q to respectively c P_EV,n and Q_tEV,n and add them respectively to P(n) and Q(n)

        4. Perform Load-Flow computation using P and Q. Store all nodal voltages and branch currents with same clustering as Input Data.
      end
    end
  end
end
```

Figure 47 Pseudo-code of LFMCSs algorithm

6.3. Results

In order to illustrate the method, we show simulation results of LFMCSs performed on two real low-voltage grids situated in the western part of Switzerland (Rolle VD). Both grids do not have EV charging stations (CSs). However, for the purpose of the simulations we artificially added charging stations in nodes corresponding to real establishments (e.g. a company, a hospital, a residential building, etc.). Furthermore, the simulation includes EV charging profiles that were synthesized by taking into account the real characteristics of each establishment (e.g. number of residents in a residential apartment etc.), all while accounting for the behavior of EV users. The method used to create the latter is detailed in Pareschi et al. (2020). For both grids, LFMCSs are performed with different penetration percentages of EV CSs in order to highlight the influence of full, partial and null electrification of private transportation on the electric grid static security constraints (i.e. voltage magnitudes, branch current magnitudes and slack apparent power magnitudes within bounds).

6.3.1. Rolle - Gare

The network map, topology and real resource allocation are depicted in Figure 48. We recall that the EV CSs were added artificially as they do not exist in the real network.

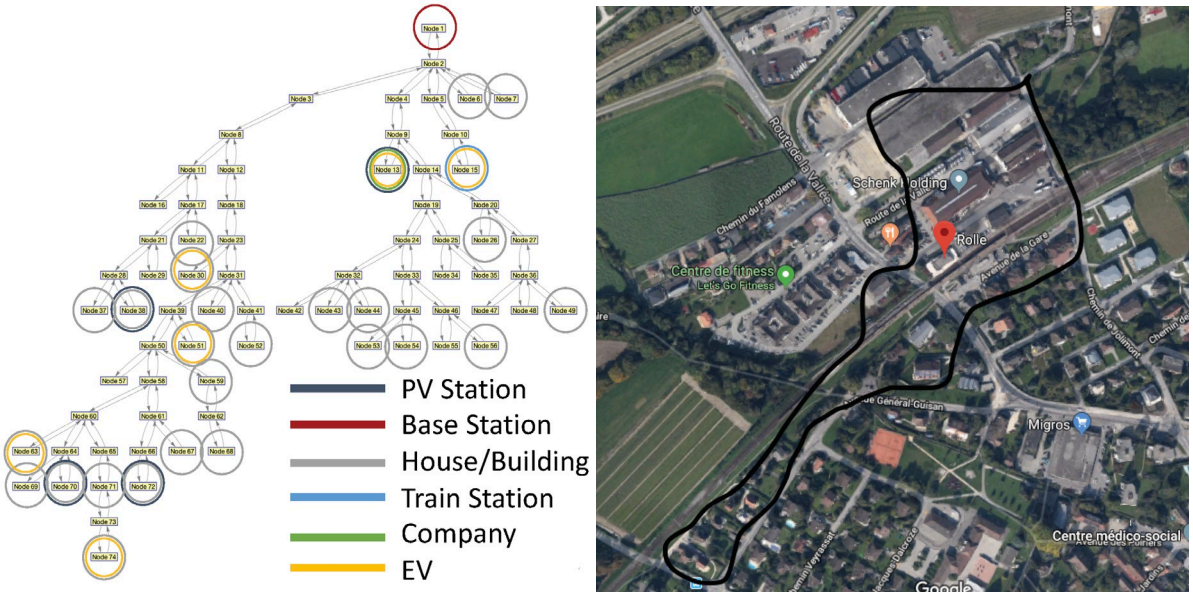

(a) Network Graph with Resource Allocation (b) Network Map

Figure 48 Rolle Gare Network Topology

The yearly profiles of every node, used to create the input CDFs needed for the LFMCSs are shown in Figure 49. The active generation profile (Figure 49(a)) is a real measured aggregated PV injection profile from the region of Rolle VD[7]. The data was not measured at the Gare network, however, with the known real maximum power ratings of each installed PV plant in the Gare network, we were able to disaggregate the profile and get the active power injection profile for each node with a PV installation. This is fair as the network radius is small enough that PV profiles of each node have most probably unitary spatial and time correlations.

[7] The data for reactive power injections for PV installations were not available and therefore assumed to be null.

The generation profile and load profiles correspond to measurements taken, respectively, from 01.01.2014 to 27.07.2016 and from 01.01.2018 to 07.11.2018. The active and reactive load profiles are shown in Figure 49(b). The trends come from real data measurements. The measurements come from three different locations: (i) USA (more information and description can be found in OEDI (2020), (ii) Italy (more information and description can be found in Terni (2020)) and (iii) Germany (more information and description can be found in Minde (2020)). Note that, only a subset of profiles were used in our simulations. The latter were all scaled using the real known peak active/reactive power load of the Rolle-Gare grid. As a result, each non-EV load injection encapsulates the behavior of the node (i.e. restaurant, train-station, household, etc.) and is scaled properly to have the correct order of magnitudes. Two sets of absorption (i.e. only EV charging) profiles of EV CSs (see Figure 50) were synthesized for this grid[8]: the first (see Figure 50(a)) assumes that EV chargers can be placed everywhere (i.e. residential and point-of-interest chargers), and, the second (see Figure 50(b)) assumes that EV chargers can be placed only at home (i.e. only residential charging). To synthesize them, 100% electrification of vehicles was assumed. Home chargers were assumed to be rated at 2.3 kW while all other chargers were rated at 3.7 kW. All EVs were assumed battery EVs with 80 kWh of nominal capacity. Each profile was synthesized while taking into account the exact nature (e.g. number of vehicles, peak hours, etc.) of each node (e.g. hospital, work place, home etc.) it is connected to. More specifically, in Figure 50.

1. EV-Home corresponds to the aggregated charging profile (CP) of all residential buildings of the grid. That profile was then disaggregated on the different real residential nodes proportionally to the number of habitants per node,
2. EV-Work corresponds to the aggregated CP of Schenk SA Warehouse. To create the profile it was estimated that about 126 employees worked there,
3. EV-Station corresponds to the CP of the potential commuters passing by the Rolle train-station.

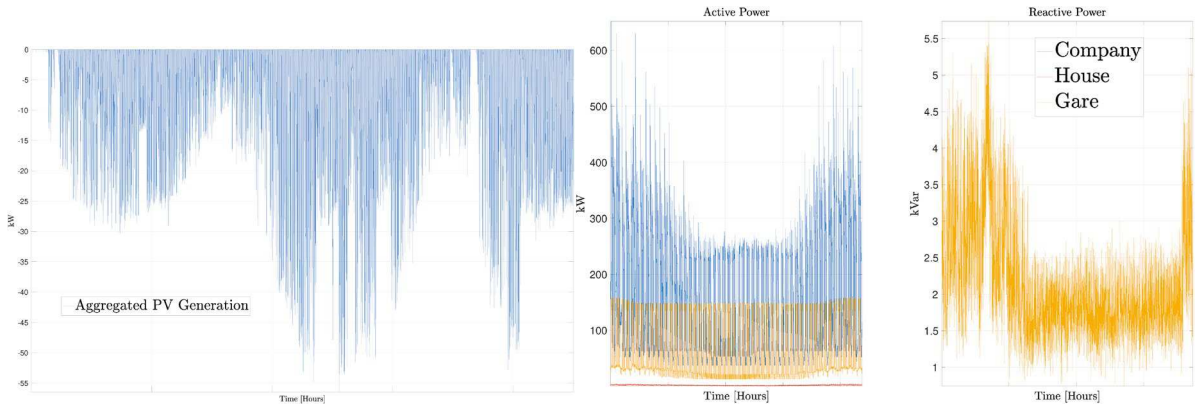

(a) Aggregated PV Generation Hourly Profile

(b) Aggregated Load Hourly Profile

Figure 49 - Inputted non-EV active and reactive nodal injection profiles

[8] Provided by Aerothermochemistry and Combustion Systems Laboratory, ETH Zurich, Switzerland

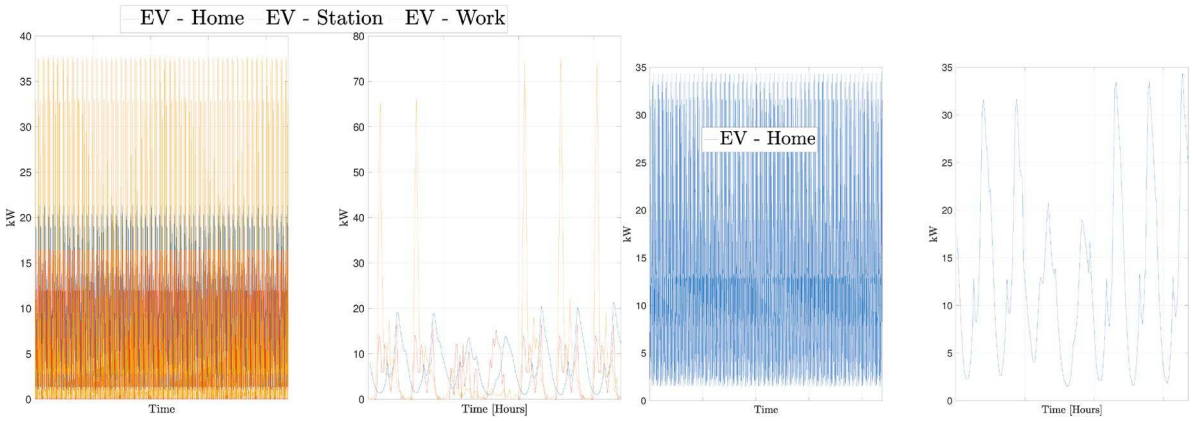

(a) Chargers everywhere (b) Only-home charging

Figure 50 - Inputted EV active (charging) nodal injection profiles

The post-LFMCSs results can be found in Figure 51 - Figure 61. All LFMCSs assume a voltage tolerance around nominal voltage of $\beta = 10\%$and use the real branch ampacity limits of the grid. Figure 51 - Figure 54 show the quantiles computed over the K load-flow simulations, of the voltage and branch current magnitudes for all seasons, day-types and hours, for three different EV injection scenarios: no EV injection, home charging and home-and-point-of-interests (POI) charging. Figure 55 shows the boxplot representation of the slack apparent power over the Kload-flow simulations for all seasons, day-types and hours, for all three EV injection scenarios. In the figures, the scales (color axis) are either in per unit (voltage and slack apparent power) or in per unit ampacity (branch currents). It is clear from these figures that without EV injections the Rolle-Gare grid does not suffer any grid security violations, with only home charging, the grid suffers from voltage, branch current and slack apparent power violations, and, with home-and-POIs charging, the grid only suffers from voltage and slack apparent power violations.

(a) Without EV charging

(b) Only home EV charging

(c) Home-and-POIs EV charging

Figure 51 - Nodal voltage magnitudes - Min, mean and max over all K simulations

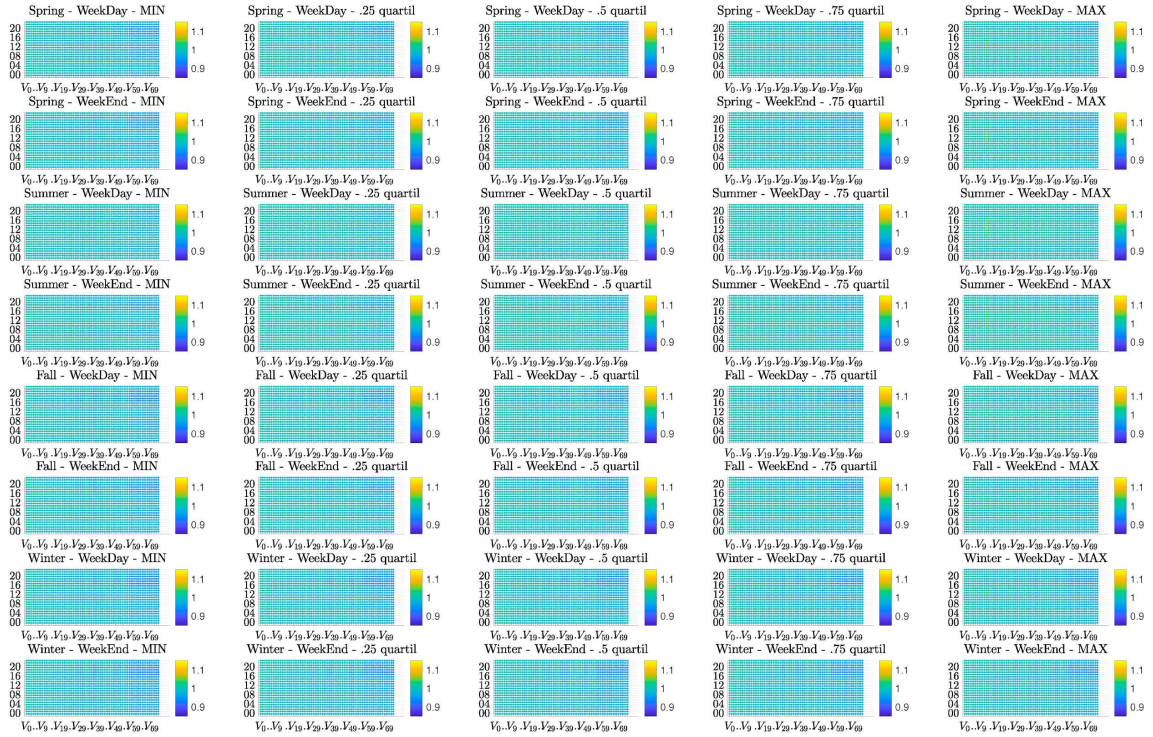

(a) Without EV charging

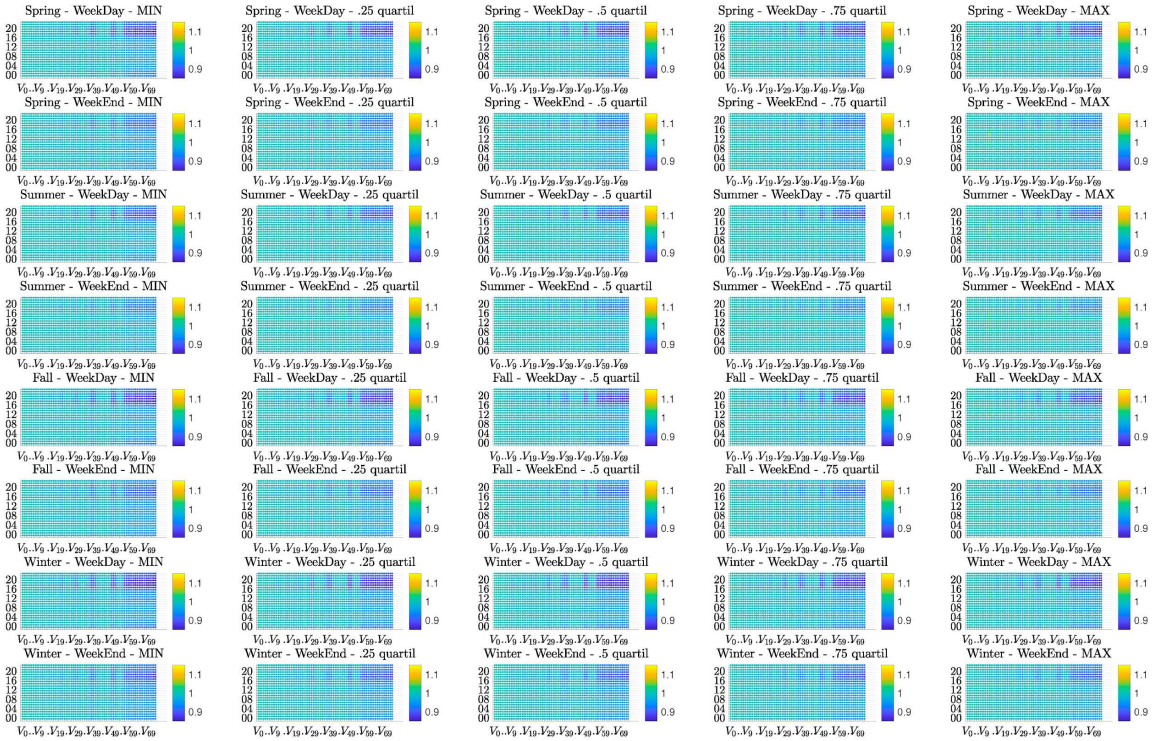

(b) Only home EV charging

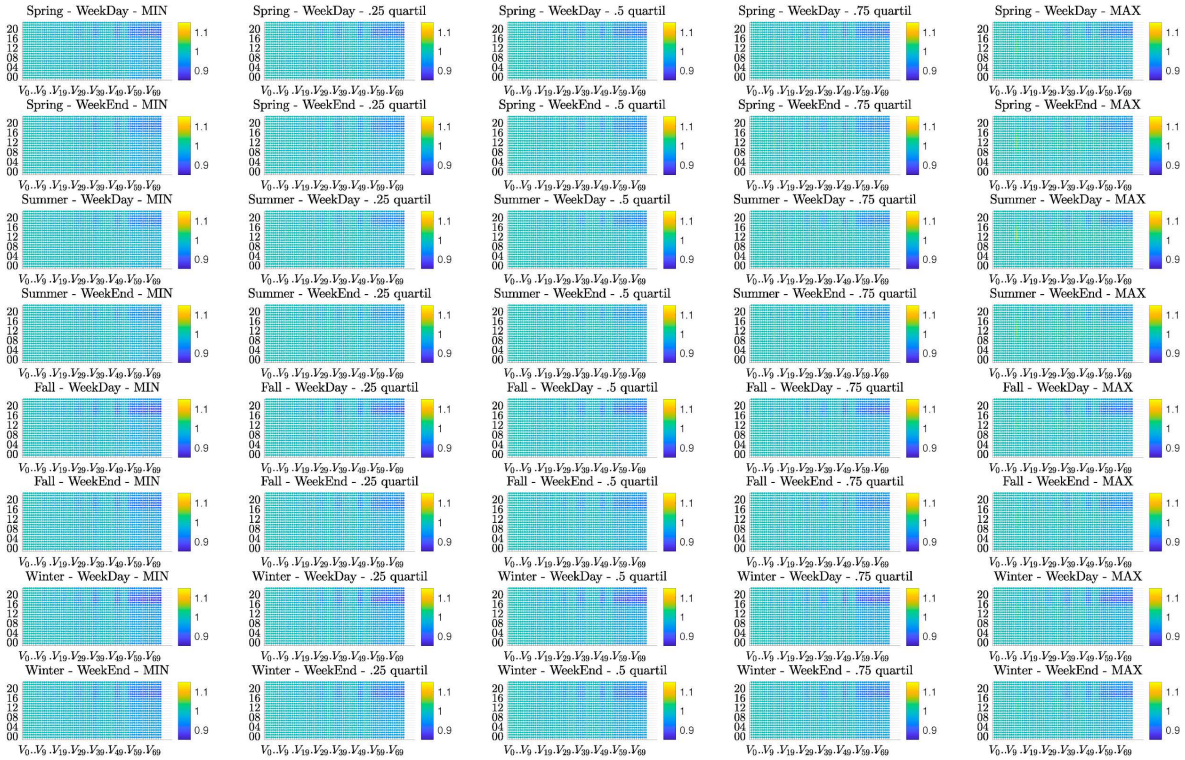

(c) Home-and-POIs EV charging

Figure 52 - Nodal voltage magnitudes - Quantiles over all K simulations

(a) Without EV charging

(b) Only home EV charging

(c) Home-and-POIs EV charging

Figure 53 - Branch current magnitudes - Min, mean and max over all K simulations

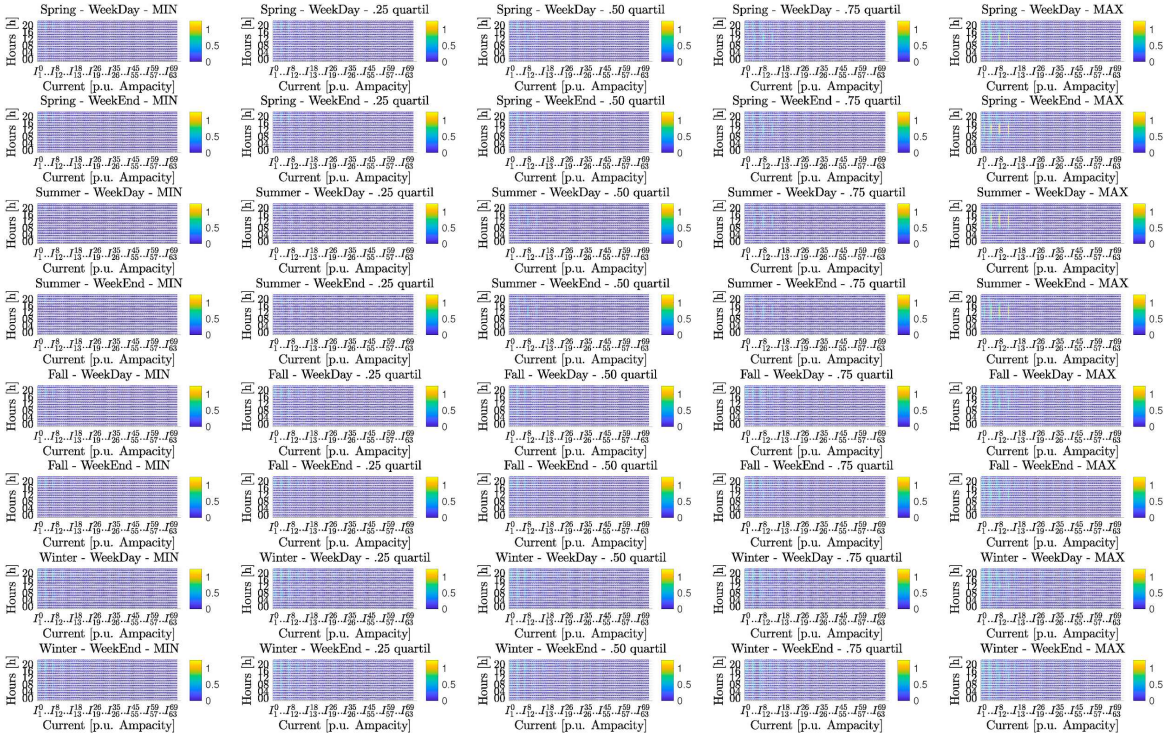

(a) Without EV charging

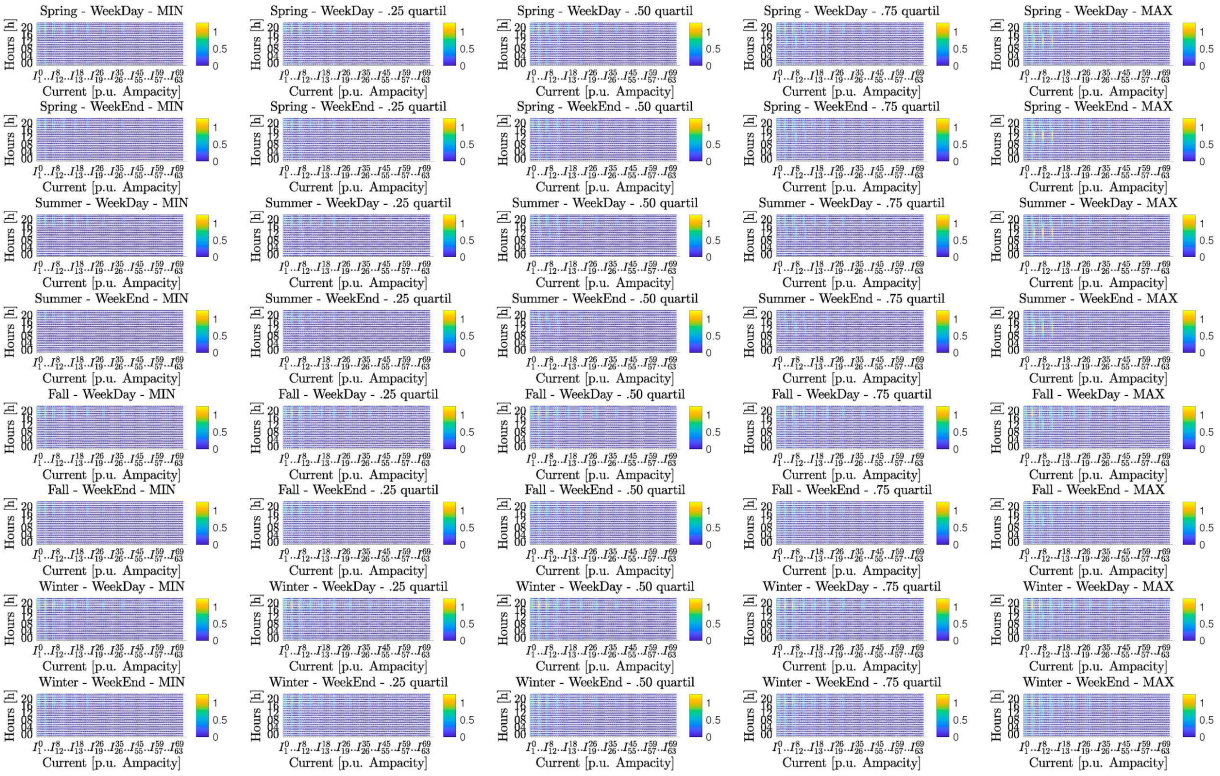

(b) Only home EV charging

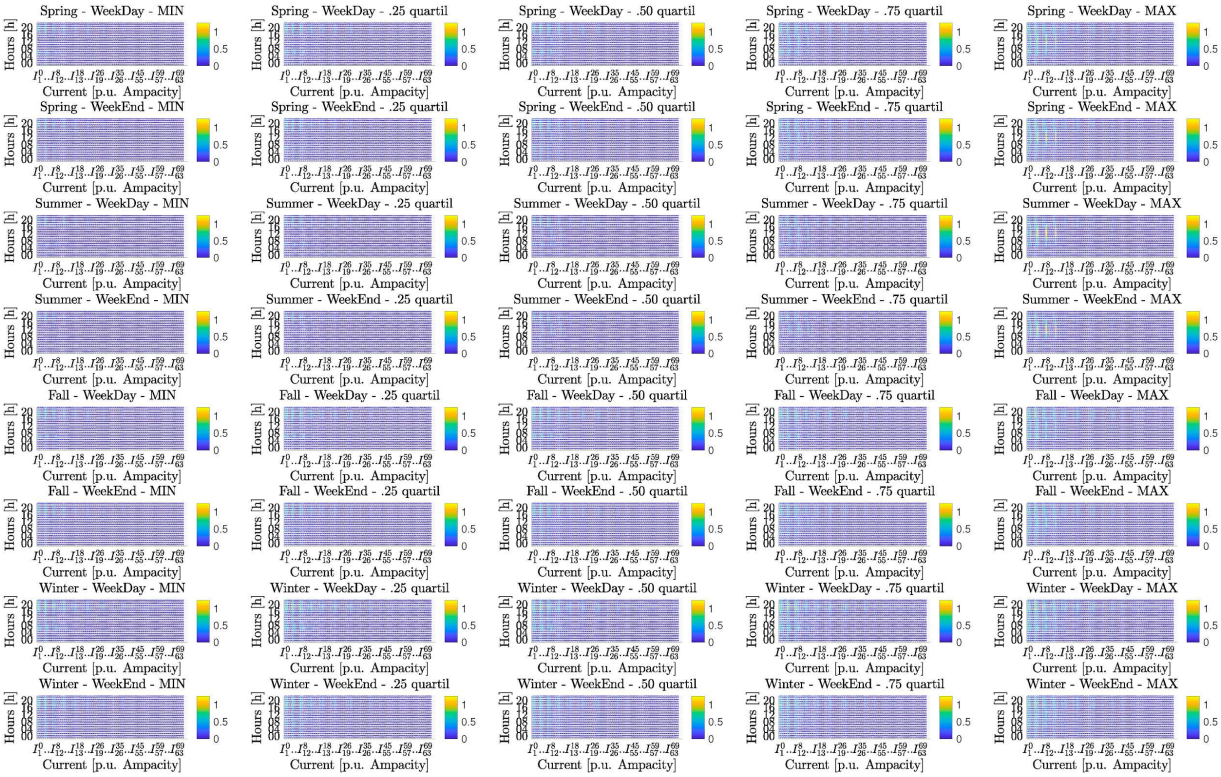

(c) Home-and-POIs EV charging

Figure 54 - Branch current magnitudes - Quantiles over all K simulations

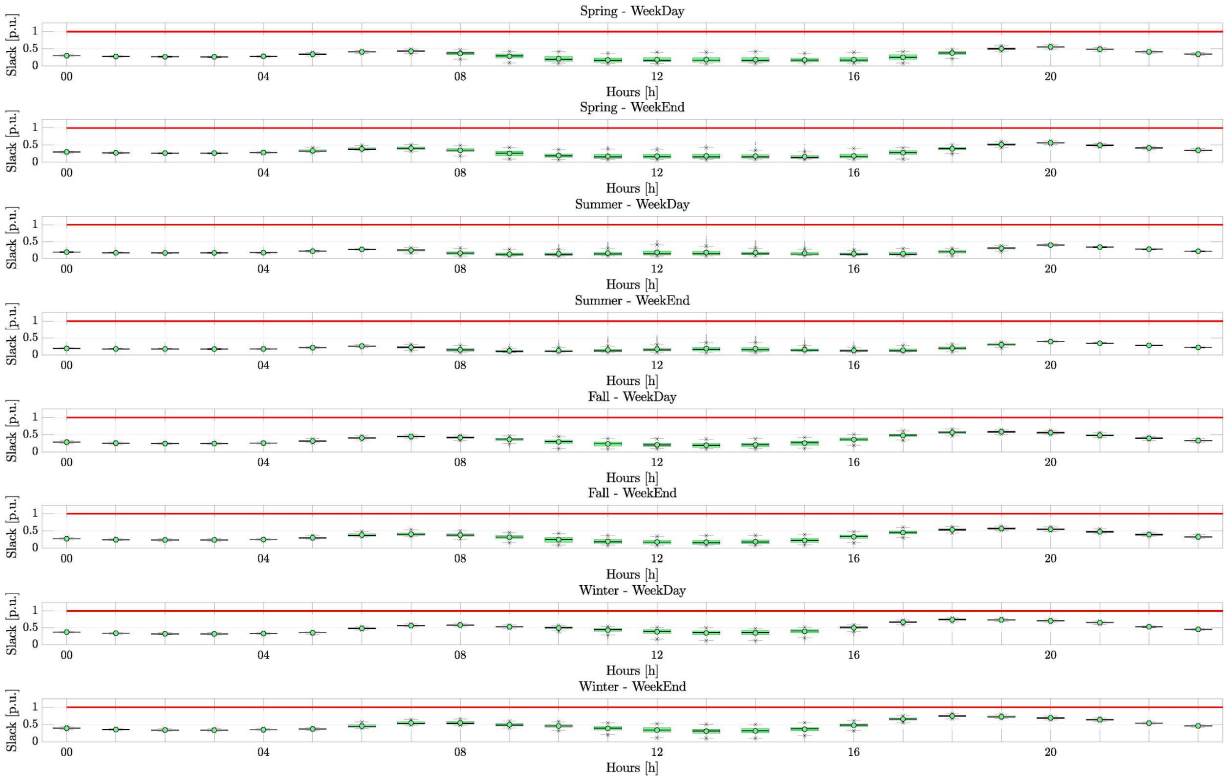

(a) Without EV charging

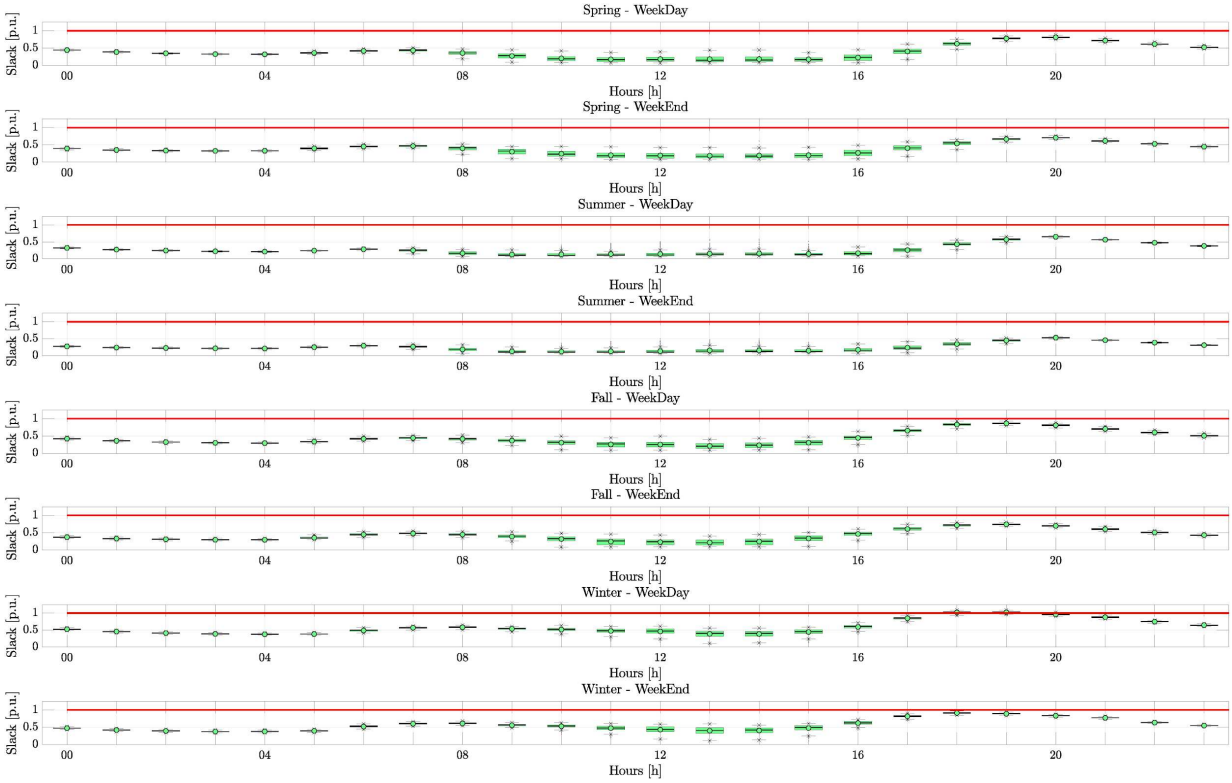

(b) Only home EV charging

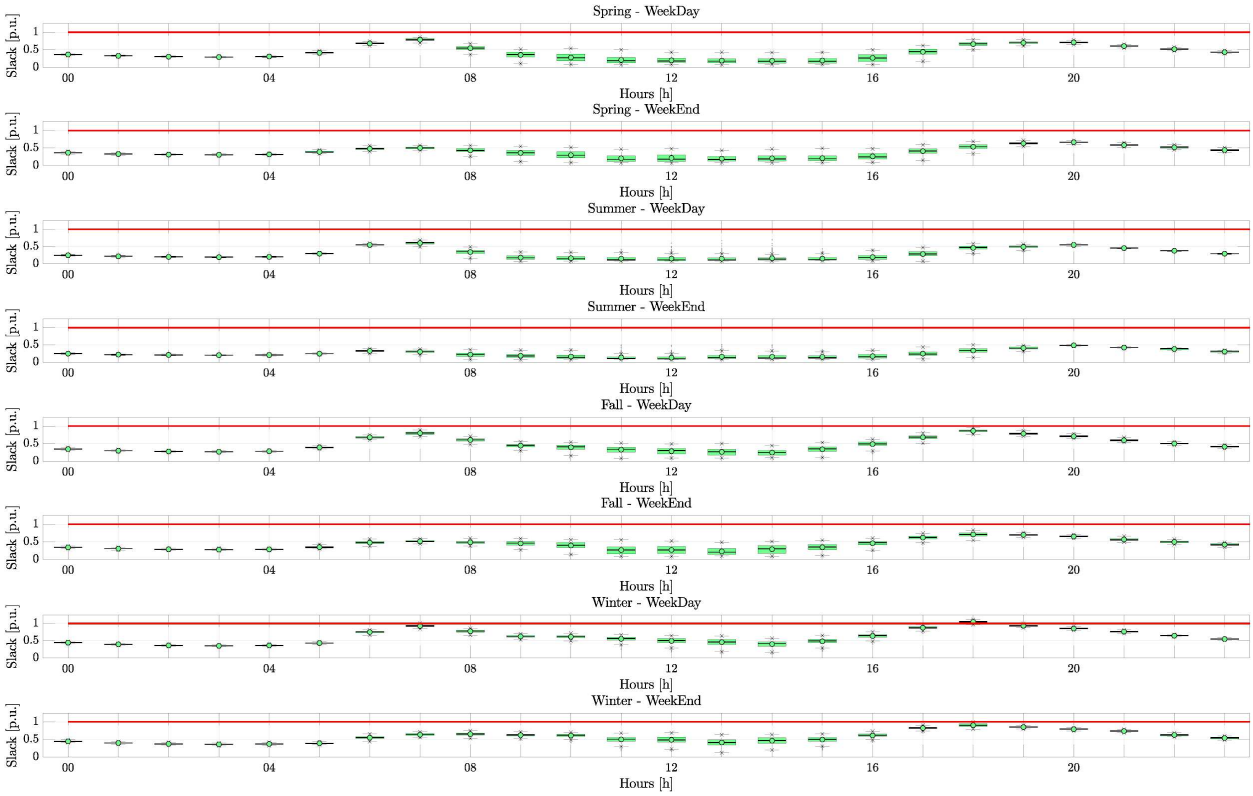

(c) Home-and-POIs EV charging

Figure 55 - Apparent power magnitudes - Boxplot over all K simulations

To go a step further and to show the sensitivity analysis vis-a-vis the percentage of transport electrification, Figures 56 to 61 show the probabilities (computed directly from the outputted CDFs of the states and auxiliary variables) to violate the grid security constraints. In principle, each figure should contain five subsub-figures encapsulating respectively, 0%, 25%, 50%, 75% and 100% EV penetration, however, in practice, for compactness, some graphs have been omitted when there were no grid violations (i.e. probability equal to 0 for all seasons, day-types and hours). One can conclude from the figures that:

1. Without EV charging there are no violations of the grid security constraints
2. With *only* home charging, at 25% EV penetration there are no grid violations, while at 50% and 75%, there are only nodal voltage magnitude violations and at 100% all grid constraints are at risk to be violated.
3. With home and POI charging, at 25% and 50% EV penetration there are no grid violations, while at 75% and 100% there are nodal voltage magnitude and apparent slack power magnitude violations.
4. The more EV injections the more likely (i.e. higher probability) the constraints can be violated.
5. Voltage magnitude constraint violations occur mostly at night when there is no PV generation injecting in the grid. Indeed, the violations are more likely to happen in the winter when heating electricity demands are increased compared to the summer. The nodes at the end of the feeder are more likely to have violations compared to the ones next to the slack node. This is in accordance with the radiality of the network topology, the line losses principle and EV load placement. More than one node suffers from potential voltage magnitude constraint violations.
6. With the exception of the branch connecting nodes 2 and 7, the ampacity limits of the Rolle-Gare grid branches are high enough to sustain extra EV loads (i.e. zero probability to violate

branch current constraints). However, it is clear that at night in the winter, the branch connecting nodes 2 to 7 risks having branch current violations with up to 90%. This is unacceptable as it can damage the electrical grid, which suggests that in grids such as this one, even though uncontrolled night charging at home is acceptable most of the year, in the winter it can have damaging consequences.

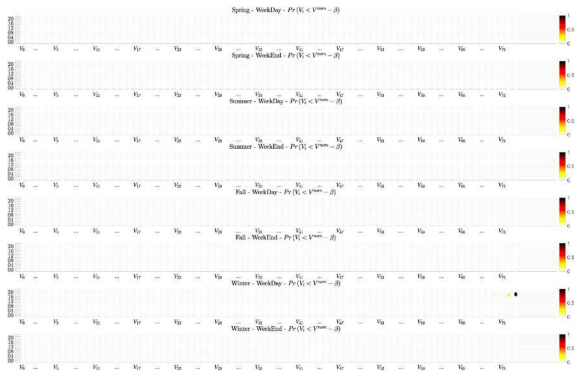

(a.i) 50% EV Penetration / only home EV charging

(a.ii) 75% EV Penetration / only home EV charging

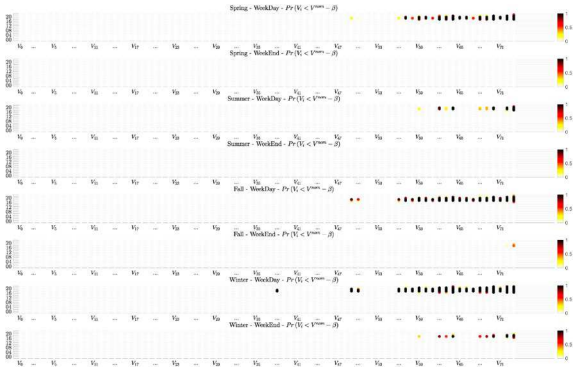

(a.iii) 100% EV Penetration / only home EV charging

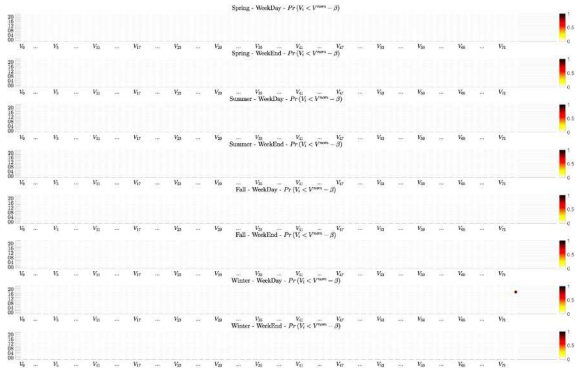

(b.i) 75% EV Penetration / Home-and-POIs EV charging

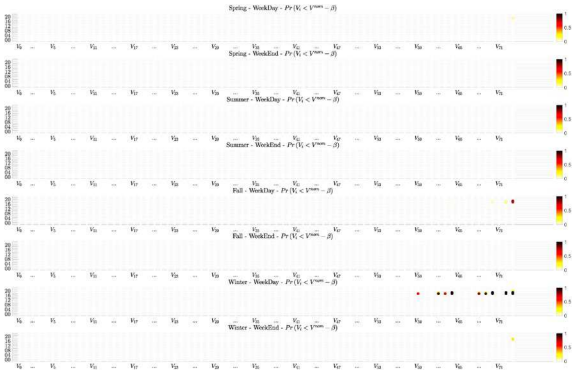

(b.ii) 100% EV Penetration / Home-and-POIs EV charging

Figure 56 - Probability to violate nodal voltage magnitudes

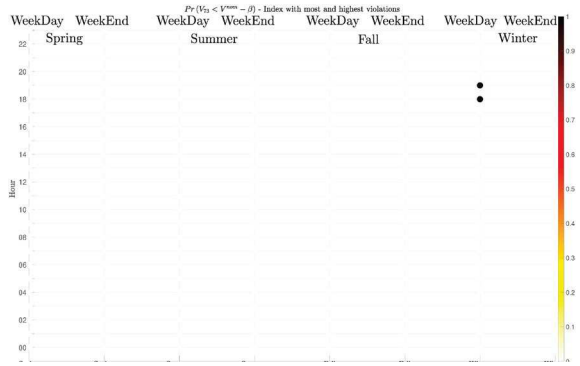

(a.i) 50% EV Penetration / Only home EV charging

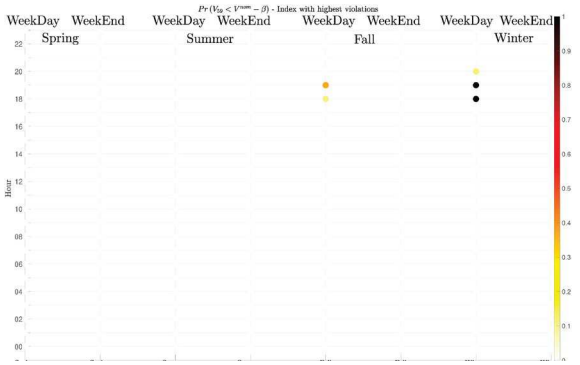

(a.ii) 75% EV Penetration / Only home EV charging

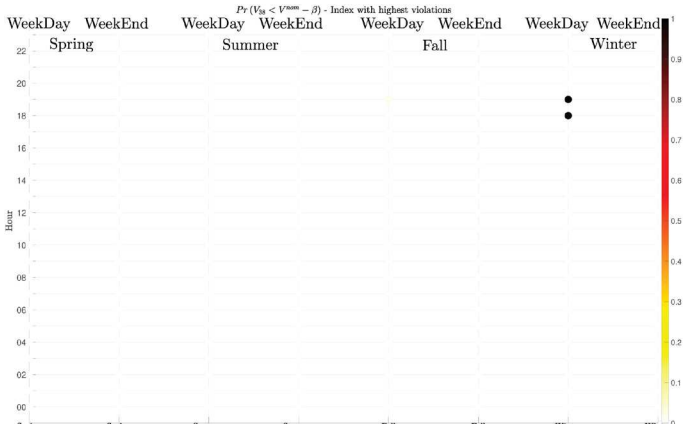

(a.iii) 100% EV Penetration / Only home EV charging

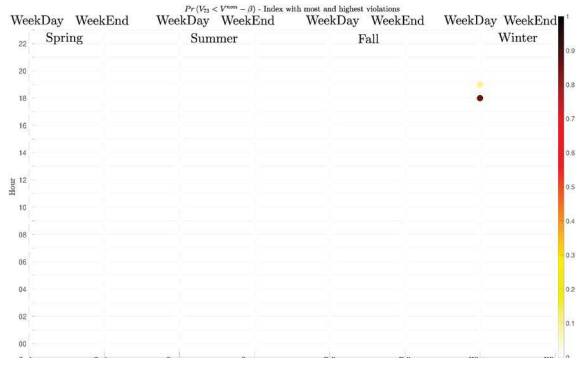

(b.i) 75% EV Penetration / Home-and-POIs EV charging

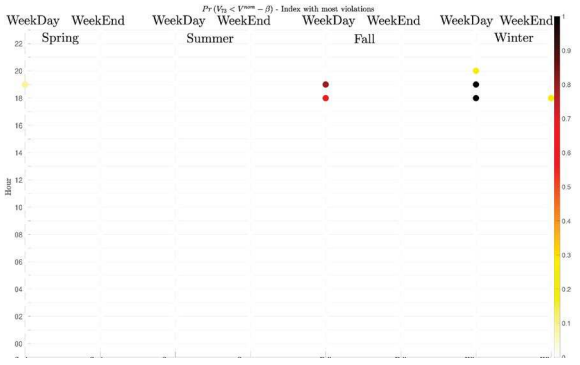

(b.ii) 100% EV Penetration / Home-and-POIs EV charging

Figure 57 - Probability to violate nodal voltage magnitudes of node with highest violations

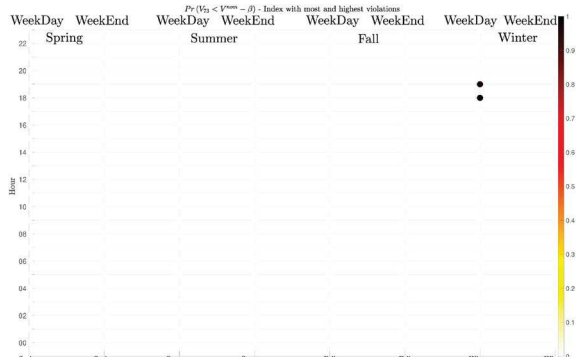

(a.i) 50% EV Penetration / Only home EV charging

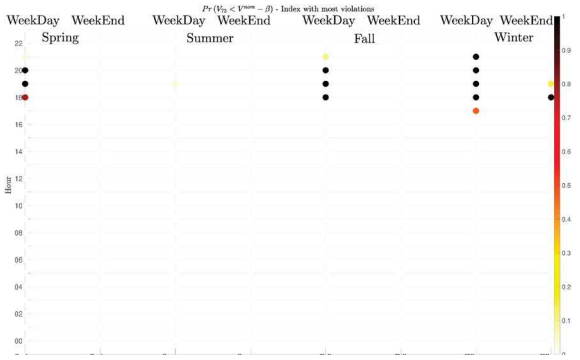

(a.ii) 75% EV Penetration / Only home EV charging

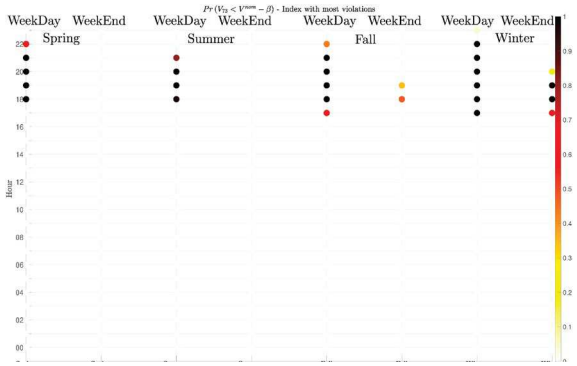

(a.iii) 100% EV Penetration / Only home EV charging

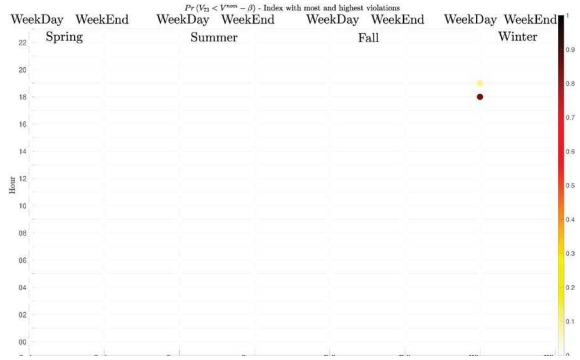

(b.i) 75% EV Penetration / Home-and-POIs EV charging

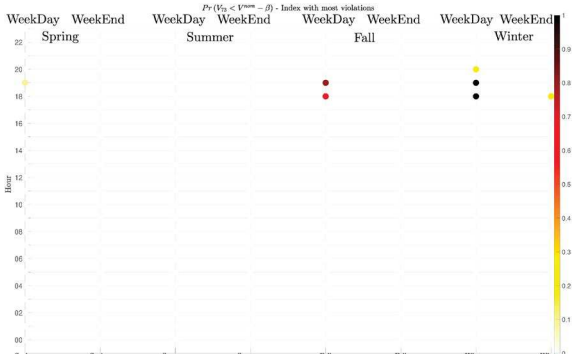

(b.ii) 100% EV Penetration / Home-and-POIs EV charging

Figure 58 - Probability to violate nodal voltage magnitudes of node with most violations

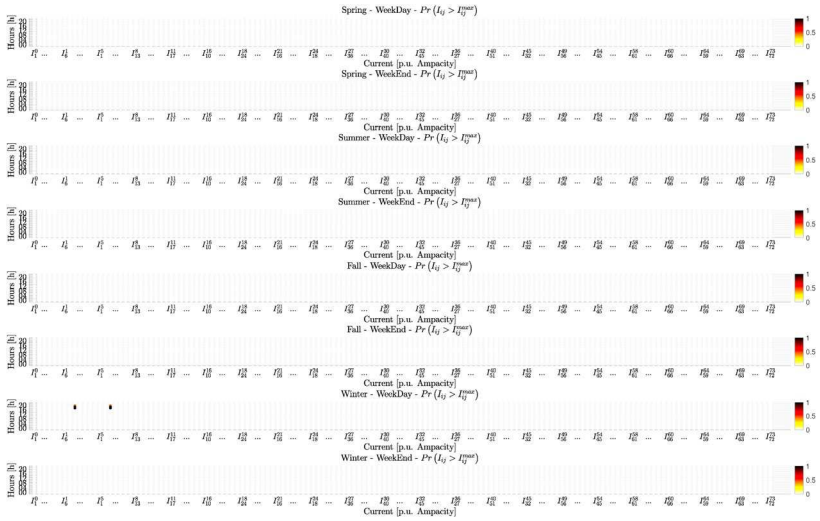

Figure 59 - Probability to violate branch current magnitudes - Only home EV charging- 100% EV Penetration

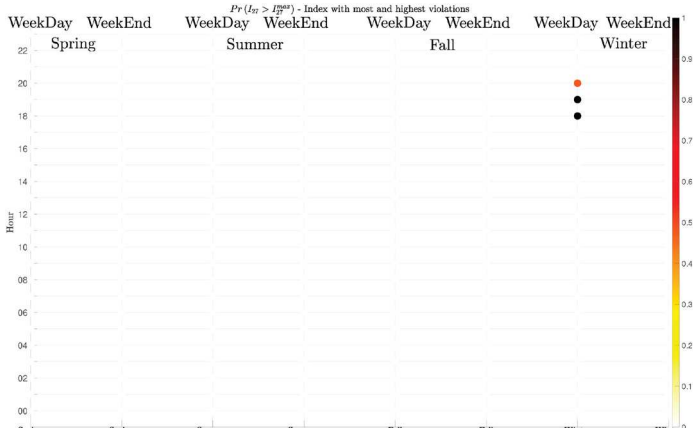

Figure 60 - Probability to violate branch current magnitudes of branch with highest & most violations - Only home EV charging- 100% EV Penetration

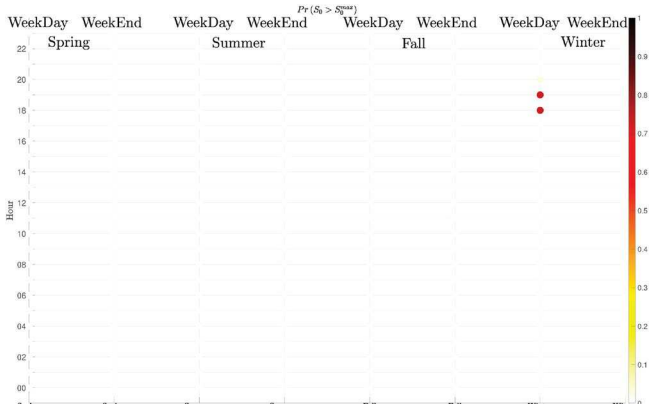

(a) 100% EV Penetration / Only home EV charging

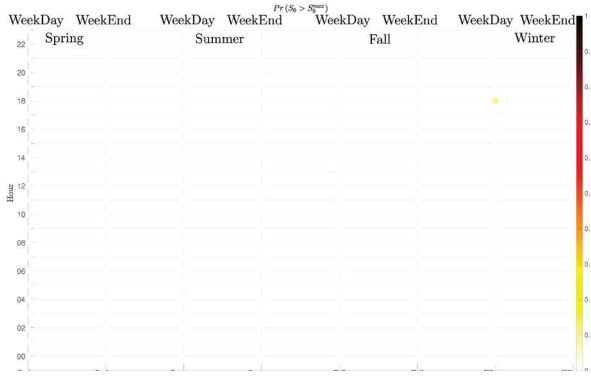

(b.i) 75% EV Penetration / Home-and-POIs EV charging

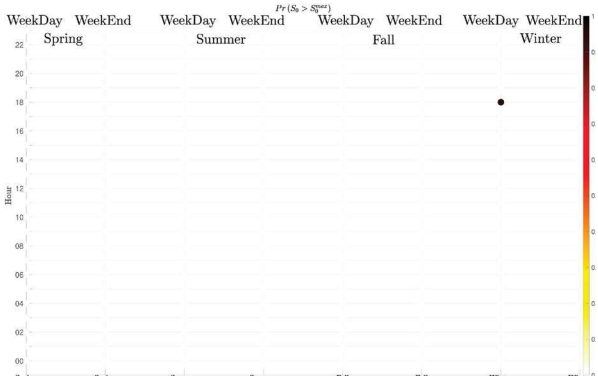

(b.ii) 100% EV Penetration / Home-and-POIs EV charging

Figure 61 - Probability to violate slack apparent power magnitude

6.3.2. Rolle - Hopital

The network map, topology and real resource allocation are depicted in Figure 62. We recall that the EV CSs were added artificially as they do not exist in the real network.

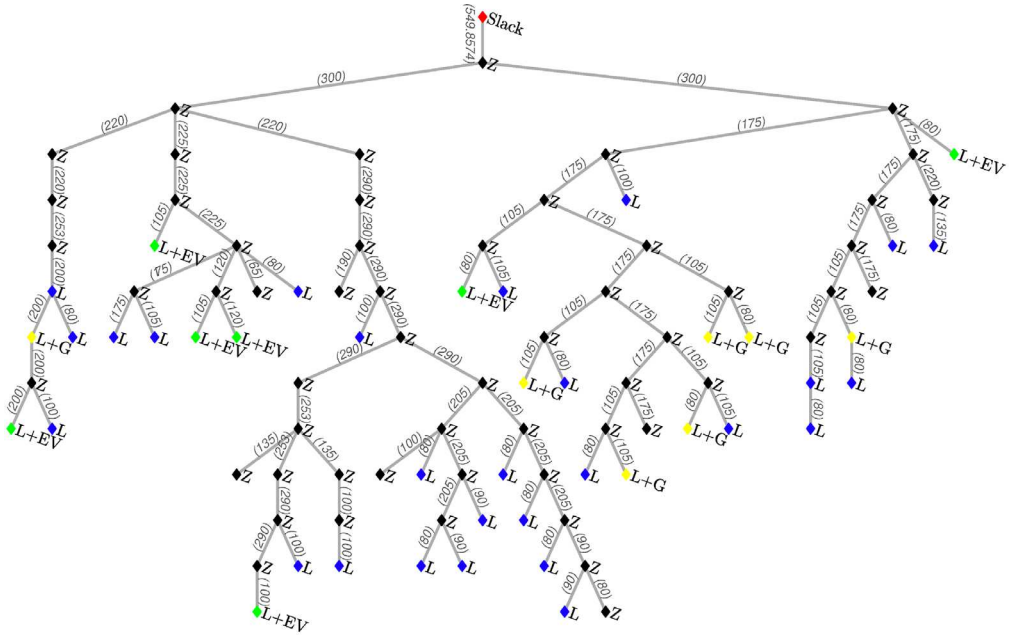

(a) Network Graph with Resource Allocation. Slack (red) is the slack node, Z (black) are zero-injection nodes, L (blue), L+EV (green) and L+G (yellow) are resource nodes with, respectively, only loads, loads and EV CSs and, loads and PV generation. In parenthesis are the branch ampacity limits in amperes.

(b) Network Map

Figure 62 - Rolle Hopital Network Topology

The yearly profiles of every node, used to create the input CDFs needed for the LFMCSs are shown in Figure 63. The active generation profile (Figure 63a) is a real measured aggregated PV injection profile from the region of Rolle VD[9]. The data was not measured at the Hospital network, however, with the known real maximum power ratings of each installed PV plant in the network, we were able to disaggregate the profile and get the active power injection profile for each node with a PV installation. As previously explained, this is fair as the network radius is small enough that PV profiles of each node have most probably unitary spatial and time correlations. The generation profile and load profiles correspond to measurements taken, respectively, from 01.01.2014 to 27.07.2016 and from 01.01.2018 to 07.11.2018.

The active and reactive load profiles are shown in Figure 63b. The trends come from real data measurements. The measurements come from three different locations: (i) USA (more information and description can be found in OEDI (2020)), (ii) Italy (more information and description can be found in Terni (2020)) and (iii) Germany (more information and description can be found in Minde (2020)). Note that, only a subset of profiles were used in our simulations. The latter were all scaled using the real known peak active/reactive power load of the Rolle-Hôpital grid. As a result, each non-EV load injection encapsulates the behavior of the node (i.e. restaurant, train-station, household, etc.) and is scaled properly to have the correct order of magnitudes. Two sets of absorption (i.e. only EV charging) profiles of EV CSs (see Figure 64) were synthesized[10] for this grid: the first (see Figure 64a) assumes that EV chargers can be placed everywhere (i.e. residential and point-of-interest chargers), and, the second (see Figure 64b) assumes that EV chargers can be placed only at home (i.e. only residential charging). To synthesize them, as before, 100% electrification of vehicles was assumed.

Home chargers were assumed to be rated at 2.3 kW while all other chargers were rated at 3.7 kW. All EVs were assumed battery EVs with 80 kWh of nominal capacity. Each profile was synthesized while taking into account the exact nature (e.g. number of vehicles, peak hours, etc.) of each node (e.g. hospital, work place, home etc.) it is connected to. More specifically, in Figure 64.

1. EV-Home corresponds to the aggregated charging profile (CP) of all residential buildings of the grid. That profile was then disaggregated on the different real residential nodes while considering that buildings on the eastern side of the grid have higher population density,
2. EV-Restaurant corresponds to the aggregated CP of the bakery (Café Milo) and the restaurant (Il Puulcinella) present in the grid. The CP is then split between the two nodes accounting for the fact that dinner demand peaks correspond to the restaurant while during lunch time both bakery and restaurant have comparable peaks,
3. EV-Hospital corresponds to the CP of the hospital node. This profile considers two types of EV users: (i) the permanent hospital employees (estimated to be 128 people), and, (ii) the profiles from walk-in patients that drove themselves to the hospital.

[9] The data for reactive power injections for PV installations were not available and therefore assumed to be null.

[10] Provided by Aerothermochemistry and Combustion Systems Laboratory, ETH Zurich, Switzerland

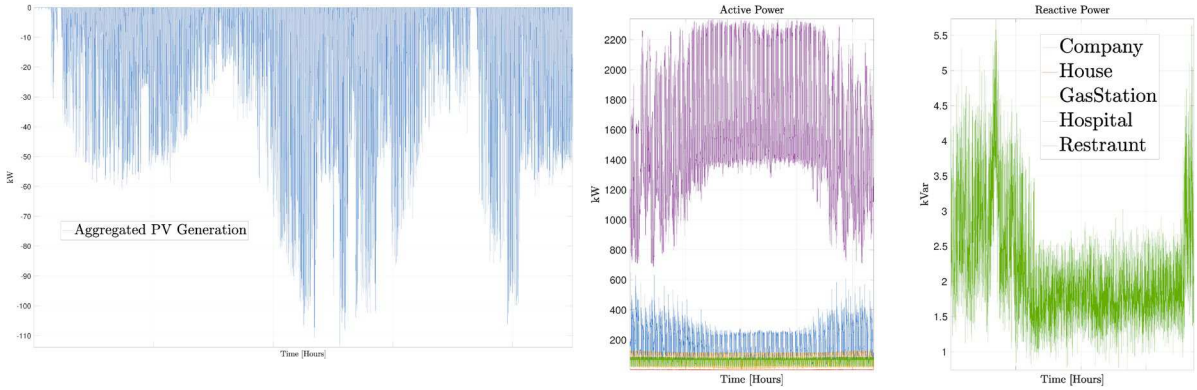

(a) Aggregated PV Generation Hourly Profile (b) Aggregated Load Hourly Profile

Figure 63 - Inputted non-EV active and reactive nodal injection profiles

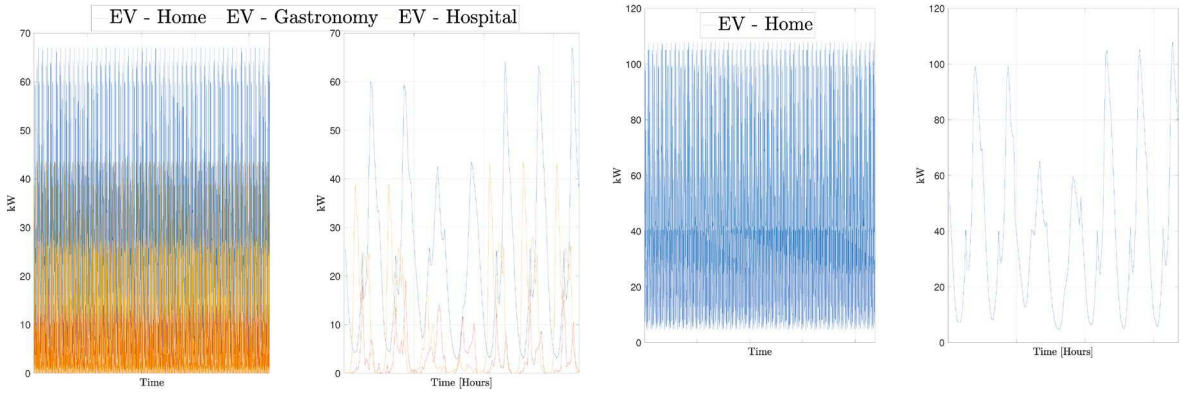

(a) Chargers everywhere (b) Only-home charging

Figure 64 - Inputted EV active (charging) nodal injection profiles

The post-LFMCSs results can be found in Figure 65 to Figure 76. All LFMCSs assume a voltage tolerance around nominal voltage of $\beta = 10\%$and use the real branch ampacity limits of the grid. Figure 65 - Figure 68 show the quantiles computed over the K load-flow simulations of the voltage and branch current magnitudes for all seasons, day-types and hours, for three different EV injection scenarios: no EV injection, home charging and home-and-point-of-interests (POI) charging.

Figure 69 shows the boxplot representation of the slack apparent power over the K load-flow simulations for all seasons, day-types and hours, for all three EV injection scenarios. As before, in the figures, the scales (color axis) are either in per unit (voltage and slack apparent power) or in per unit ampacity (branch currents). Unlike the previous grid, without EV injections the Hospital grid suffers from nodal voltage magnitude violations. Furthermore, with only home and home-and-POIs charging, the grid suffers from voltage, branch current and slack apparent power violations.

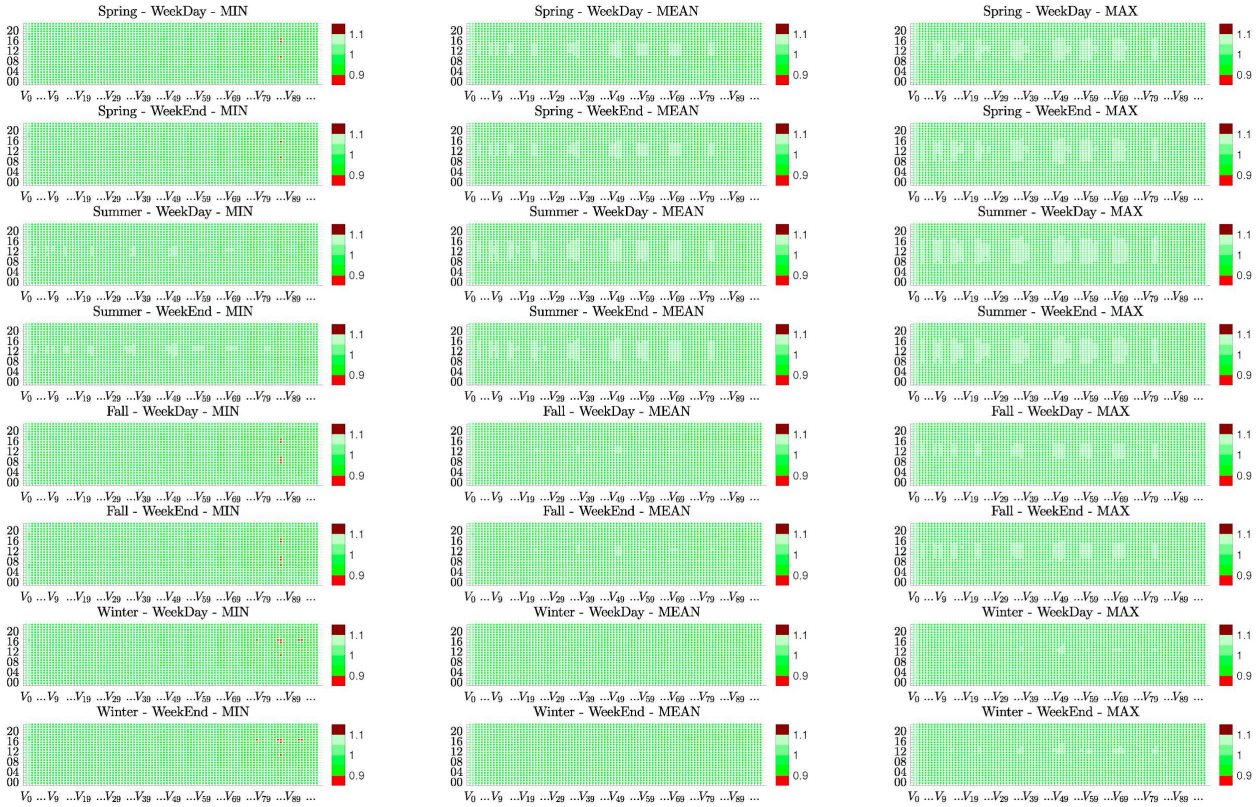

(a) Without EV charging

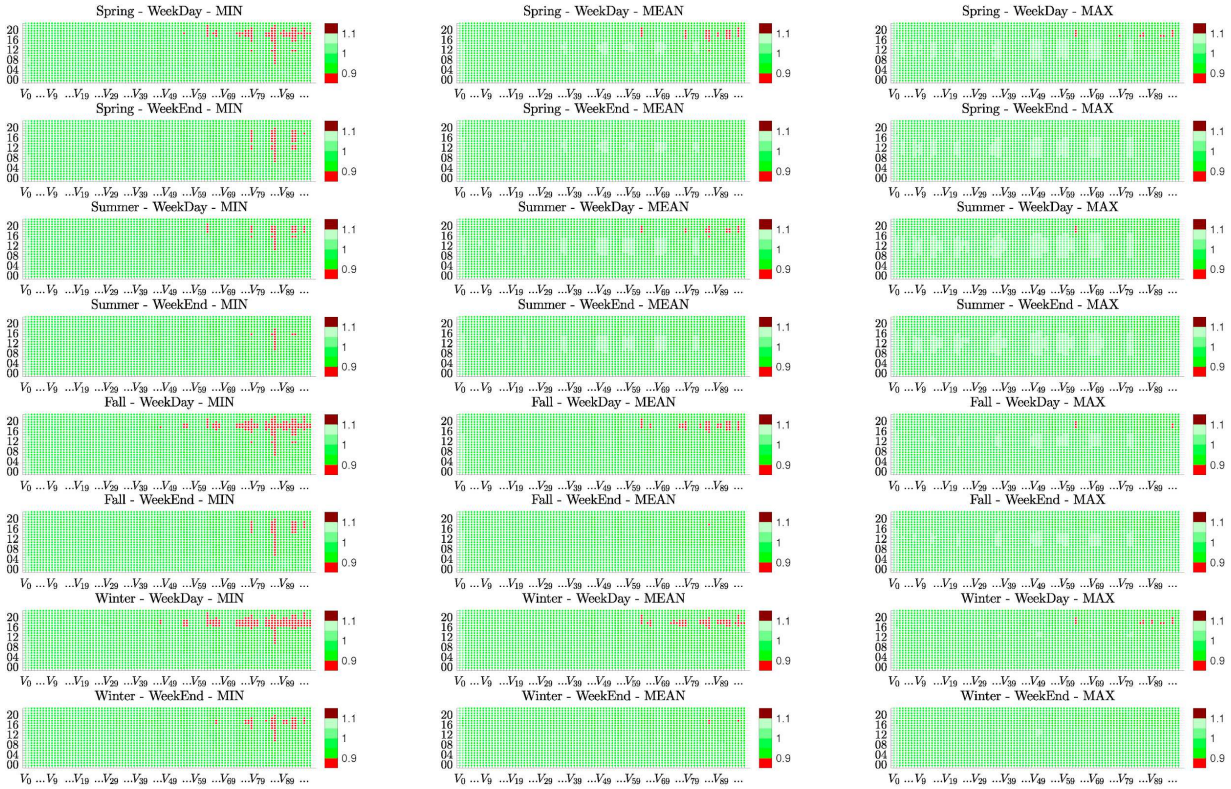

(b) Only home EV charging

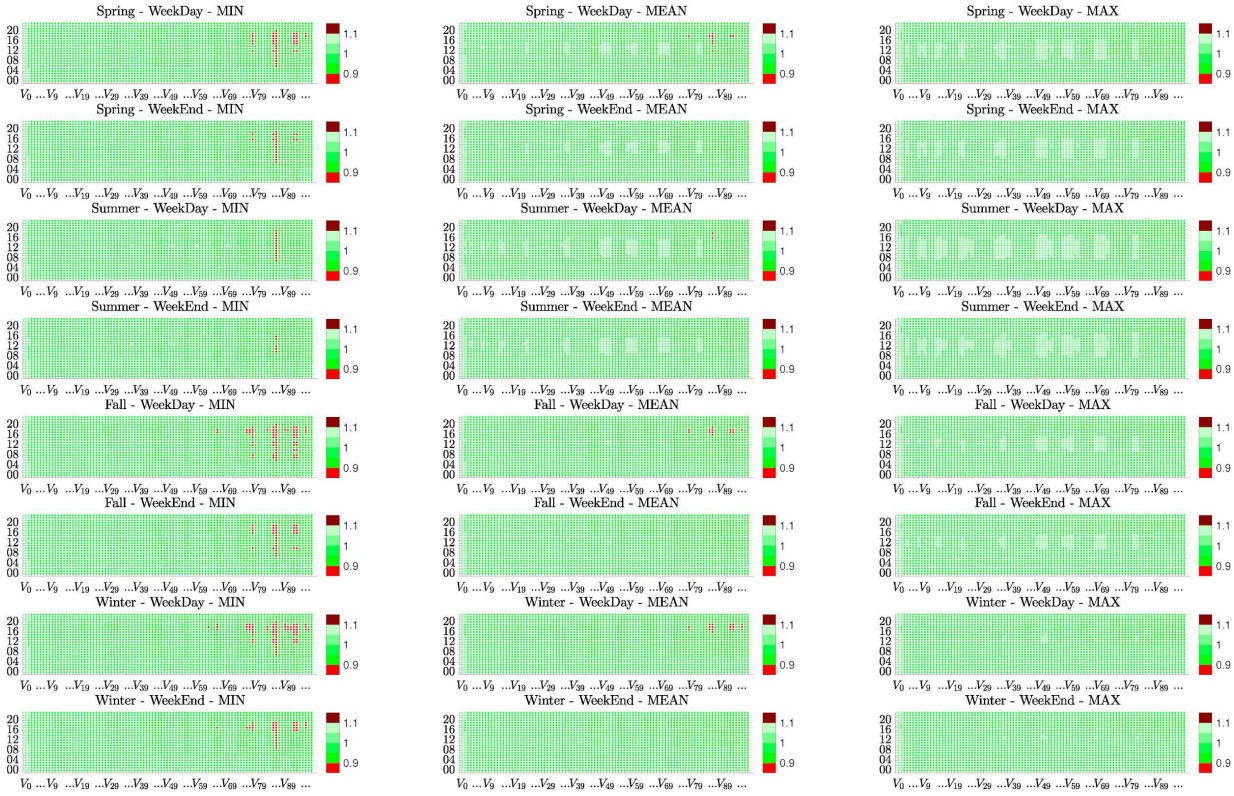

(c) Home-and-POIs EV charging

Figure 65 - Nodal voltage magnitudes - Min, mean and max over all K simulations

(a) Without EV charging

(b) Only home EV charging

(c) Home-and-POIs EV charging

Figure 66 - Nodal voltage magnitudes - Quantiles over all K simulations

(a) Without EV charging

(b) Only home EV charging

(c) Home-and-POIs EV charging

Figure 67 - Branch current magnitudes - Min, mean and max over all K simulations

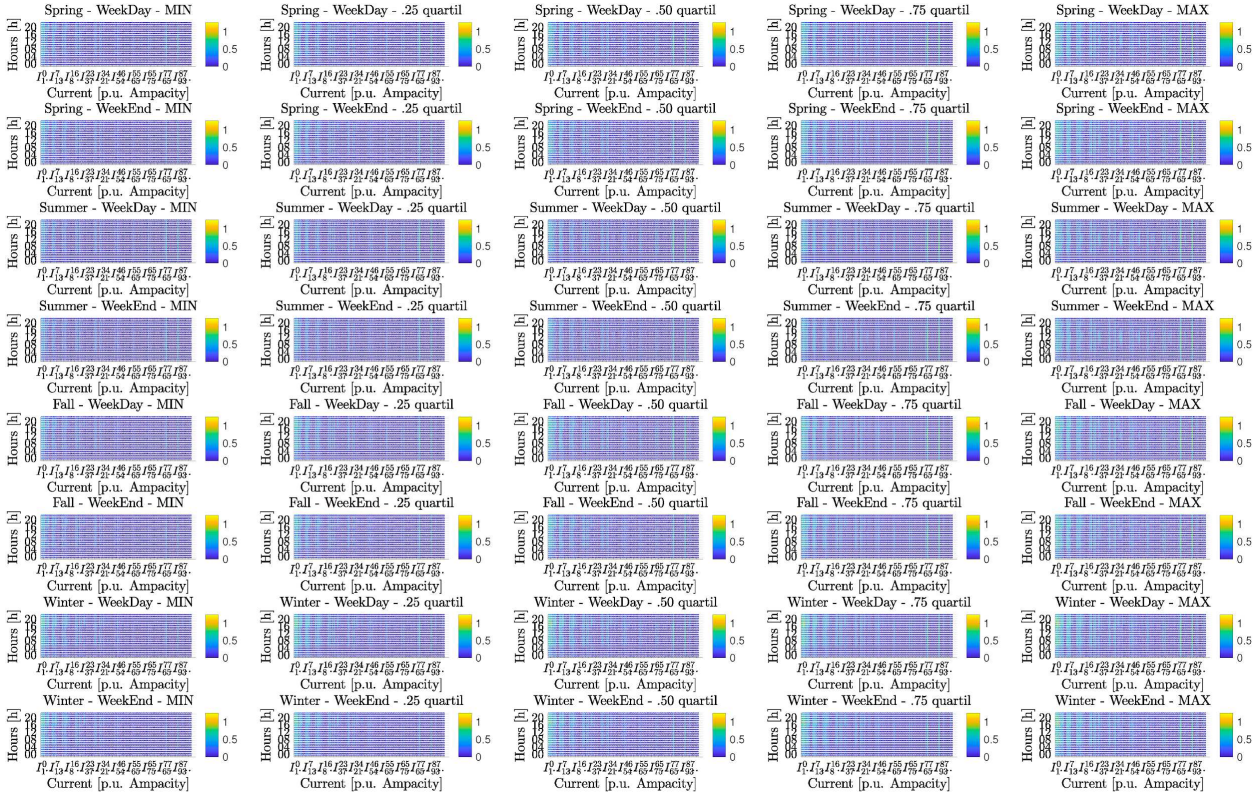

(a) Without EV charging

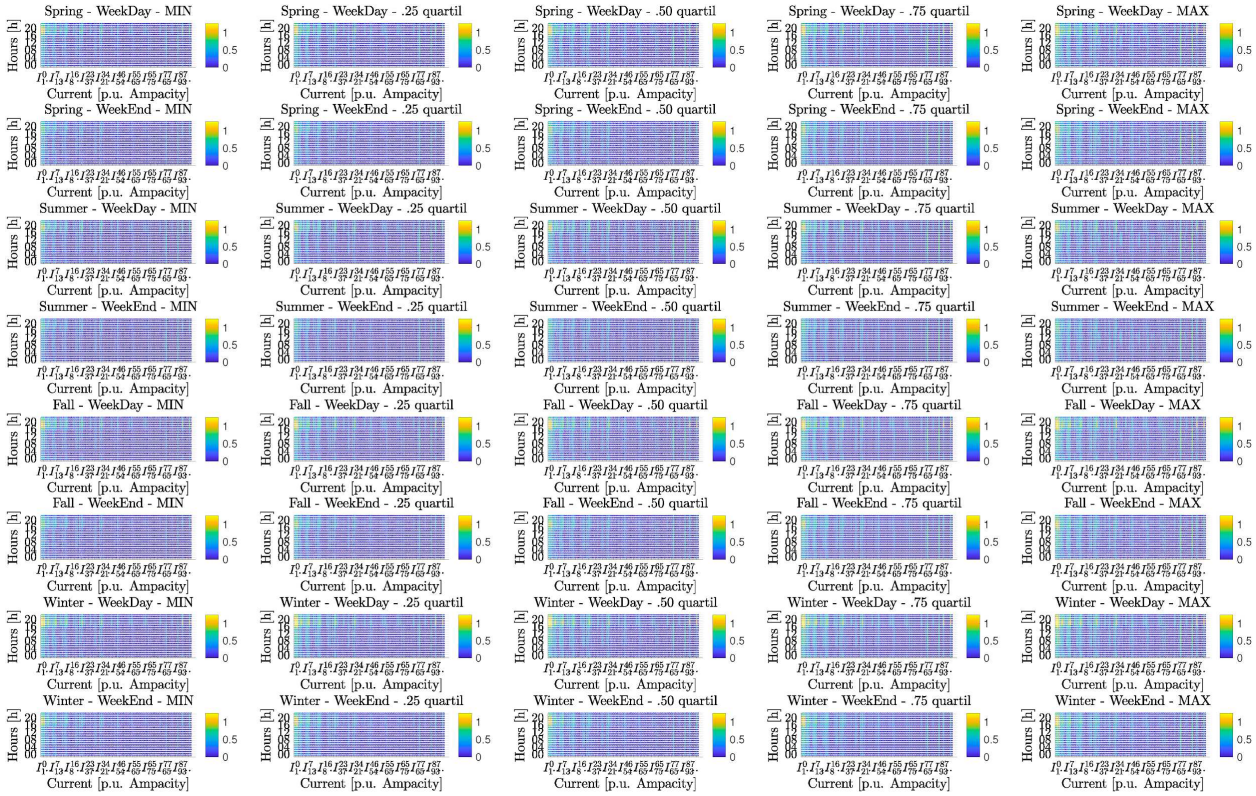

(b) Only home EV charging

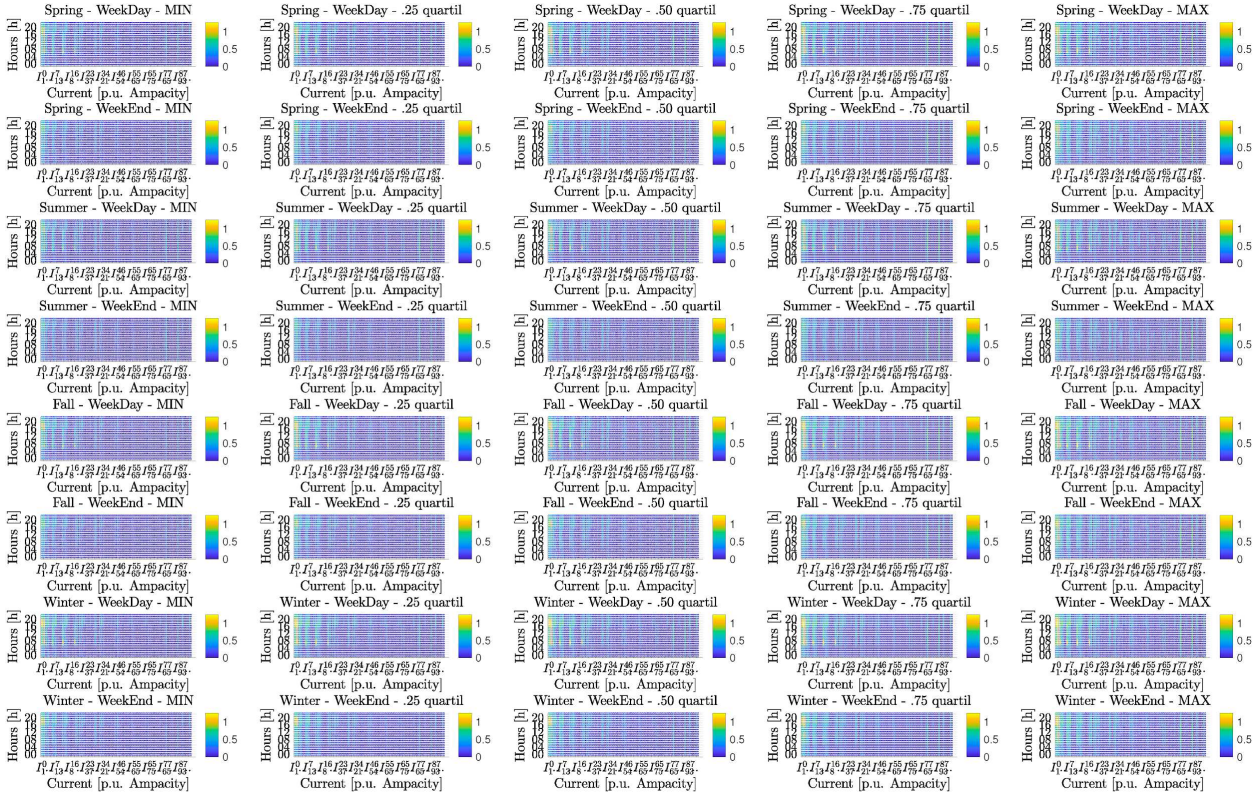

(c) Home-and-POIs EV charging

Figure 68 - Branch current magnitudes - Quantiles over all K simulations

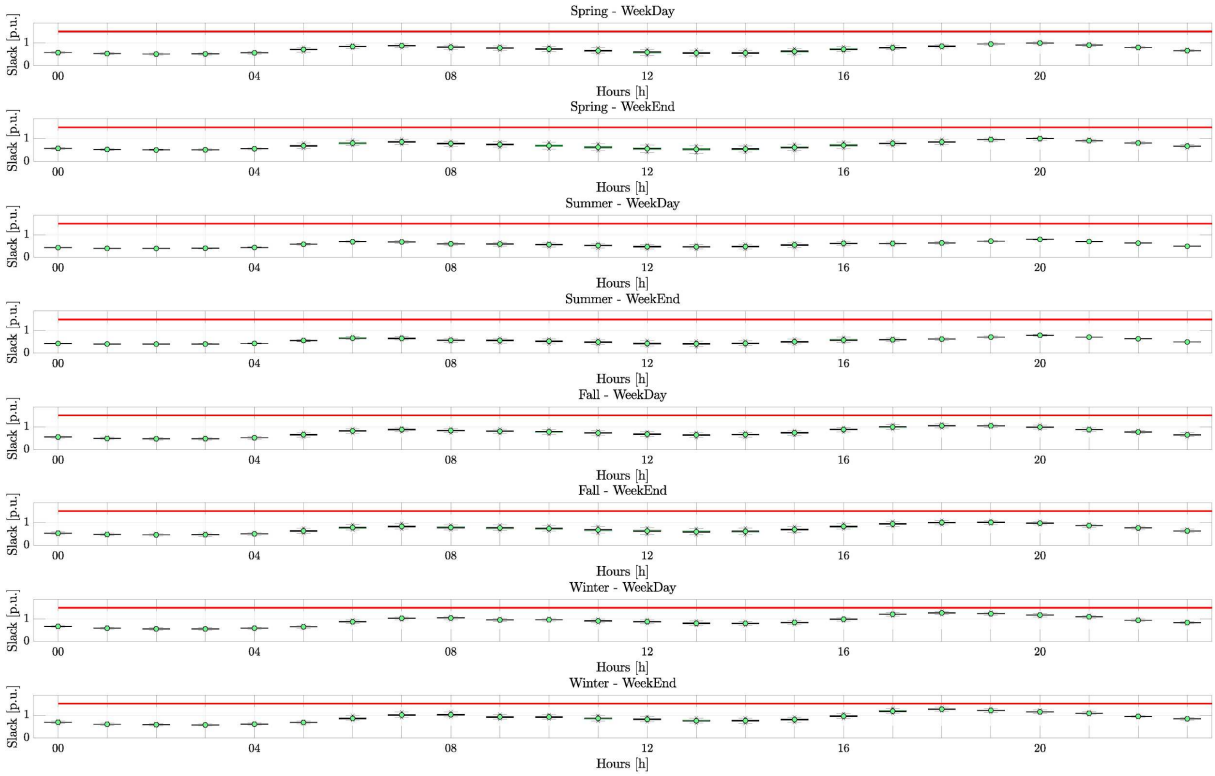

(a) Without EV charging

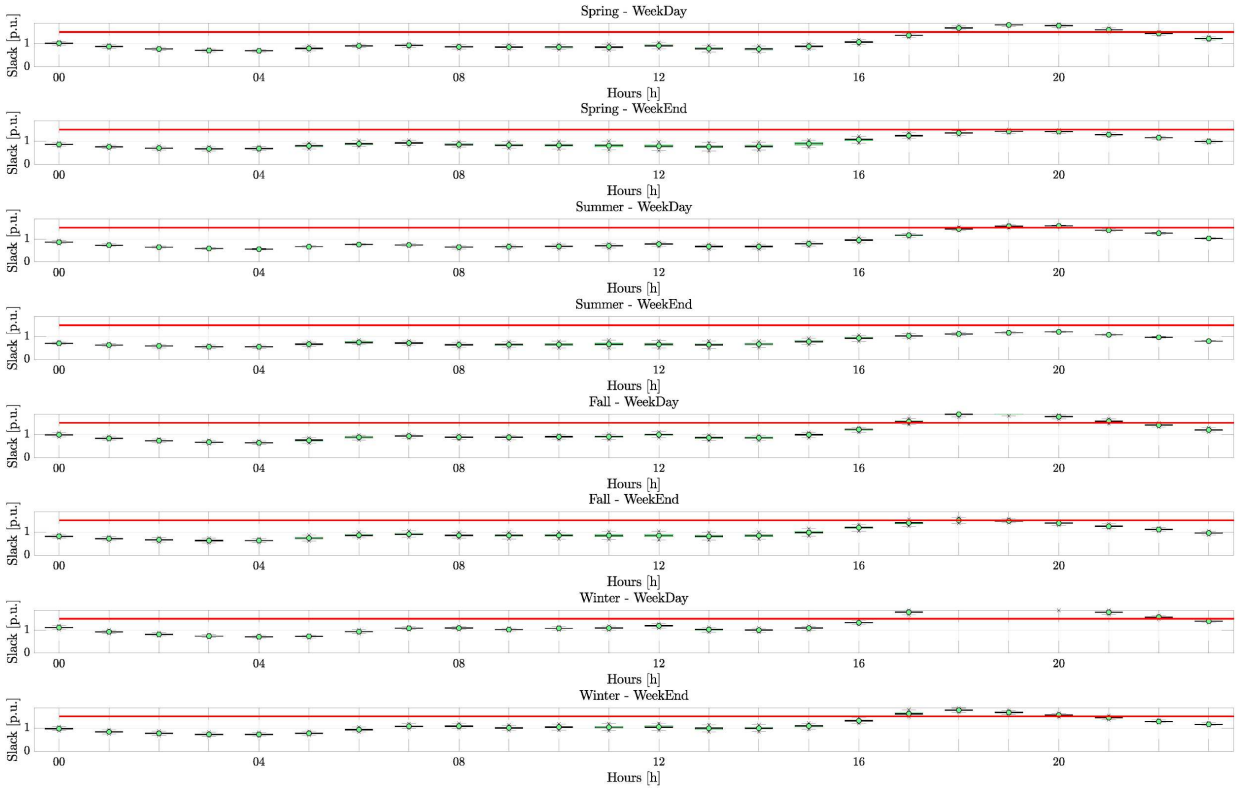

(b) Only home EV charging

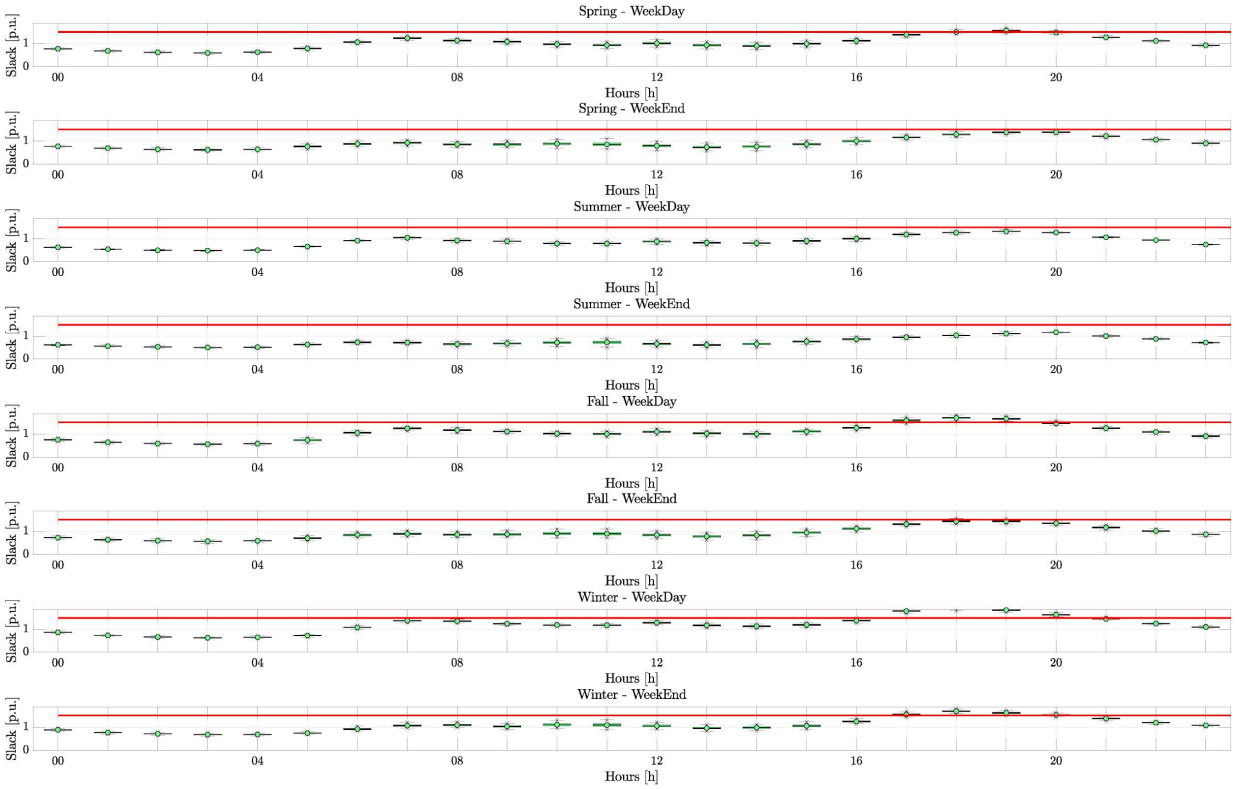

(c) Home-and-POIs EV charging

Figure 69 - Apparent power magnitudes - Boxplot over all K simulations

To go a step further and to show the sensitivity analysis vis-a-vis the percentage of transport electrification, Figure 70 - Figure 76 show the probabilities (computed directly from the outputted CDFs of the states and auxiliary variables) to violate the grid security constraints. In principle, each figure should contain five subsub-figures encapsulating respectively, 0%, 25%, 50%, 75% and 100% EV penetration, however, in practice, for compactness, some graphs have been omitted when there were no grid violations (i.e. probability equal to 0 for all seasons, day-types and hours). One can conclude from the figures that:

1. Without EV charging there are minor nodal voltage magnitude violations.
2. With only home charging, at 100%, 75% and 50% EV penetration all grid security constraints are violated. However, at 25% EV penetration there are no branch current magnitudes violations and only minor slack apparent power violations.
3. With home and POI charging, at 100%, 75% and 50% EV penetration all grid security constraints are violated. However, at 25% EV penetration there are no slack apparent power violations and only minor branch current magnitudes violations.
4. As previously concluded, it is clear that the more EV injections the more likely (i.e. higher probability) the constraints can be violated.
5. Compared to the previous grid, there are risks of violating voltage magnitude security constraints during multiple seasons and hours of the day. For instance, several branches are at high-risk of have overcurrents during multiple periods of the year (see Figure 73).

6. Similar to the previous grid, winter nights present the most at-risk time period to incur grid violations. However, in this grid, it is clear the problem occurs also during other seasons and during other periods of the day.
7. This grid is obviously a weaker grid compared to the previous one and it is clear that satisfying EV user need without a smart-grid control infrastructure or major grid reinforcements is quasi-impossible.

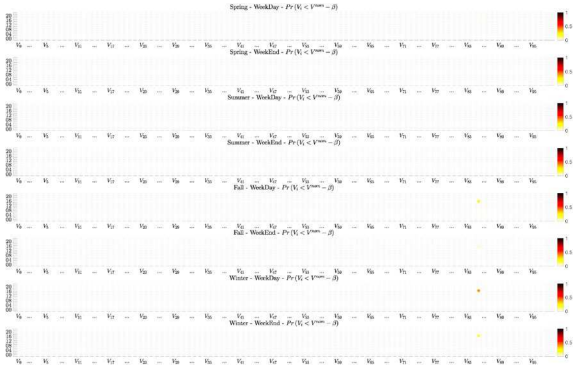

(a.i) 0% EV

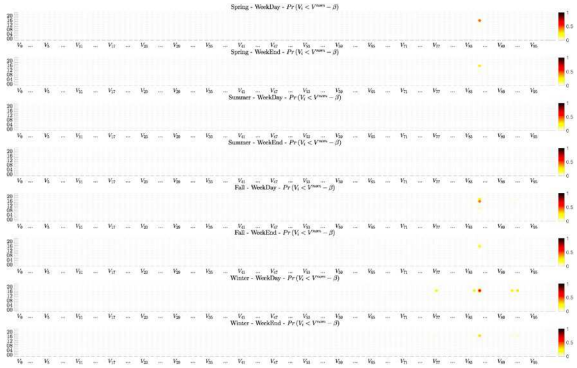

(a.ii) 25% EV

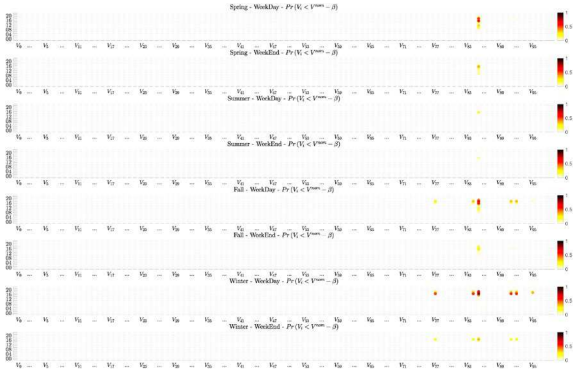

(a.iii) 50% EV / Only home EV charging

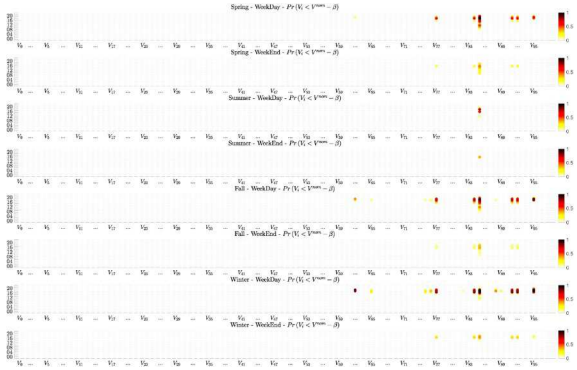

(a.iv) 75% EV / Only home EV charging

(a.v) 100% EV / Only home EV charging

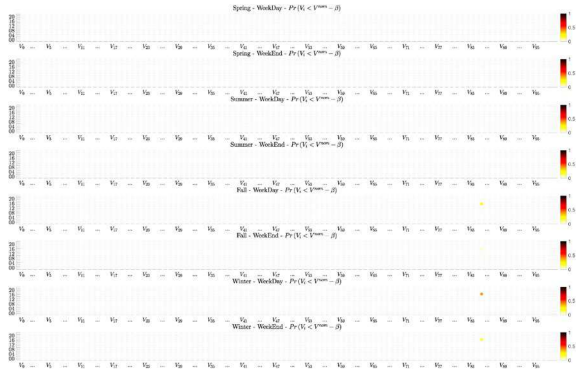

(b.i) 0% EV / Home-and-POIs EV charging

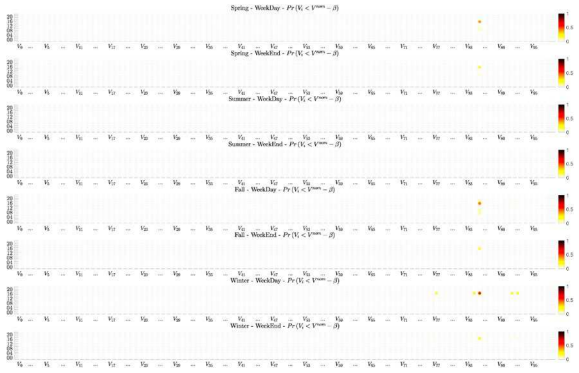

(b.ii) 25% EV / Home-and-POIs EV charging

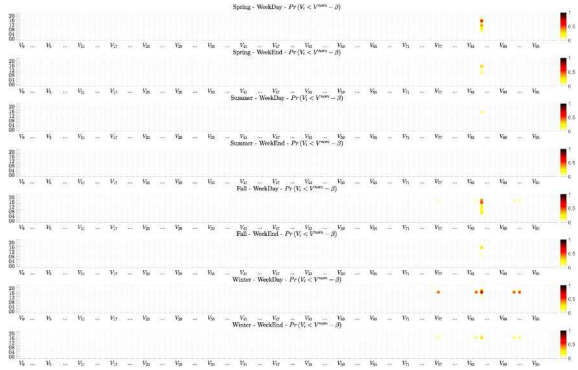

(b.iii) 50% EV / Home-and-POIs EV charging

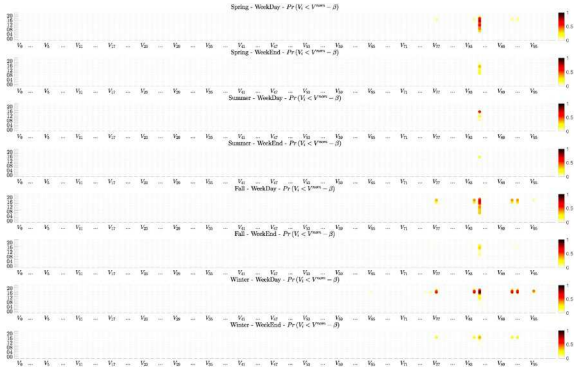

(b.iv) 75% EV / Home-and-POIs EV charging

(b.v) 100% EV / Home-and-POIs EV charging

Figure 70 - Probability to violate nodal voltage magnitudes

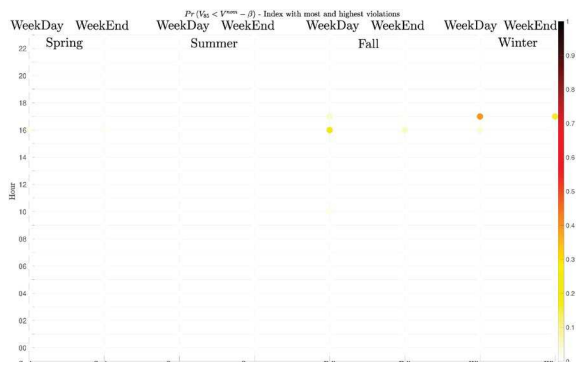

(a.i) 0% EV / Only home EV charging

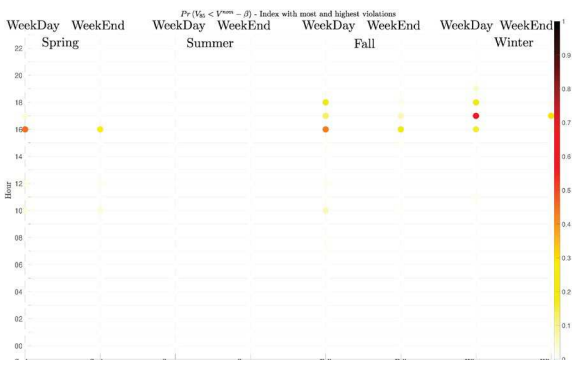

(a.ii) 25% EV / Only home EV charging

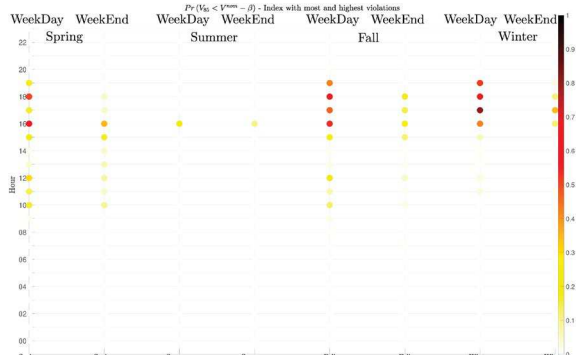

(a.iii) 50% EV / Only home EV charging

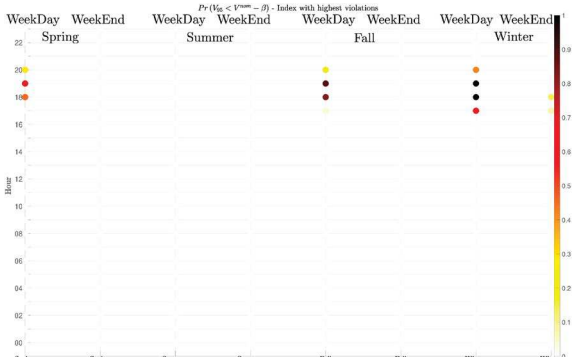

(a.iv) 75% EV / Only home EV charging

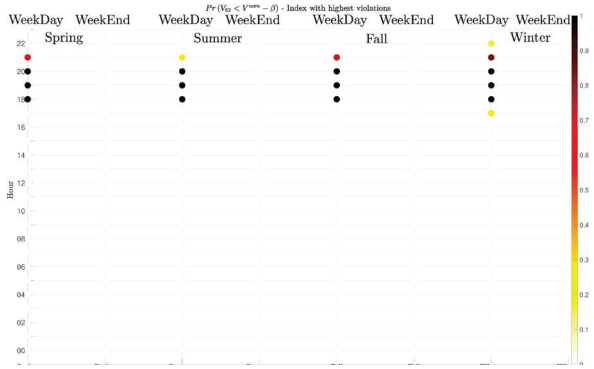

(a.v) 100% EV / Only home EV charging

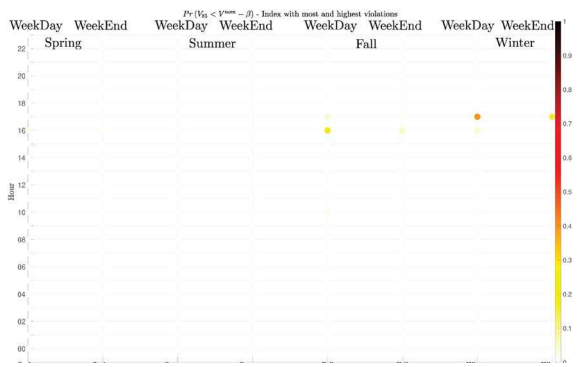

(b.i) 0% EV / Home-and-POIs EV charging

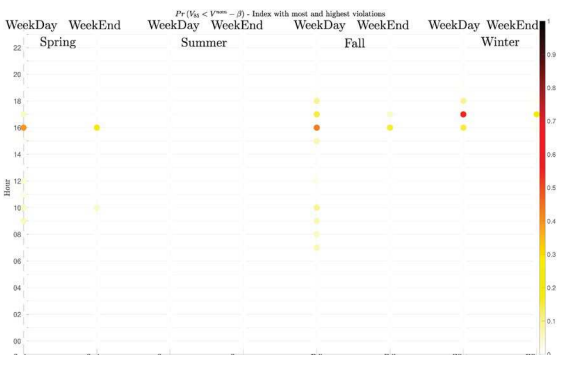

(b.ii) 25% EV / Home-and-POIs EV charging

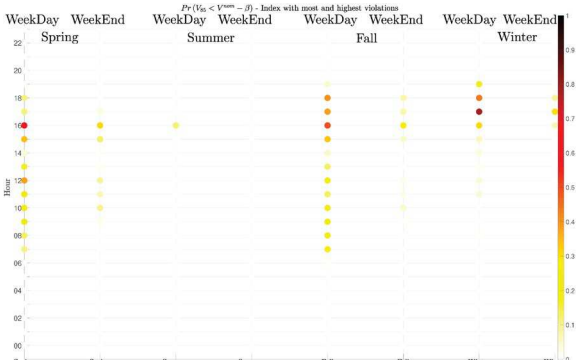

(b.iii) 50% EV / Home-and-POIs EV charging

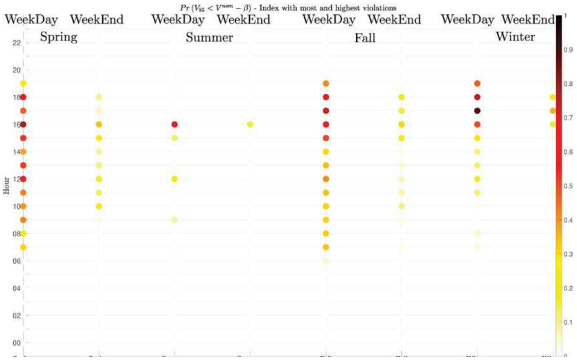

(b.iv) 75% EV / Home-and-POIs EV charging

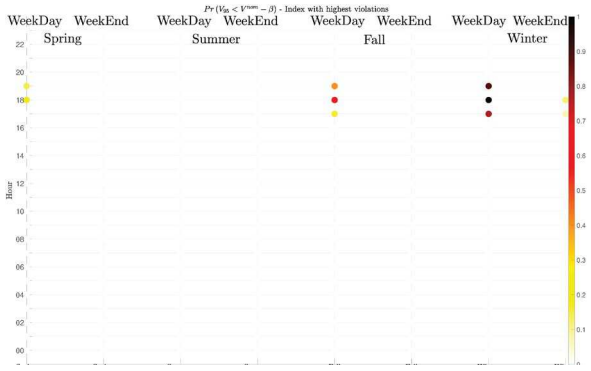

(b.v) 100% EV

Figure 71 - Probability to violate nodal voltage magnitudes of node with highest violations

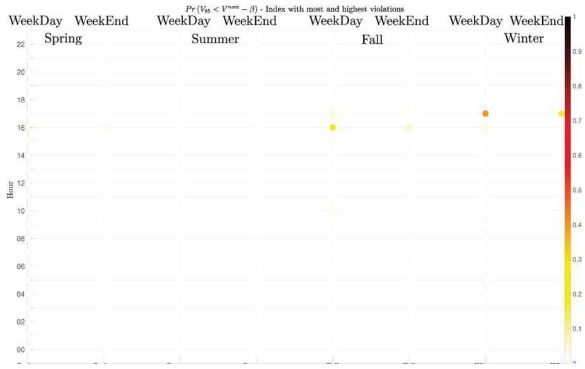

(a.i) 0% EV / Only home EV charging

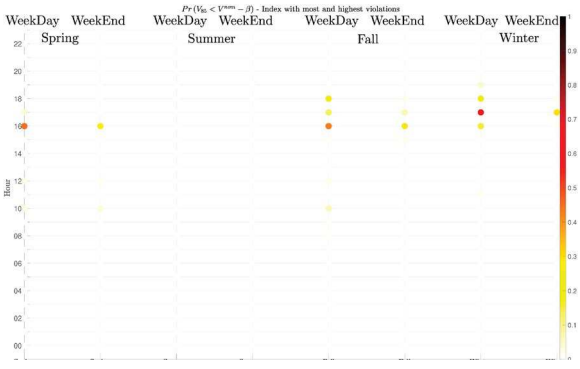

(a.ii) 25% EV / Only home EV charging

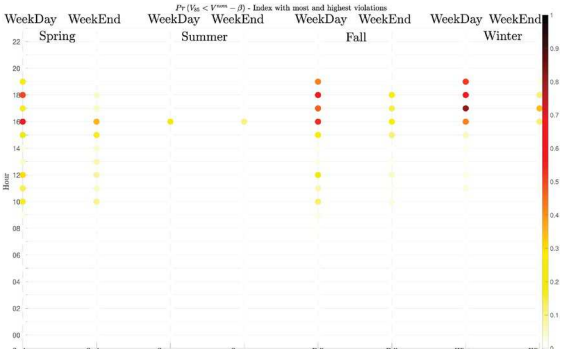

(a.iii) 50% EV / Only home EV charging

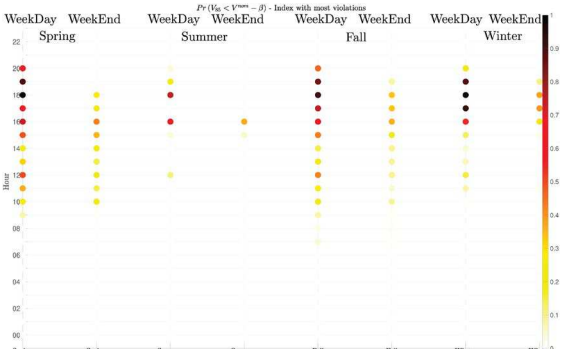

(a.iv) 75% EV / Only home EV charging

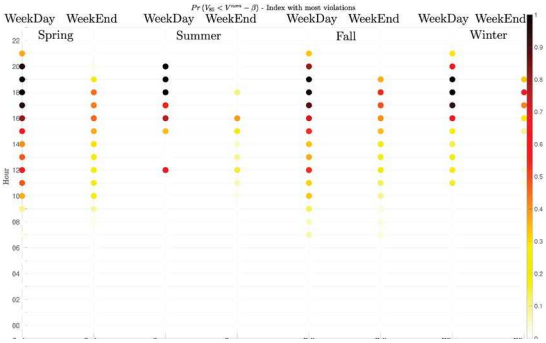

(a.v) 100% EV / Only home EV charging

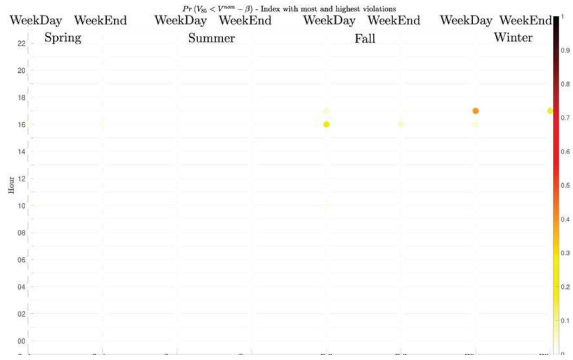

(b.i) 0% EV / Home-and-POIs EV charging

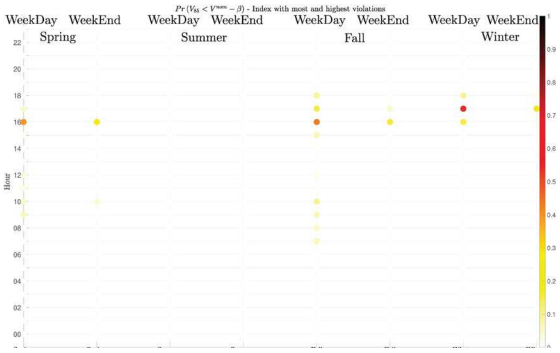

(b.ii) 25% EV / Home-and-POIs EV charging

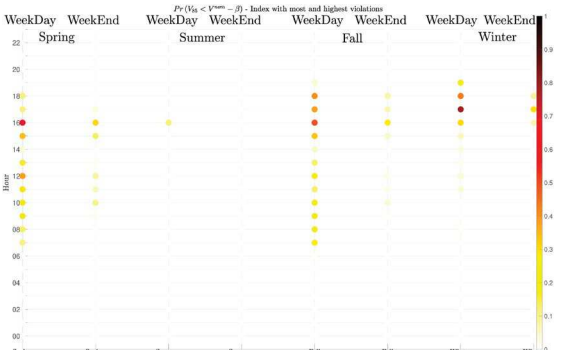

(b.iii) 50% EV / Home-and-POIs EV charging

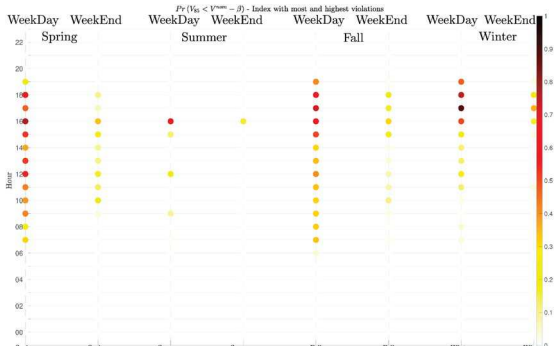

(b.iv) 75% EV / Home-and-POIs EV charging

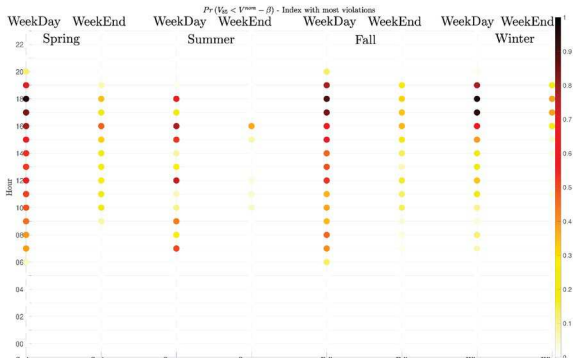

(b.v) 100% EV / Home-and-POIs EV charging

Figure 72 - Probability to violate nodal voltage magnitudes of node with most violations

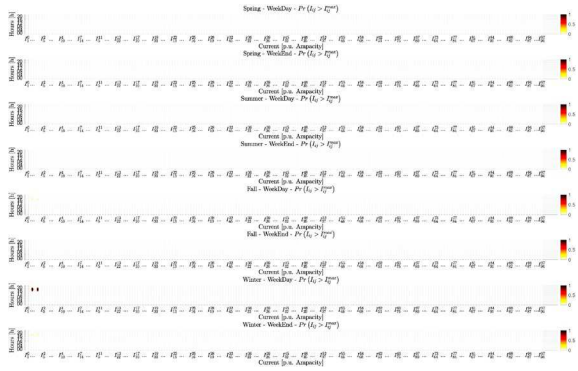

(a.i) 50% EV / Only home EV charging

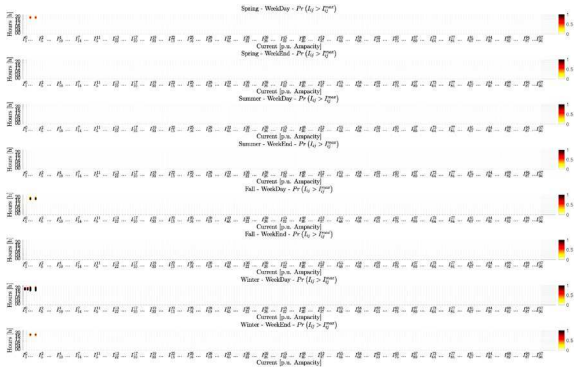

(a.ii) 75% EV / Only home EV charging

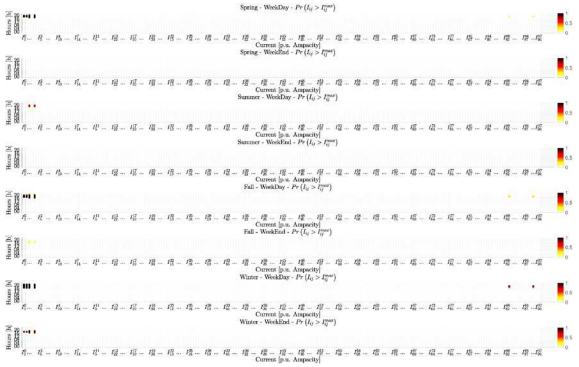

(a.iii) 100% EV / Only home EV charging

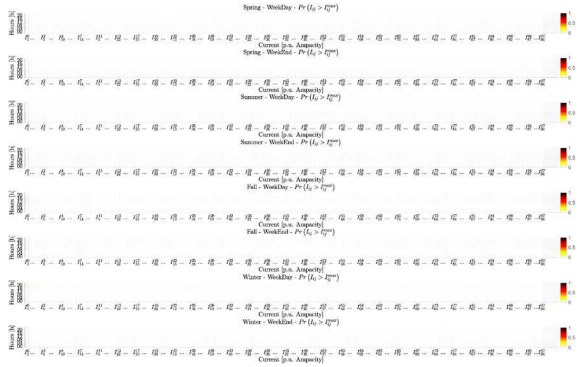

(b.i) 25% EV / Home-and-POIs EV charging

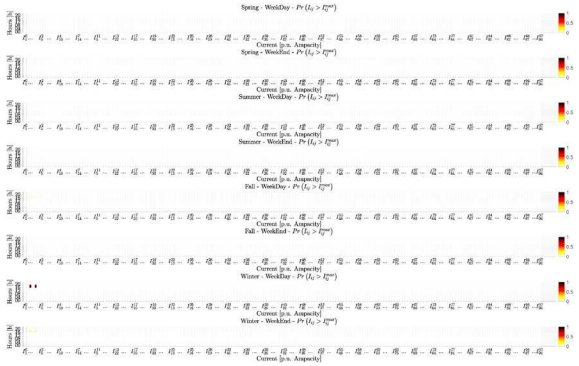

(b.ii) 50% EV / Home-and-POIs EV charging

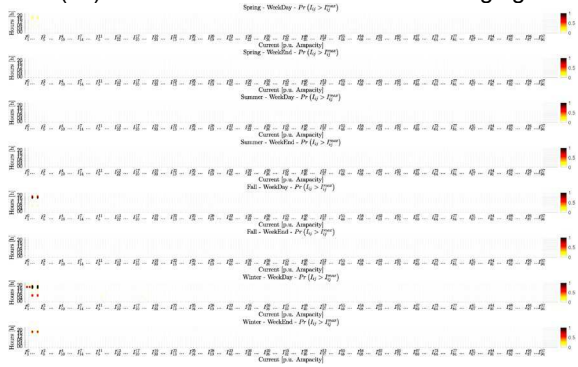

(b.iii) 75% EV / Home-and-POIs EV charging

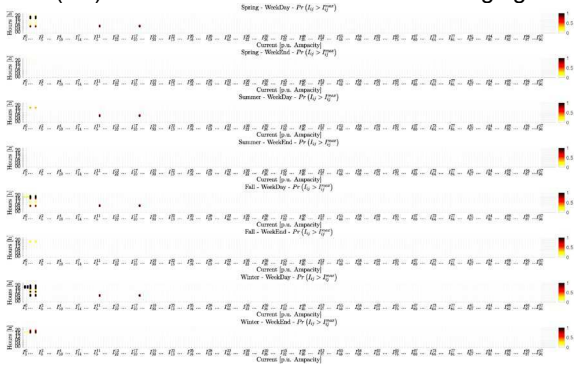

(b.iv) 100% EV / Home-and-POIs EV charging

Figure 73 - Probability to violate branch current magnitudes

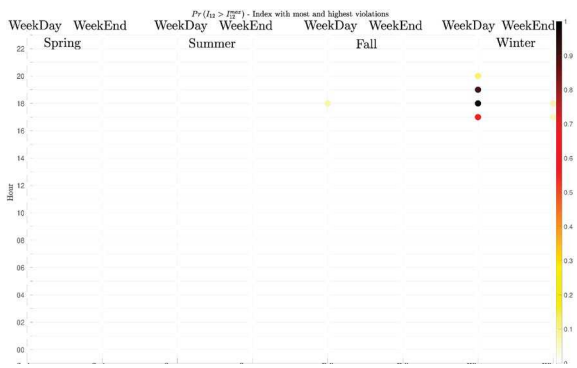

(a.i) 50% EV / Only home EV charging

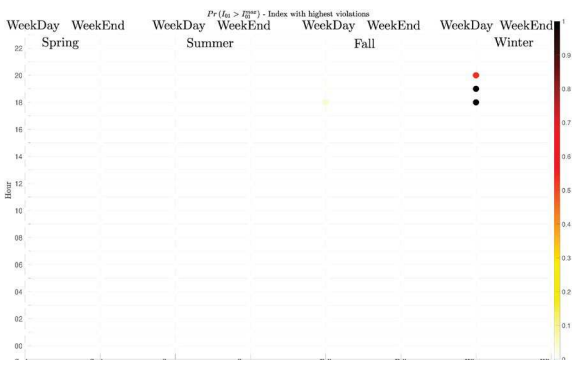

(a.ii) 75% EV / Only home EV charging

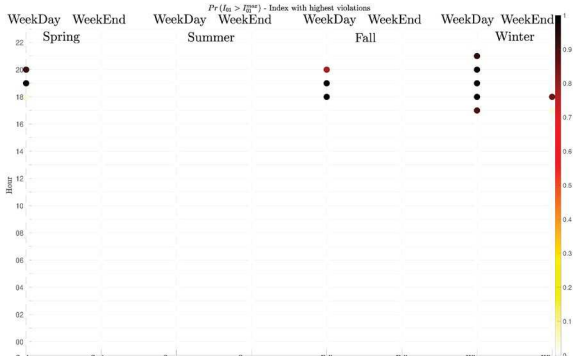

(a.iii) 100% EV / Only home EV charging

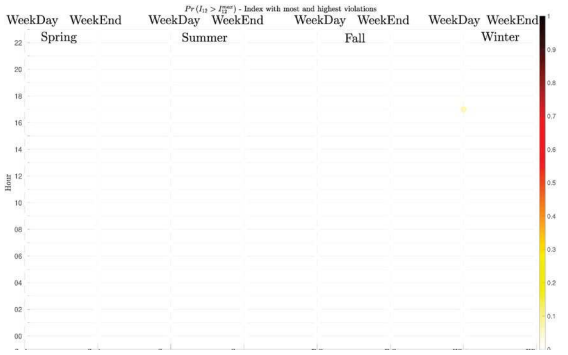

(b.i) 25% EV

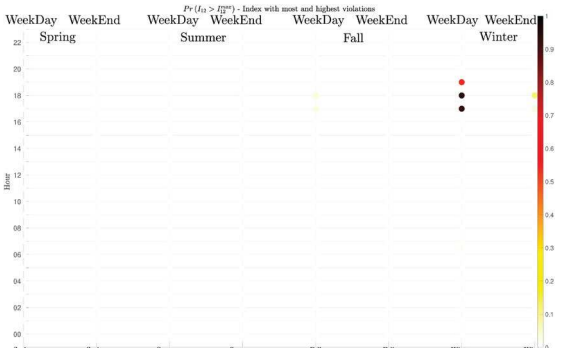

(b.ii) 50% EV

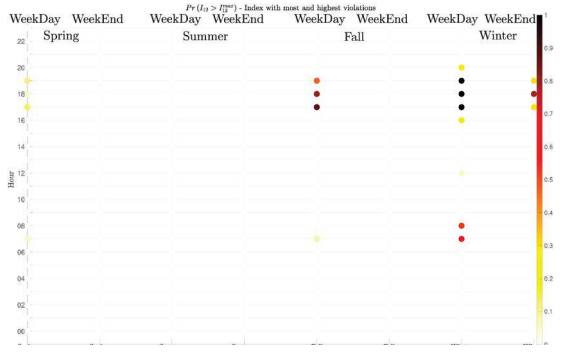

(b.iii) 75% EV

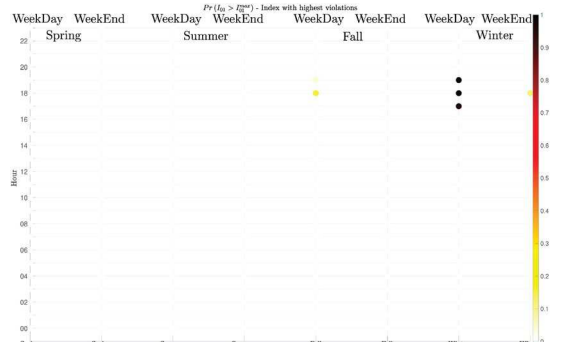

(b.iv) 100% EV

Figure 74 - Probability to violate branch current magnitudes of branch with highest violations

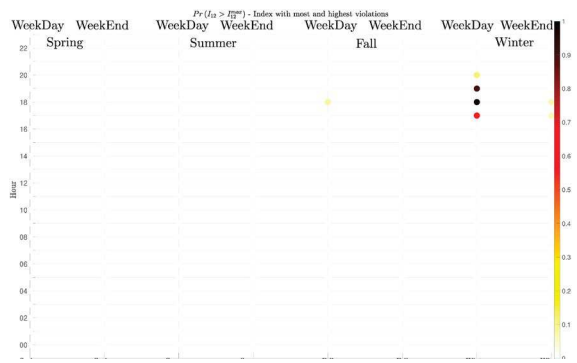

(a.i) 50% EV / Only home EV charging

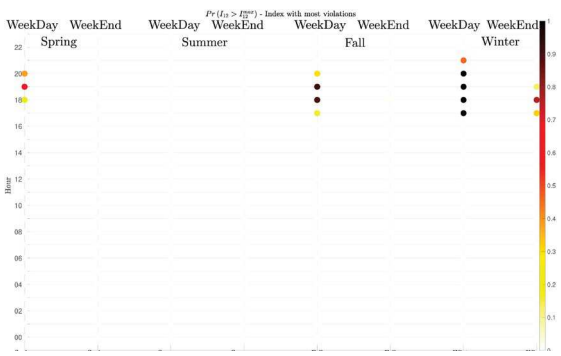

(a.ii) 75% EV / Only home EV charging

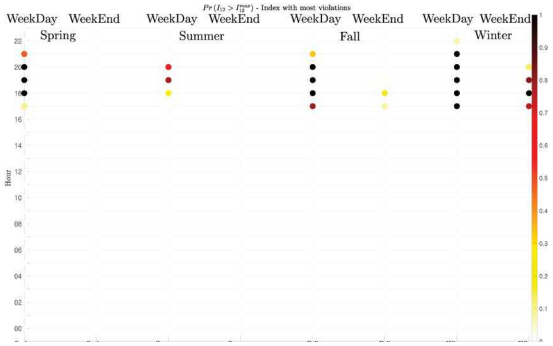

(a.iii) 100% EV / Only home EV charging

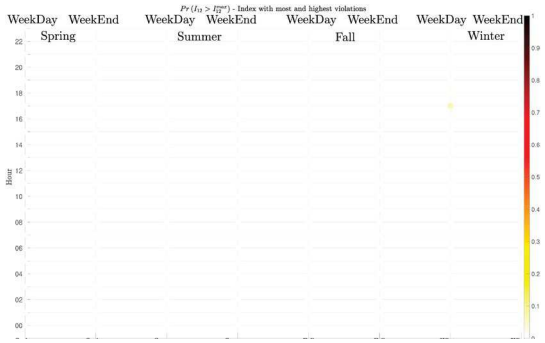

(b.i) 25% EV / Home-and-POIs EV charging

(b.ii) 50% EV / Home-and-POIs EV charging

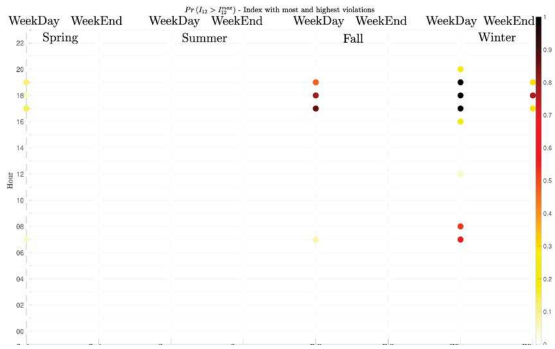

(b.iii) 75% EV / Home-and-POIs EV charging

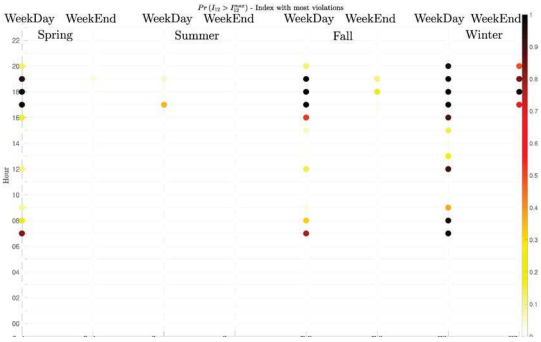

(b.iv) 100% EV / Home-and-POIs EV charging

Figure 75 - Probability to violate branch current magnitudes of node with most violations

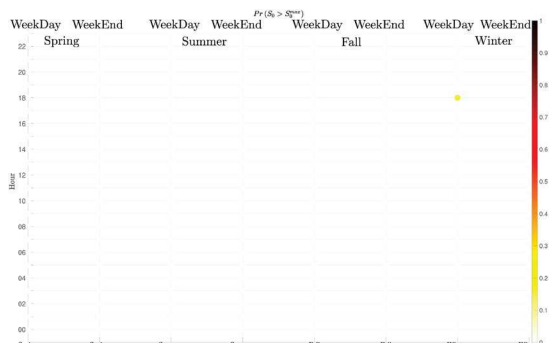

(a.i) 25% EV / Only home EV charging

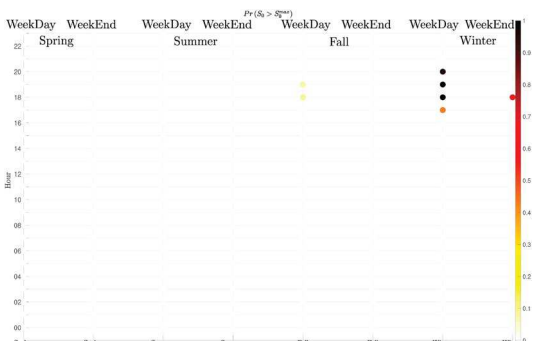

(a.ii) 50% EV / Only home EV charging

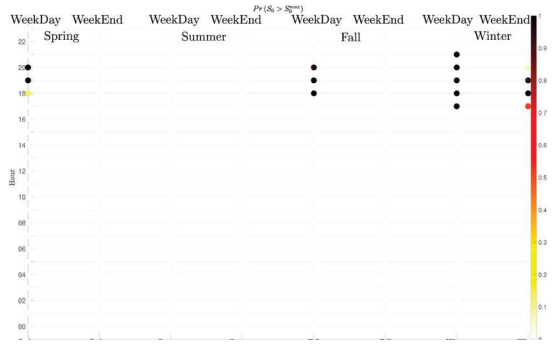

(a.iii) 75% EV / Only home EV charging

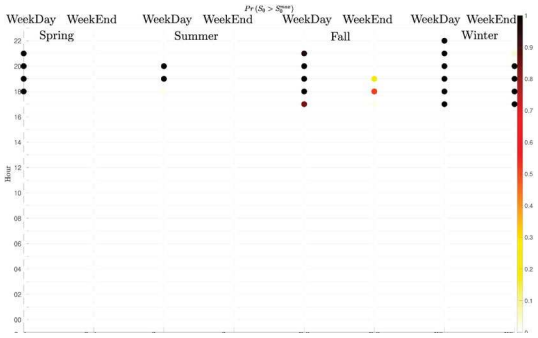

(a.iv) 100% EV / Only home EV charging

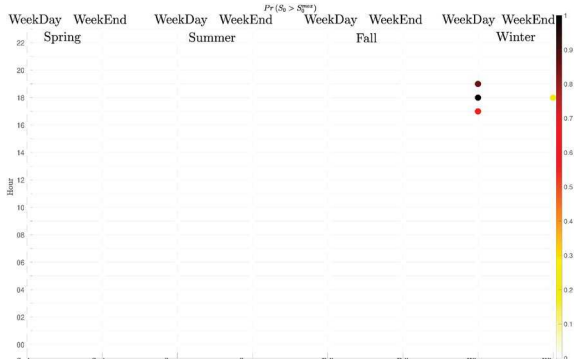

(b.i) 50% EV / Home-and-POIs EV charging

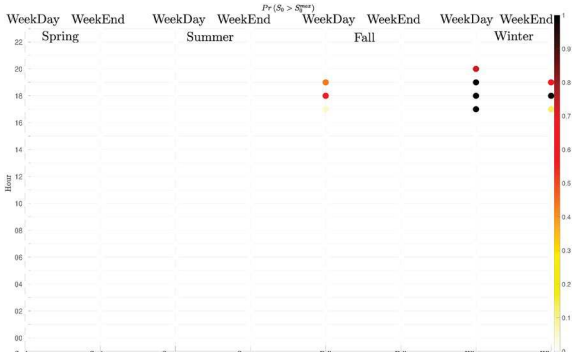

(b.ii) 75% EV / Home-and-POIs EV charging

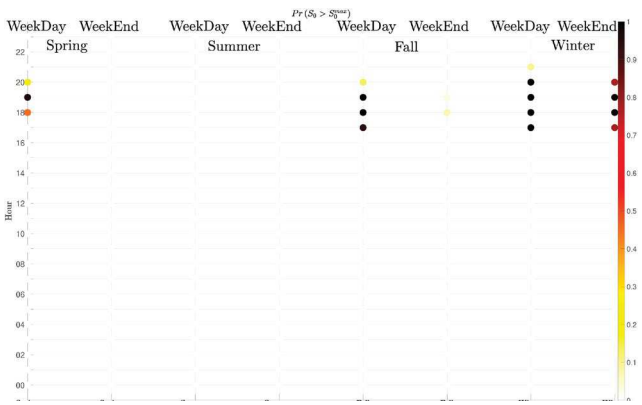

(b.iii) 100% EV / Home-and-POIs EV charging

Figure 76 - Probability to violate slack apparent power magnitudes

6.4. Conclusions EV charging

In this chapter the impact of the presence of EV charging stations (CSs) in low-voltage electric grids was investigated. More specifically, we presented a Monte-Carlo-based method that quantifies the impact of EV charging on the grid's static security constraints (i.e. nodal voltage magnitudes, branch current magnitudes and slack apparent power all within bounds) while accounting for the stochastic nature of: (i) renewable generation, (ii) non-EV loads, and, (iii) EV loads. The method was used on two real low-voltage networks situated in the south-eastern part of Switzerland (Rolle VD).

The simulations revealed that the method should be used in the planning stage to understand the degree of influence EV charger placement will have on the grids. Indeed, both simulations showed that EV loads are harmful on grid static security. Even though the Rolle-Gare network had fewer issues than the Rolle-Hôpital network, both simulations revealed that non-negligible actions are needed if a full electrification of private transport is planned. For instance, seeing that the Rolle-Gare network only had minor overcurrent issues and mostly under-voltages, one can argue that some minor grid reinforcements coupled with voltage regulation are enough to anticipate full electrification in that grid. On the other hand, the Rolle-Hôpital network presented major overcurrents, under-voltages and transformer overloads (i.e. slack apparent power larger than 1 p.u.), thus, grid reinforcements might implicate major economical expenses, therefore, in such cases, a smart charging algorithm can be used to satisfy the EV user needs as best as possible all while protecting the electrical grid.

In other situations, a grid-aware CS placement-planning problem could be used to anticipate grid static violations by placing less CSs in nodes that can accommodate higher power loading. As a final note, it is clear that every grid will behave differently and simulations using the presented tool can give insights on the strategy to be adopted in order to prepare the grid for 100% electrification of private transport.

7. Conclusions and Recommendations

Significant GHG emissions reductions are possible by introducing electricity-based mobility (EBM) such as BEV, H_2-FCEV and SNG-V. Due to the fluctuating and seasonal unbalanced availability of renewable electricity, the comparison of these three technologies is complex, despite many simplifications, as this study shows. The following conclusions and recommendations can be given:

1. All EBM scenarios show significantly less GHG emissions than the reference scenario with fossil fuels operated ICEV/HEV. Depending on the scenario and underlying assumptions, EBM results in a life-cycle GHG emissions reduction of roughly 2 - 4 Mt by 2050, while about 4 - 8 Mt of GHG emissions remain in the considered energy system.

   The authors recommend policy makers to develop a phase-out of fossil fuels for mobility and to intensify the further market and technology development of EBM technologies.

2. Three main boundary conditions are affecting the GHG emissions reduction of EBM significantly: the installed PV power, the possibility to avoid curtailment of renewable electricity and the GHG content of imported electricity during electricity shortages.

   Due to the additional electricity demand in case of EBM, the authors recommend to intensify the PV installations and to invest in curtailment-avoidance such as demand side management and both short-term storage by batteries, etc. and long-term (seasonal) storage by H_2 or SNG production.

   Because high-carbon electricity imports limit the GHG emissions reduction of EBM, concepts for low-carbon imports during electricity shortages *should be developed (seasonal energy storage concepts, import of renewable chemical energy).*

3. The electricity demand of EBM may locally overcharge the electric infrastructure.

   The authors recommend to promote (or even to prescribe) smart charging management systems on neighborhood and household level to achieve fast installation of charging infrastructure.

4. The actual CO_2 legislation for the immatriculation of new passenger cars does not consider all life-cycle GHG emissions of EBM and therefore is overestimating the impact.

   The authors recommend supporting the European Commission by developing life cycle (LCA) based CO_2 emission assessment methods for vehicle registration.

8. Outlook

In this study, the impacts of electricity-based mobility (EBM) powertrains (BEV, H_2-FCEV and SNG-V) are investigated with respect to systemic and marginal specific life-cycle (LCA) greenhouse gas (GHG) emissions as well as compared to a corresponding “non-” (60% gasoline and 40% diesel) passenger cars fleet in the case of Switzerland. To this end, several scenarios with respect to the domestic PV expansion, the GHG content of imported electricity and the use of “excess” electricity (curtailment or sector coupling) have been investigated by means of an energy system optimization model.

Irrespective of the domestic PV expansion and GHG content of imported electricity, generally feature significantly lower GHG emissions than a corresponding “non-EBM” fleet. If no electricity must be curtailed due to additional sector coupling (power-to-gas), BEV generally feature the lowest systemic and marginal specific GHG emissions. In turn, if a certain part of “excess” electricity must be curtailed, BEV are only the most GHG-efficient powertrain in an energy system with low domestic PV expansion and low-carbon (LC) imports. In all other scenarios, H_2-FCEV and SNG-V are at least equally GHG-efficient, or with a high PV expansion and high-carbon (CCGT) imports, even more GHG-efficient than BEV. This is due to the fact the H_2-FCEV and SNG-V, despite their lower TTW powertrain efficiency and additional losses in the conversion steps of electrolysis (ELYSE) and methanation (METH), feature a higher flexibility with regard to the selection of their used electricity and its varying GHG content due to the long-term (seasonal) storability of their fuels (e.g. as SNG in the NG grid) and also with respect to using grid NG (for H_2-FCEV via SMR), in times when the GHG of electricity is higher. This is in particular the case, if grid NG has a high share of renewable biomethane or SNG. However, with (partial) curtailment, generally differences in terms of GHG emissions between powertrains are small, except for those «extreme» cases regarding domestic PV expansion and GHG content of import electricity.

Eventually, regarding the specific GHG emissions pertaining to each powertrain (in g $CO_{2\text{-eq}}$/km), there are quite substantial differences, whether a marginal or average electricity mix approach is used; with the marginal approach typically attributing lower specific GHG emissions to H_2-FCEV and SNG-V than BEV (in particular with a high PV expansion and high-carbon imports), and the average approach always favoring BEV over H_2-FCEV and SNG-V in terms of their specific GHG emissions. Both approaches have their justification and shortcomings.

In this study, only the technological potential for GHG mitigation of powertrains has been investigated without considering economical (and sociological) aspects in their implementation. However, it could be shown that the required electrolysis capacities for H_2-FCEV and SNG-V, or to avoid curtailment in the BEV case, range - depending on the domestic PV expansion scenario - between 7 and 34 GW_{el} with equivalent full load hours (eqFLH) of typically less than 1'000 hours. In order to become more economically viable, these eqFLH must be increased, however, typically at the expense of higher GHG emissions. Moreover, if it is considered that a large penetration of BEV will more likely lead to local electricity grid failure, in practice (without costly grid reinforcements) a «mixed fleet» of BEV and H_2-FCEV / SNG-V will most likely be the most sustainable option. Such techno-economical aspects - including “mixed fleets”, demand response of BEV charging as well as a simultaneous electrification of the heat sector (heat pumps) and decarbonization of the heavy-duty transportation and industry sectors - need to be included in further studies.

Limitations of the study

- The study does not cover energy demand besides the electricity and passenger cars mobility sectors, such as heating, industry or heavy-duty transportation. These sectors may also have a potential to use excess electricity. In turn, especially space heating is supposed to increase electricity demand and hence, potentially electricity imports required in winter, which could have an impact on the mix of imported electricity.
- For EBM vehicles, average mileages are assumed. In reality, they differ quite strongly depending on vehicle category and use patterns. If mainly low or high mileage vehicles became EBM, this would have a significant impact on GHG emissions.
- It is assumed that all excess electricity can be converted to H_2 and SNG. Because the equivalent full load hour requirement of H2 and SNG production plants is in the range of 4'500 h/a to be economically viable, actual H_2 and SNG production may be overestimated.
- Non-renewable (synthetic) gasoline or diesel is assumed to be used for non-EBM vehicles. Such synfuels could reduce the difference in achieved GHG mitigation between EBM and non-EBM scenarios.
- No "mixed fleet" of different EBM powertrains in the same energy system is considered. Due to synergetic effects, this may further reduce GHG emissions.
- Fixed battery charging profiles without flexibility in terms of demand of BEV charging are considered. Such flexibility options may further reduce GHG emissions of BEV scenarios.

9. References

Ajanovic, A., Haas, R., 2019. Economic and Environmental Prospects for Battery Electric- and Fuel Cell Vehicles: A Review. Fuel Cells 19, 515–529. https://doi.org/10.1002/fuce.201800171

Antonini, C., Treyer, K., Streb, A., van der Spek, M., Bauer, C., Mazzotti, M., 2020. Hydrogen production from natural gas and biomethane with carbon capture and storage - A techno-environmental analysis. Sustain. Energy Fuels 4, 2967–2986. https://doi.org/10.1039/d0se00222d

ARE, 2016. Perspektiven des Schweizerischen Personen- und Güterverkehrs bis 2040 (Perspectives for Swiss passenger and freight traffic up to 2040).

Arnhold, O., Fleck, M., Goldammer, K., Grüger, F., Hoch, O., Schachler, B., 2017. Transformation of the German energy and transport sector – a national analysis. pp. 9–21. https://doi.org/10.1007/978-3-658-19293-8_3

ASTRA, 2020. Fahrzeughalterregister (MOFIS).

BAFU, 2019. Treibhausgasinventar der Schweiz (Switzerland's greenhouse gas inventory).

Bauer, C., Bäuerle, Y., Biollaz, S., Calbry-Muzyka, A., Cox, B., Heck, T., Hirschberg, S., Lehnert, M., Meier, A., Prasser, H.-M., Schenler, W., Treyer, K., Vogel, F., Wieckert, H., Zhang, X., Zimmermann, M., Burg, V., Bowman, G., Erni, M., Saar, M., Tran, M., 2017. Potentials, costs and environmental assessment of electricity generation technologies. Paul Scherrer Institut, Villigen PSI, Switzerland.

Bauer, C., Hofer, J., Althaus, H.J., Del Duce, A., Simons, A., 2015. The environmental performance of current and future passenger vehicles: Life Cycle Assessment based on a novel scenario analysis framework. Appl. Energy 157, 871–883. https://doi.org/10.1016/j.apenergy.2015.01.019

Beer, M., 2018. Abschätzung des Potenzials der Schweizer Speicherseen zur Lastdeckung bei Importrestriktionen (Assessment of the potential of Swiss storage lakes to cover loads in the event of import restrictions). Zeitschrift für Energiewirtschaft 42, 1–12. https://doi.org/10.1007/s12398-018-0220-8

Berrill, P., Arvesen, A., Scholz, Y., Gils, H.C., Hertwich, E.G., 2016. Environmental impacts of high penetration renewable energy scenarios for Europe. Environ. Res. Lett. 11, 14012. https://doi.org/10.1088/1748-9326/11/1/014012

BFE, 2020. Kennzahlen alternative Antriebe Neuwagen (Key data relating to alternative drives).

BFE, 2019. Analyse des schweizerischen Energieverbrauchs 2000-2018 -- Auswertung nach Verwendungszwecken (Analysis of Swiss energy consumption 2000-2018 - evaluation according to purpose). Bundesamt für Energie BFE (Swiss Federal Office of Energy (SFOE), Bern.

BFE, 2017. Schweizerische Gesamtenergiestatistik (Swiss total energy statistics), Bundesamt für Energie BFE. Bundesamt für Energie BFE (Swiss Federal Office of Energy SFOE).

BFE, 2015. Schweizerische Elektrizitätsstatistik (Swiss Electricity Statistics) 2015.

BFS, 2020a. Road vehicles - New registrations.

BFS, 2020b. Mikrozensus Mobilität und Verkehr (MZMV).

BFS, 2019. Leistungen des privaten Personenverkehrs auf der Strasse.

Bolla, M., Held, M., Küng, L., Georges, G., Boulouchos, K., 2018. Vehicle motion patterns for energy research: Comparison of annual mileage using vehicle and person-based data, in: 18th Swiss Transport Research Conference. https://doi.org/https://doi.org/10.3929/ethz-b-000315035

Bundesrat, 2020. Ordinance on the Reduction of CO2 Emissions 641.711.

Cabalzar, U., 2019. Aufbau und Betrieb der ersten Wasserstofftankstellen in der Schweiz mit einem Nenndruck von 70 MPa (Construction and operation of the first hydrogen filling stations in Switzerland with a nominal pressure of 70 MPa). Bundesamt für Energie BFE (Swiss Federal Office of Energy (SFOE), Dübendorf (Switzerland).

Capros, P., De Vita, A., Tasios, N., Siskos, P., Kannavou, M., Petropoulos, A., Evangelopoulou, S., Zampara, M., Papadopoulos, D., Nakos, C., others, 2016. EU Reference Scenario 2016-Energy, transport and GHG emissions Trends to 2050. European Commission Directorate-General for Energy, Directorate-General for~….

Cox, B., 2018. Mobility and the Energy Transition: A Life Cycle Assessment of Swiss Passenger Transport Technologies including Developments until 2050. ETH Zurich. https://doi.org/10.3929/ethz-b-000276298

Cox, B., Bauer, C., 2018. The environmental burdens of passenger cars: today and tomorrow (Background report).

Cox, B., Bauer, C., Mendoza Beltran, A., van Vuuren, D.P., Mutel, C.L., 2020. Life cycle environmental and cost comparison of current and future passenger cars under different energy scenarios. Appl. Energy 269, 115021. https://doi.org/10.1016/j.apenergy.2020.115021

De Vos, K., 2015. Negative Wholesale Electricity Prices in the German, French and Belgian Day-Ahead, Intra-Day and Real-Time Markets. Electr. J. 28, 36–50. https://doi.org/10.1016/j.tej.2015.04.001

Díaz Redondo, P., van Vliet, O., 2015. Modelling the Energy Future of Switzerland after the Phase Out of Nuclear Power Plants. Energy Procedia 76, 49–58. https://doi.org/10.1016/J.EGYPRO.2015.07.843

Dillig, M., Jung, M., Karl, J., 2016. The impact of renewables on electricity prices in Germany - An estimation based on historic spot prices in the years 2011-2013. Renew. Sustain. Energy Rev. 57, 7–15. https://doi.org/10.1016/j.rser.2015.12.003

EAFO, 2020. European Alternative Fuels Observatory (EAFO) [WWW Document]. URL https://www.eafo.eu/ (accessed 2.5.21).

EU, 2019. Regulation (EU) 2019/631 of the European Parliament and of the Commission.

EU, 2011. White Paper on transport - Roadmap to a single European transport area - Towards a competitive and resource-efficient transport system. https://doi.org/10.2832/30955

Garimella, R.V., 2017. A Simple Introduction to Moving Least Squares and Local Regression Estimation. Los Alamos, NM (United States). https://doi.org/10.2172/1367799

Götz, P., Henkel, J., Lenck, T., Lenz, K., 2014. Negative Electricity Prices: Causes and Effects. Agora Energiewende, Berlin.

Gül, T., 2008. An energy-economic scenario analysis of alternative fuels for transport. ETH Zurich.

Hänggi, S., Elbert, P., Bütler, T., Cabalzar, U., Teske, S., Bach, C., Onder, C., 2019. A review of synthetic fuels for passenger vehicles. Energy Reports. https://doi.org/10.1016/j.egyr.2019.04.007

Hawkins, T.R., Gausen, O.M., Strømman, A.H., 2012. Environmental impacts of hybrid and electric vehicles-a review. Int. J. Life Cycle Assess. https://doi.org/10.1007/s11367-012-0440-9

Hertwich, E.G., Gibon, T., Bouman, E.A., Arvesen, A., Suh, S., Heath, G.A., Bergesen, J.D., Ramirez, A., Vega, M.I., Shi, L., 2015. Integrated life-cycle assessment of electricity-supply scenarios confirms global environmental benefit of low-carbon technologies. Proc. Natl. Acad. Sci. U. S. A. 112, 6277–6282. https://doi.org/10.1073/pnas.1312753111

Hilpert, S., Kaldemeyer, C., Krien, U., Günther, S., Wingenbach, C., Plessmann, G., 2018. The Open Energy Modelling Framework (oemof) - A new approach to facilitate open science in energy system modelling. Energy Strateg. Rev. 22, 16–25. https://doi.org/10.1016/j.esr.2018.07.001

Hirschberg, S., Bauer, C., Cox, B., Heck, T., Hofer, J., Schenler, W., Simons, A., Del Duce, A., Althaus, H.-J., Georges, G., Others, 2016. Opportunities and challenges for electric mobility: an interdisciplinary assessment of passenger vehicles: Final report of the THELMA project in co-operation with the Swiss Competence Center for Energy Research “Efficient technologies and systems for mobi. Zürich. https://doi.org/doi.org/10.3929/ethz-b-000122825

Infras, 2020. Umweltauswirkungen von Fahrzeugen im urbanen Kontext (Environmental impacts of vehicles in an urban context). Umwelt- und Gesundheitsschutz, Stadt Zürich Tiefbauamt, Stadt Zürich Amt für Abfall, Wasser, Energie und Luft, Kanton Zürich, Zürich.

IPCC, 2013. Climate Change 2013: The Physical Science Basis. Contribution of Working Group I to the Fifth Assessment Report of the Intergovernmental Panel on Climate Change. Cambridge University Press, Cambridge, United Kingdom and New York, NY, USA. https://doi.org/10.1017/CBO9781107415324

Jochem, P., Babrowski, S., Fichtner, W., 2015. Assessing CO2 emissions of electric vehicles in Germany in 2030. Transp. Res. Part A Policy Pract. 78, 68–83. https://doi.org/10.1016/j.tra.2015.05.007

Kannan, R., Hirschberg, S., 2016. Interplay between electricity and transport sectors – Integrating the Swiss car fleet and electricity system. Transp. Res. Part A Policy Pract. 94, 514–531. https://doi.org/10.1016/J.TRA.2016.10.007

Kannan, R., Turton, H., 2014. Switzerland Energy Transition Scenarios-Development and Application of the Swiss TIMES Energy System Model (STEM) Final Project Report December 2014. Bundesamt für Energie BFE (Swiss Federal Office of Energy (SFOE).

Klettke, A., Moser, A., Bossmann, T., Barberi, P., Fournie, L., 2018. Effect of electromobility on the power system and the integration of RES S13 Report. METIS Stud.

Knobloch, F., Hanssen, S. V., Lam, A., Pollitt, H., Salas, P., Chewpreecha, U., Huijbregts, M.A.J., Mercure, J.-F., 2020. Net emission reductions from electric cars and heat pumps in 59 world regions over time. Nat. Sustain. 1–11. https://doi.org/10.1038/s41893-020-0488-7

Kober, T., Bauer (eds.), C., Bach, C., Beuse, M., Georges, G., Held, M., Heselhaus, S., Korba, P., Küng, L., Malhotra, A., Moebus, S., Parra, D., Roth, J., Rüdisüli, M., Schildhauer, T., Schmidt, T.J., Schmidt, T.S., Schreiber, M., Segundo Sevilla, F.R., Steffen, B., Teske, S.L., 2019. White Paper “Power-to-X: Perspectives in Switzerland.” Villigen.

Ligen, Y., Vrubel, H., Girault, H., 2018. Mobility from Renewable Electricity: Infrastructure Comparison for Battery and Hydrogen Fuel Cell Vehicles. World Electr. Veh. J. 9, 3. https://doi.org/10.3390/wevj9010003

Longo, M., Foiadelli, F., Yaïci, W., 2019. Electric Vehicles Integrated with Renewable Energy Sources for Sustainable Mobility, in: New Trends in Electrical Vehicle Powertrains. IntechOpen. https://doi.org/10.5772/intechopen.76788

Mandel, J., McCormick, G., 2016. Combating Climate Change by Measuring Carbon Emissions Correctly - Rocky Mountain Institute [WWW Document]. URL https://rmi.org/combating-climate-change-measuring-carbon-emissions-correctly/ (accessed 2.1.21).

Minde, A., 2020. Data Platform – Open Power System Data [WWW Document]. CoSSMic. URL https://data.open-power-system-data.org/household_data/ (accessed 6.14.21).

Müller, L.J., Kätelhön, A., Bringezu, S., McCoy, S., Suh, S., Edwards, R., Sick, V., Kaiser, S., Cuéllar-Franca, R., El Khamlichi, A., Lee, J.H., Von Der Assen, N., Bardow, A., 2020. The carbon footprint of the carbon feedstock CO2. Energy Environ. Sci. 13, 2979–2992. https://doi.org/10.1039/d0ee01530j

Nordelöf, A., Messagie, Maarten, Tillman, A.-M., Ljunggren Söderman, Maria, Van Mierlo, Joeri, Van Mierlo, J, Messagie, M, Ljunggren Söderman, M, 2014. Environmental impacts of hybrid, plug-in hybrid, and battery electric vehicles-what can we learn from life cycle assessment? Int J Life Cycle Assess 19, 1866–1890. https://doi.org/10.1007/s11367-014-0788-0

Nordmann, R., 2019. Sonne für den Klimaschutz - Ein Solarplan für die Schweiz (Sun for climate protection - a solar plan for Switzerland). Zytglogge.

OEDI, 2020. OEDI: Commercial and Residential Hourly Load Profiles for all TMY3 Locations in the United States [WWW Document]. URL https://data.openei.org/submissions/153 (accessed 6.14.21).

Oguchi, M., Fuse, M., 2015. Regional and Longitudinal Estimation of Product Lifespan Distribution: A Case Study for Automobiles and a Simplified Estimation Method. Environ. Sci. Technol. 49, 1738–1743. https://doi.org/10.1021/es505245q

Pareschi, G., Georges, G., Boulouchos, K., 2017. Assessment of the Marginal Emission Factor associated with Electric Vehicle Charging. 1st E-Mobility Power System Integration Symposium. E-Proceedings, Berlin (Germany). https://doi.org/10.3929/ethz-b-000200058

Pareschi, G., Küng, L., Georges, G., Boulouchos, K., 2020. Are travel surveys a good basis for EV models? Validation of simulated charging profiles against empirical data. Appl. Energy 275, 115318. https://doi.org/10.1016/j.apenergy.2020.115318

Pattupara, R., Kannan, R., 2016. Alternative low-carbon electricity pathways in Switzerland and it's neighbouring countries under a nuclear phase-out scenario. Appl. Energy 172, 152–168. https://doi.org/10.1016/j.apenergy.2016.03.084

Pattupara, R.M., 2016. Long term evolution of the Swiss electricity system under a European electricity market. ETH Zurich. https://doi.org/https://doi.org/10.3929/ethz-a-010635090

Pfenninger, S., Staffell, I., 2016. Long-term patterns of European PV output using 30 years of validated hourly reanalysis and satellite data. Energy 114, 1251–1265. https://doi.org/10.1016/j.energy.2016.08.060

Piot, M., 2014. Bedeutung der Speicher-und Pumpspeicherkraftwerke für die Energiestrategie 2050 der Schweiz (Significance of storage and pumped storage power plants for Switzerland's 2050 energy strategy). Wasser Energ. Luft 4, 259–265.

Portmann, M., Galvagno-Erny, D., Lorenz, P., Schacher, D., 2016. Sonnendach.ch : Berechnung von Potenzialen in Gemeinden (Calculation of potentials in communities). Bundesamt für Energie BFE (Swiss Federal Office of Energy SFOE), Kriens.

Prognos, 2020. Energieperspektiven 2050+ (Kurzbericht). Bundesamt für Energie BFE (Swiss Federal Office of Energy SFOE), Bern.

Prognos, 2012. Die Energieperspektiven für die Schweiz bis 2050. Energienachgefrage und Elektrizitätsangebot in der Schweiz 2000-2050 (The energy prospects for Switzerland up to 2050. Energy demand and electricity supply in Switzerland 2000-2050). Bundesamt für Energie BFE (Swiss Federal Office of Energy (SFOE), Basel.

Reiter, G., Lindorfer, J., 2015. Global warming potential of hydrogen and methane production from renewable electricity via power-to-gas technology. Int. J. Life Cycle Assess. 20, 477–489. https://doi.org/10.1007/s11367-015-0848-0

Reynolds, D.A., 2009. Gaussian Mixture Models. Encycl. biometrics 741.

Ricardo, 2020. Determining the environmental impacts of conventional and alternatively fuelled vehicles through LCA. European Commission.

Romano, E., Hollmuller, P., Patel, M.K., 2018. Émissions horaires de gaz à effet de serre liées à la consommation d'électricité – une approche incrémentale pour une économie ouverte : Le cas de la Suisse (Real-time carbon emission due to electricity consumption - a marginal approach for an open econom. University of Geneva (Archive ouverte).

Rüdisüli, M., Teske, S.L., Elber, U., 2019. Impacts of an Increased Substitution of Fossil Energy Carriers with Electricity-Based Technologies on the Swiss Electricity System. Energies 12, 2399. https://doi.org/10.3390/en12122399

Sacchi, R., Bauer, C., Cox, B., Mutel, C., 2020. carculator: an open-source tool for prospective environmental and economic life cycle assessment of vehicles. When, Where and How can battery-electric vehicles help reduce greenhouse gas emissions? submitted.

Schaber, C., Mazza, P., Hammerschlag, R., 2004. Utility-scale storage of renewable energy. Electr. J. 17, 21–29. https://doi.org/10.1016/j.tej.2004.05.005

Schlögl, R., 2017. E-Mobility and the Energy Transition. Angew. Chemie Int. Ed. 56, 11019–11022. https://doi.org/10.1002/anie.201701633

Schmidt, U., 2020. Elektromobilität und Klimaschutz: Die große Fehlkalkulation (Electromobility and climate protection: the big miscalculation). Kiel Policy Br.

Schram, W., Lampropoulos, I., AlSkaif, T., van Sark, W., 2019. On the Use of Average versus Marginal Emission Factors, in: Proceedings of the 8th International Conference on Smart Cities and Green ICT Systems. SCITEPRESS - Science and Technology Publications, pp. 187–193. https://doi.org/10.5220/0007765701870193

Seixas, J., Simões, S., Dias, L., Kanudia, A., Fortes, P., Gargiulo, M., 2015. Assessing the cost-effectiveness of electric vehicles in European countries using integrated modeling. Energy Policy 80, 165–176. https://doi.org/10.1016/j.enpol.2015.01.032

Solaymani, S., 2019. CO2 emissions patterns in 7 top carbon emitter economies: The case of transport sector. Energy 168, 989–1001. https://doi.org/10.1016/j.energy.2018.11.145

Staffell, I., Pfenninger, S., 2016. Using bias-corrected reanalysis to simulate current and future wind power output. Energy 114, 1224–1239. https://doi.org/10.1016/J.ENERGY.2016.08.068

Stolz, P., Frischknecht, R., 2019. Energieetikette für Personenwagen: Umweltkennwerte 2019 der Strom- und Treibstoffbereitstellung (Energy label for passenger cars: Environmental parameters 2019 for electricity and fuel supply. Bundesamt für Energie BFE (Swiss Federal Office of Energy SFOE), Bern.

Suisse Eole, 2020. Plan éolien pour le climat : la solution énergétique hivernale. Analyse et actualisation du potentiel de l'énergie éolienne en Suisse. Bundesamt für Energie BFE (Swiss Federal Office of Energy (SFOE), Yverdon.

Swissgrid, 2020. Aggregierte Energiedaten aus dem Regelblock Schweiz (Aggregated energy data from the Swiss control block) [WWW Document]. URL https://www.swissgrid.ch/de/home/customers/topics/energy-data-ch.html (accessed 11.24.20).

Swissgrid, 2018. Aggregated energy data of the control block Switzerland [WWW Document]. URL https://www.swissgrid.ch/de/home/operation/grid-data/generation.html

Swissnuclear, 2020. Energieproduktion der Kernkraftwerke - swissnuclear [WWW Document]. URL https://www.swissnuclear.ch/de/energieproduktion-der-kernkraftwerke-_content---1--1014.html (accessed 11.24.20).

Taylor, A.M.K.P., 2008. Science review of internal combustion engines. Energy Policy 36, 4657–4667. https://doi.org/10.1016/j.enpol.2008.09.001

Terni, 2020. Smart Energy Data: Terni Power Demand/ Supply Profiles - Datasets - FIWARE Lab Data Portal [WWW Document]. URL https://data.lab.fiware.org/dataset/smart_energy_data-_terni_power_demand__supply_profiles (accessed 6.14.21).

Teske, S.L., Rüdisüli, M., Schildhauer, T.J., Bach, C., 2019. Potentialanalyse Power-to-Gas in der Schweiz (Potential analysis of power-to-gas in Switzerland). Empa, Dübendorf. https://doi.org/https://doi.org/10.5281/zenodo.2649817

Van Der Giesen, C., Kleijn, R., Kramer, G.J., 2014. Energy and climate impacts of producing synthetic hydrocarbon fuels from CO2. Environ. Sci. Technol. 48, 7111–7121. https://doi.org/10.1021/es500191g

Von Roon, S., Huber, M., 2010. Modeling Spot Market Pricing with the Residual Load. Enerday - 5th Conference on Energy Economics and Technology, 16.04.2010, Dresden, Munich.

VSG, 2020. Thesen 2020 der Schweizer Gaswirtschaft (2020 theses of the Swiss gas industry). Verband der Schweizerischen Gasindustrie VSG, Zürich.

Walch, A., Castello, R., Mohajeri, N., Scartezzini, J.-L., 2020. Big data mining for the estimation of hourly rooftop photovoltaic potential and its uncertainty. Appl. Energy 262, 114404. https://doi.org/10.1016/j.apenergy.2019.114404

Wang, A., Leun, K. van der, Peters, D., Buseman, M., 2020. European Hydrogen Backbone - How a dedicated hydrogen infrastructure can be created. Guidehouse, Stadsplateau (NL).

Wernet, G., Bauer, C., Steubing, B., Reinhard, J., Moreno-Ruiz, E., Weidema, B., 2016. The ecoinvent database version 3 (part I): overview and methodology. Int. J. Life Cycle Assess. 21, 1218–1230. https://doi.org/10.1007/s11367-016-1087-8

Wikipedia contributors, 2020. Phase-out of fossil fuel vehicles.

Wulf, C., Kaltschmitt, M., 2018. Hydrogen supply chains for mobility-Environmental and economic assessment. Sustain. 10, Art.-Nr. 1699. https://doi.org/10.3390/su10061699

Zappa, W., Junginger, M., van den Broek, M., 2019. Is a 100% renewable European power system feasible by 2050? Appl. Energy 233–234, 1027–1050. https://doi.org/10.1016/j.apenergy.2018.08.109

Zhang, X., Bauer, C., Mutel, C.L., Volkart, K., 2017. Life Cycle Assessment of Power-to-Gas: Approaches, system variations and their environmental implications. Appl. Energy 190, 326–338. https://doi.org/10.1016/j.apenergy.2016.12.098

Zhang, X., Witte, J., Schildhauer, T., Bauer, C., 2020. Life cycle assessment of power-to-gas with biogas as the carbon source. Sustain. Energy Fuels 4, 1427–1436. https://doi.org/10.1039/c9se00986h

Züttel, A., Remhof, A., Borgschulte, A., Friedrichs, O., 2010. Hydrogen: The future energy carrier. Philos. Trans. R. Soc. A Math. Phys. Eng. Sci. https://doi.org/10.1098/rsta.2010.0113